LYOPHOBIC COLLOIDAL SYSTEMS

(The “lyophilic/lyophobic” classification makes sense only for particles dispersed in a liquid)

By definition, the dispersed systems are **lyophobic** if they are **thermodynamically unstable**.

Hence, the dispersion of a solid or liquid sample in water with formation of micelles runs unspontaneously: $\Delta G_{disp} = \Delta H_{disp} - T\Delta S_{disp} > 0$,

and is irreversible.

On the other hand, $\pi d^2\sigma >> k_B T$

Nanodispersed systems

The systems of interest: $d \le 10^{-6}$ m

Especially, systems with nano-sized particles, *i.e.*,

$$d \le 10^{-7}\ \text{m, or}\ 1\text{–}100\ \text{nm}$$

$$1\,\text{nm} = 10^{-9}\ \text{m}$$

Such systems may be either **polydispersed** or (almost) **monodispersed**.

They may be either **well-defined** or **ill-defined.**

Some examples of most popular lyophobic nanodispersed systems

Typical lyophobic colloidal systems:
hydrosols of metals, e.g., Pt, Cu, Au, Ag, Hg,
metal iodides, e.g., AgI,
sulfides, ZnS, CdS, HgS, As_2S_3, Sb_2S_3, Bi_2S_3,
and chalcogenes: S, Se.

Their coagulation occurs at low concentrations of indifferent electrolytes, and the deposits as a rule cannot be peptized.

The surface tension values of the solid/liquid interface may reach tenths or even $J \cdot m^{-2}$ units.

Their stability is caused only by the formation of a double electrical layer. They are stable against sedimentation owing to small size of particles.

Some examples of most popular lyophobic nanodispersed systems

Lyophobic, i.e., thermodynamically unstable are **emulsions** and **foams**. They cannot exist during a long time without an added stabilizer (surfactant of polymer).

Air (and other gases) **bubbles**

An important kind of lyophobic colloidal systems are **latexes**.

[recycled rubber tree sap (*hevea brasiliensis*)]

Nanocarbon: **fullerenes; carbon nanotubes (SWCNT, MWCNT); graphene; nanodiamonds** – we'll talk about them later.

Unique applications in nanotechnologies !!

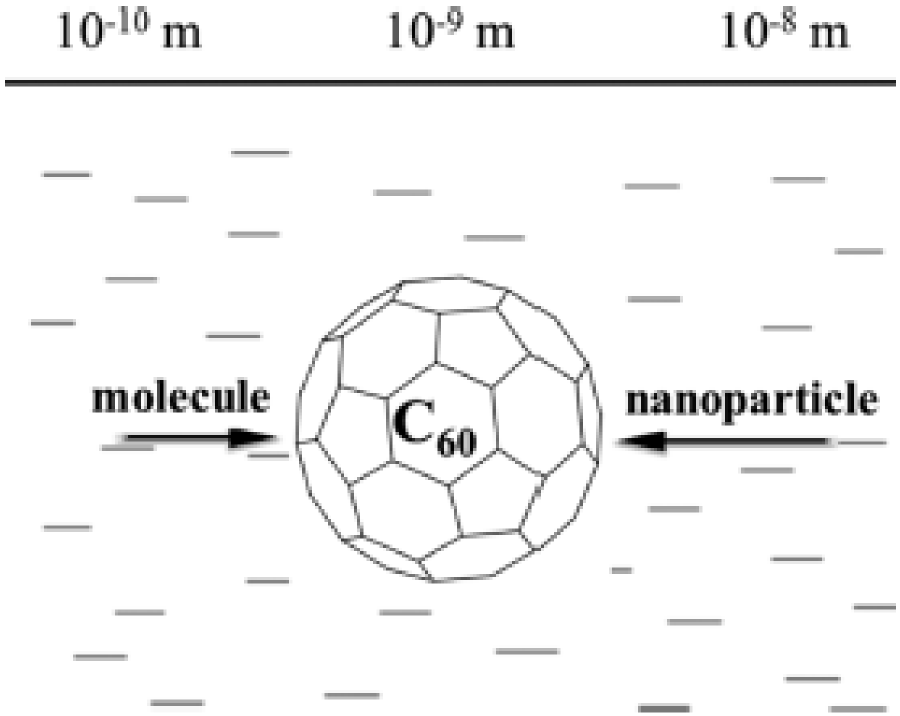

Fullerenes C_N : 12 pentagons and (N/2) – 10 hexagons

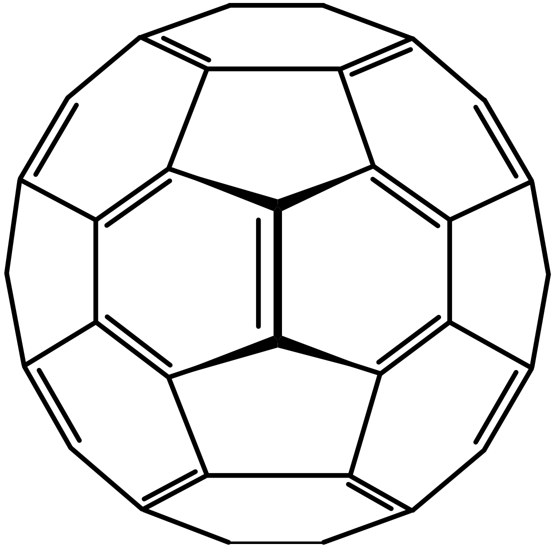

C_{60} , C_{70} , C_{76} , C_{78} , C_{84}, and so on …

12 pentagons and $(N/2) - 10$ hexagons

Теорема Эйлера:
число вершин + число граней = число ребер + 2

The Euler theorem: number of vertexes + number of planes = number of edges + 2.

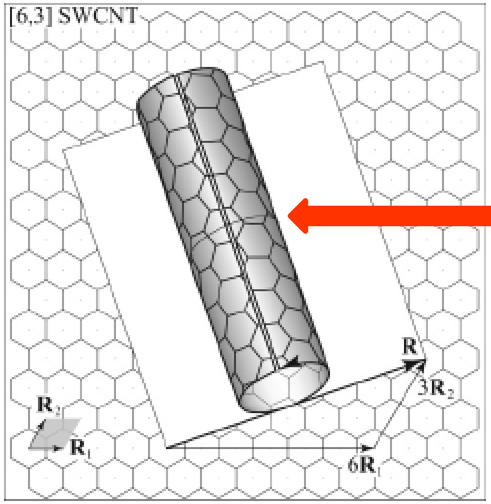

Carbon nanotube

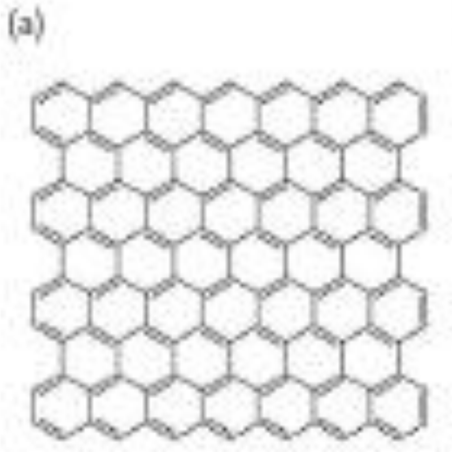

Graphene

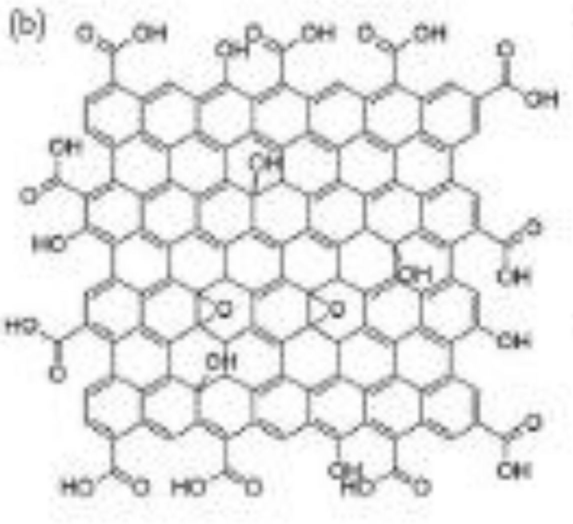

Oxidized graphene

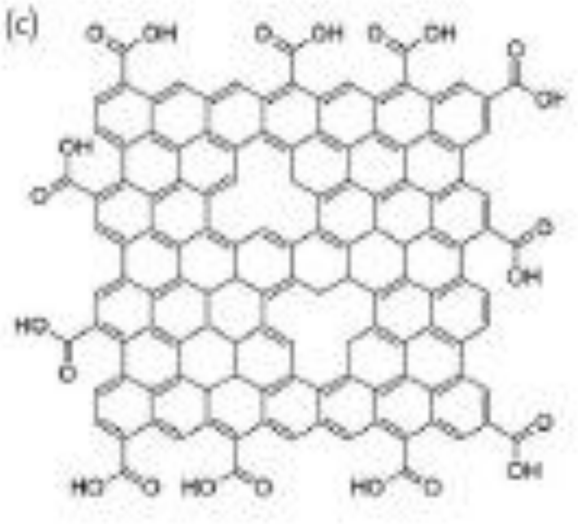

Reduced graphene

Detonation nanodiamond

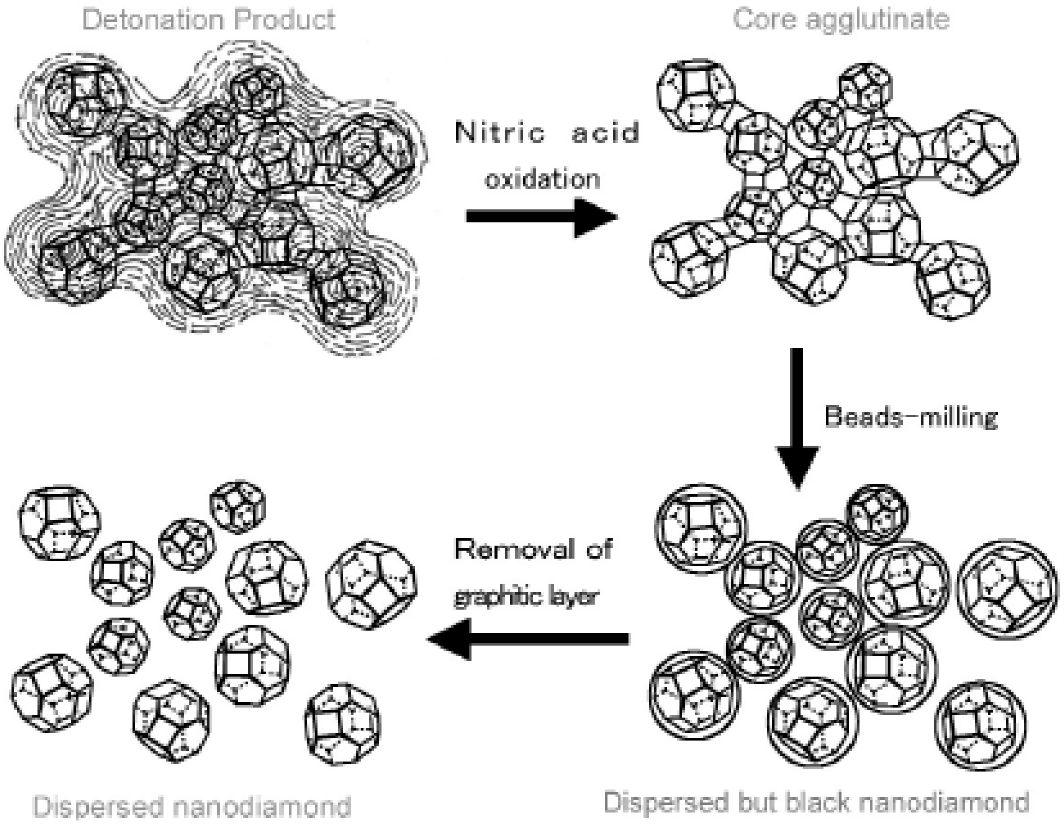

Colloidal systems of intermediate type

Fe_2O_3, $FeO(OH)$, $Fe(OH)_3$, SiO_2, SnO_2, TiO_2, Al_2O_3, etc.

Inorganic polymers:

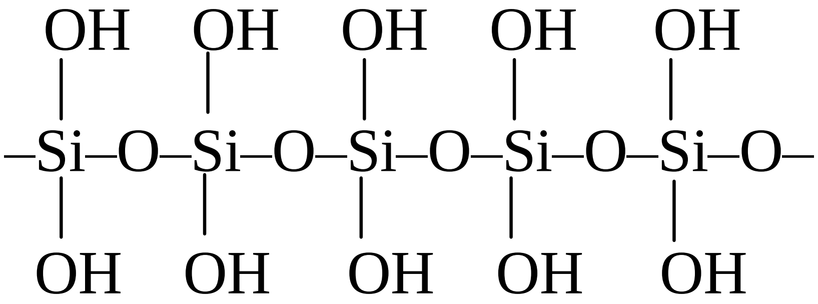

$$-\underset{\underset{OH}{|}}{\overset{\overset{OH}{|}}{Si}}-O-\underset{\underset{OH}{|}}{\overset{\overset{OH}{|}}{Si}}-O-\underset{\underset{OH}{|}}{\overset{\overset{OH}{|}}{Si}}-O-\underset{\underset{OH}{|}}{\overset{\overset{OH}{|}}{Si}}-O-\underset{\underset{OH}{|}}{\overset{\overset{OH}{|}}{Si}}-O-$$

Bentonite clays: minerals of the montmorilonite group, saturated with lithium and sodium chlorides

$$Al_4Si_8O_{16}(OH)_{12}\cdot nH_2O \text{ or } [Al(OH)_3]_4[SiO_2]_8\cdot nH_2O$$

Nanoparticles in the environment

Fate of the engineered colloidal species in soils and freshwater (rivers, lakes, etc.).

Interactions of nanoparticles with natural organic matter (humates, fulvates).

Detection and removal of nanoparticles from natural waters.

The impact of the engineered nanoparticles on the environment and on the human body is not yet fully understood !!

COMMENTARY

Safe handling of nanotechnology

The pursuit of responsible nanotechnologies can be tackled through a series of grand challenges, argue **Andrew D. Maynard** and his co-authors.

When the physicist and Nobel laureate Richard Feynman challenged the science community to think small in his 1959 lecture 'There's Plenty of Room at the Bottom', he planted the seeds of a new era in science and technology. Nanotechnology, which is about controlling matter at near-atomic scales to produce unique or enhanced materials, products and devices, is now maturing rapidly with more than 300 claimed nanotechnology products already on the market[1]. Yet concerns have been raised that the very properties of nanostructured materials that make them so attractive could potentially lead to unforeseen health or environmental hazards[2].

The spectre of possible harm — whether real or imagined — is threatening to slow the development of nanotechnology unless sound, independent and authoritative information is developed on what the risks are, and how to avoid them[3]. In what may be unprecedented pre-emptive action in the face of a new technology, governments, industries and research organizations around the world are beginning to address how the benefits of emerging nanotechnologies can be realized while minimizing potential risks[4]. Yet despite a clear commitment to support risk-focused research, opportunities to establish collaborative, integrated and targeted research programmes are being missed[5]. In September, Sherwood Boehlert, chair of the US House Science Committee, commented in a hearing that "we're on the right path to dealing with the problem, but we're sauntering down it when a sense of urgency is required". And in October, Britain's Royal Society raised concerns that the UK government had not made enough progress on reducing the uncertainties surrounding the health and environmental impacts of nanomaterials[6].

"Understanding and preventing risk often has a low priority in the competitive world of research funding."

The risks

As research leaders in our respective fields, we recognize that systematic risk research is needed if emerging nano-industries are to thrive. We cannot set the international research agenda on our own, but we can inspire the scientific community — including government, industry, academia and other stakeholders — to move in the right direction. So we propose five grand challenges to stimulate research that is imaginative, innovative and above all relevant to the safety of nanotechnology.

DR AKEY

Potential health risks from exposure to engineered nanomaterials must be understood and minimized.

Fears over the possible dangers of some nanotechnologies may be exaggerated, but they are not necessarily unfounded. Recent studies examining the toxicity of engineered nanomaterials in cell cultures and animals have shown that size, surface area, surface chemistry, solubility and possibly shape all play a role in determining the potential for engineered nanomaterials to cause harm[7]. This is not surprising: we have known for many years that inhaled dusts cause disease, and that their harmfulness depends on both what they are made of and their physical nature. For instance, small particles of inhaled quartz lead to lung damage and the potential development of progressive lung disease, yet the same particles with a thin coating of clay are less harmful[8]. Asbestos presents a far more dramatic example: thin, long fibres of the material can lead to lung disease if inhaled, but grind the fibres down to shorter particles with the same chemical make-up and the harmfulness is significantly reduced[9].

It is generally accepted that, in principle, some nanomaterials may have the potential to cause harm to people and the environment. But the way science is done is often ill-equipped to address novel risks associated with emerging technologies. Research into understanding and preventing risk often has a low priority in the competitive worlds of intellectual property, research funding and technology development. And yet there is much at stake in how potential nano-specific risks are understood and managed. Without strategic and targeted risk research, people producing and using nanomaterials could develop unanticipated illness arising from their exposure; public confidence in nanotechnologies could be reduced through real or perceived dangers; and fears of litigation may make nanotechnologies less attractive to investors and the insurance industry.

The science community needs to act now if strategic research is to support sustainable nanotechnologies, in which risks are minimized and benefits maximized. Our five grand challenges are chosen to stimulate such research, as well as bring focus to a range of complex multidisciplinary issues. The challenges span the next 15 years, and their successful achievement will depend on coordination, collaboration, resources and ingenuity. They are not comprehensive — there is essential research that is not covered here — but they do form a framework on which others can build.

Getting Nanotechnology Right the First Time

Statement to the National Research Council
Committee to Review the National Nanotechnology Initiative
25 March 2005
Richard A. Denison, Ph.D., Senior Scientist
Health Program, Environmental Defense

Thank you for this opportunity to offer the perspective of Environmental Defense to this panel. Environmental Defense, formerly known as Environmental Defense Fund, was established in 1967 by scientists who were among the first to discern the devastating effects of aerial spraying of DDT on wildlife. Today, Environmental Defense is one of the country's leading environmental advocacy organizations, with an annual budget of nearly $50 million.

e

ENVIRONMENTAL DEFENSE
finding the ways that work

Nanotoxicology References

A bibliography of references and abstracts of risk-related research studies on nanomaterials compiled by Environmental Defense

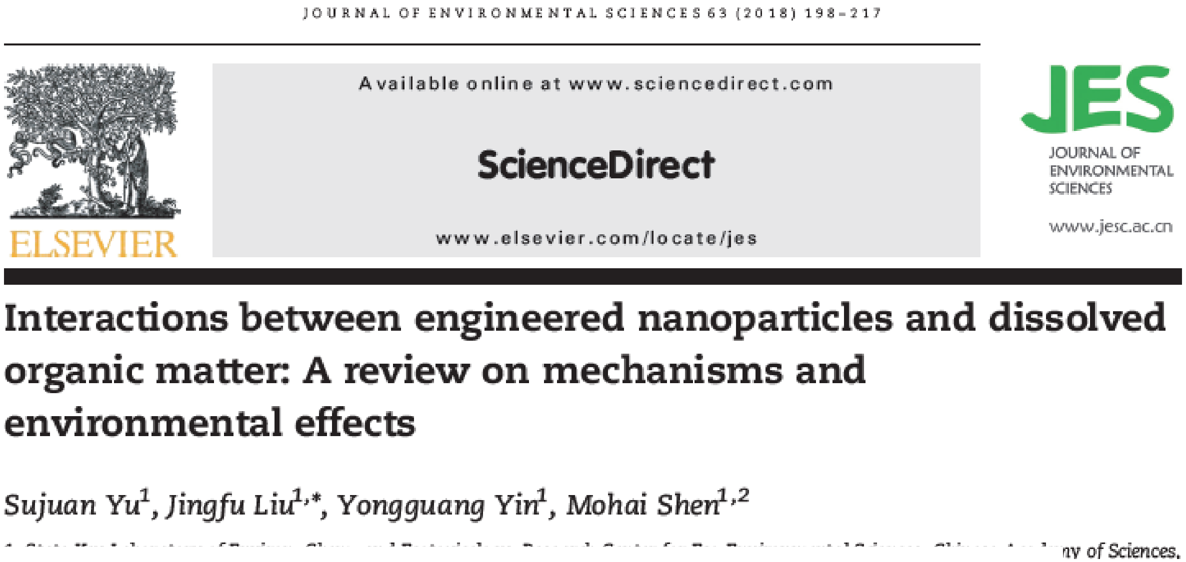

JOURNAL OF ENVIRONMENTAL SCIENCES 63 (2018) 198–217

Available online at www.sciencedirect.com

ScienceDirect

www.elsevier.com/locate/jes

JES JOURNAL OF ENVIRONMENTAL SCIENCES

www.jesc.ac.cn

Interactions between engineered nanoparticles and dissolved organic matter: A review on mechanisms and environmental effects

Sujuan Yu[1], Jingfu Liu[1,*], Yongguang Yin[1], Mohai Shen[1,2]

ny of Sciences,

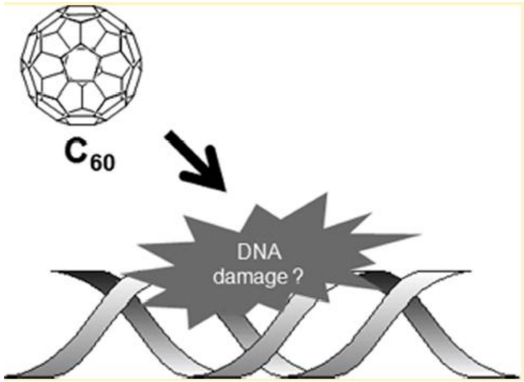

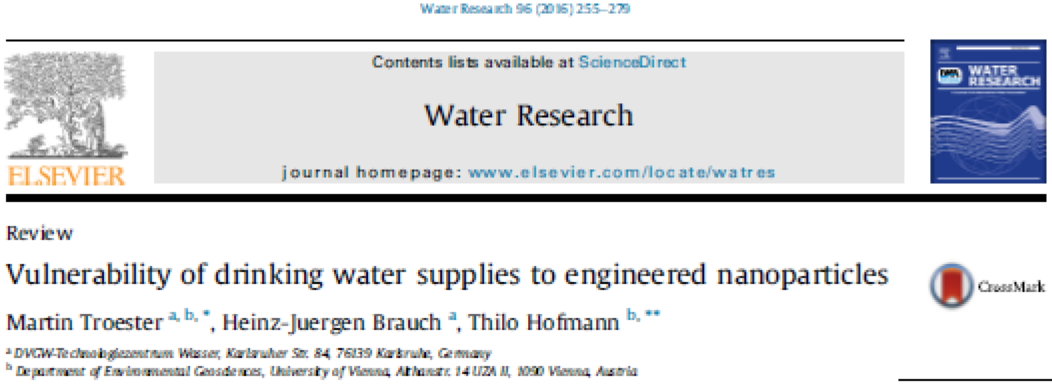

Water Research 96 (2016) 255–279

Contents lists available at ScienceDirect

Water Research

journal homepage: www.elsevier.com/locate/watres

Review

Vulnerability of drinking water supplies to engineered nanoparticles

Martin Troester [a, b, *], Heinz-Juergen Brauch [a], Thilo Hofmann [b, **]

[a] DVGW-Technologiezentrum Wasser, Karlsruher Str. 84, 76139 Karlsruhe, Germany
[b] Department of Environmental Geosciences, University of Vienna, Althanstr. 14 UZA II, 1090 Vienna, Austria

Genotoxicity ??!!

Cytotoxicity??!!

Photocytotoxicity??!!

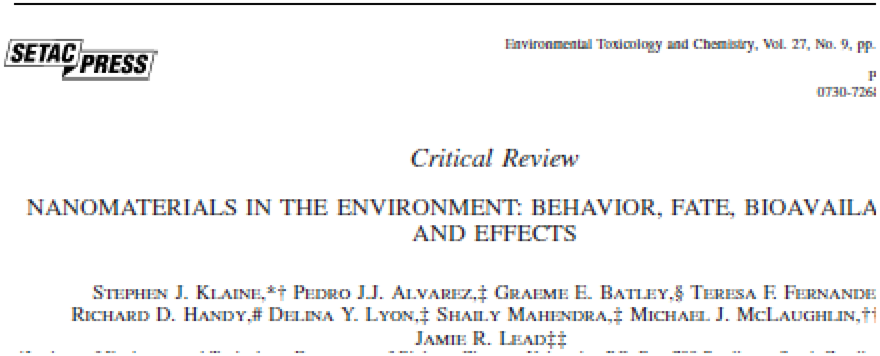

SETAC PRESS

Environmental Toxicology and Chemistry, Vol. 27, No. 9, pp.

0730-726

Critical Review

NANOMATERIALS IN THE ENVIRONMENT: BEHAVIOR, FATE, BIOAVAILA AND EFFECTS

STEPHEN J. KLAINE,*† PEDRO J.J. ALVAREZ,‡ GRAEME E. BATLEY,§ TERESA F. FERNANDE
RICHARD D. HANDY,# DELINA Y. LYON,‡ SHAILY MAHENDRA,‡ MICHAEL J. MCLAUGHLIN,†
JAMIE R. LEAD‡‡

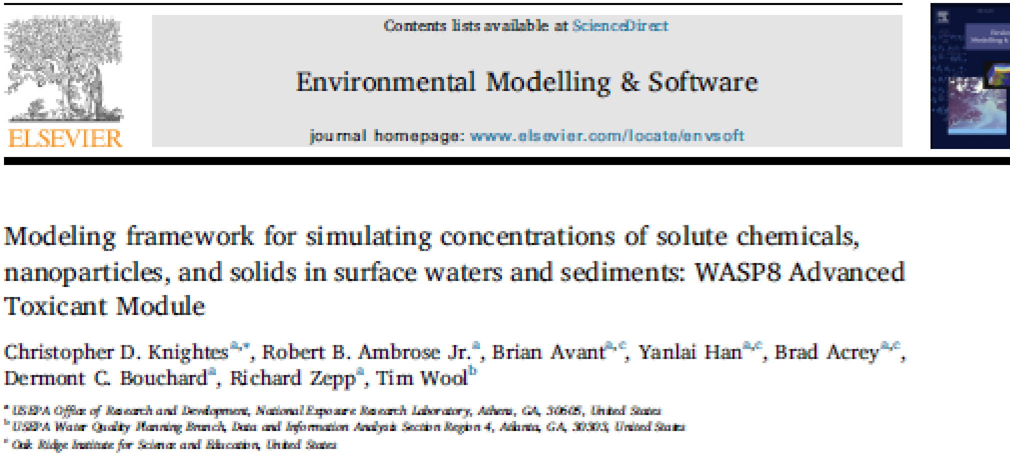

Contents lists available at ScienceDirect

Environmental Modelling & Software

journal homepage: www.elsevier.com/locate/envsoft

Modeling framework for simulating concentrations of solute chemicals, nanoparticles, and solids in surface waters and sediments: WASP8 Advanced Toxicant Module

Christopher D. Knightes[a,*], Robert B. Ambrose Jr.[a], Brian Avant[a,c], Yanlai Han[a,c], Brad Acrey[a,c], Dermont C. Bouchard[a], Richard Zepp[a], Tim Wool[b]

[a] USEPA Office of Research and Development, National Exposure Research Laboratory, Athens, GA, 30605, United States
[b] USEPA Water Quality Planning Branch, Data and Information Analysis Section Region 4, Atlanta, GA, 30303, United States
[c] Oak Ridge Institute for Science and Education, United States

SYNTHESIS OF NANOPARTICLES

Two main methods:

1) **Top-down** (from macroscopic body to suspensions or sols)

2) **Bottom-up** (from molecules to colloidal particles)

Top-down methods: dispergation

1) work of volumetric dispersion (i.e. work of elastic and plastic deformation);
2) work of creating new surfaces

$$W = kV + \sigma \Delta s = d^2(k_1 d + k_2 \sigma)$$

The Rehbinder effect: grinding is facilitated in the presence of surfactants

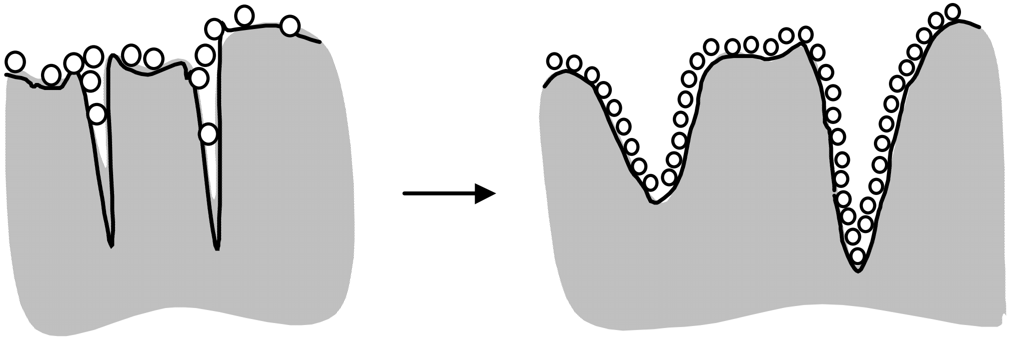

Dispergation of macroscopic solid

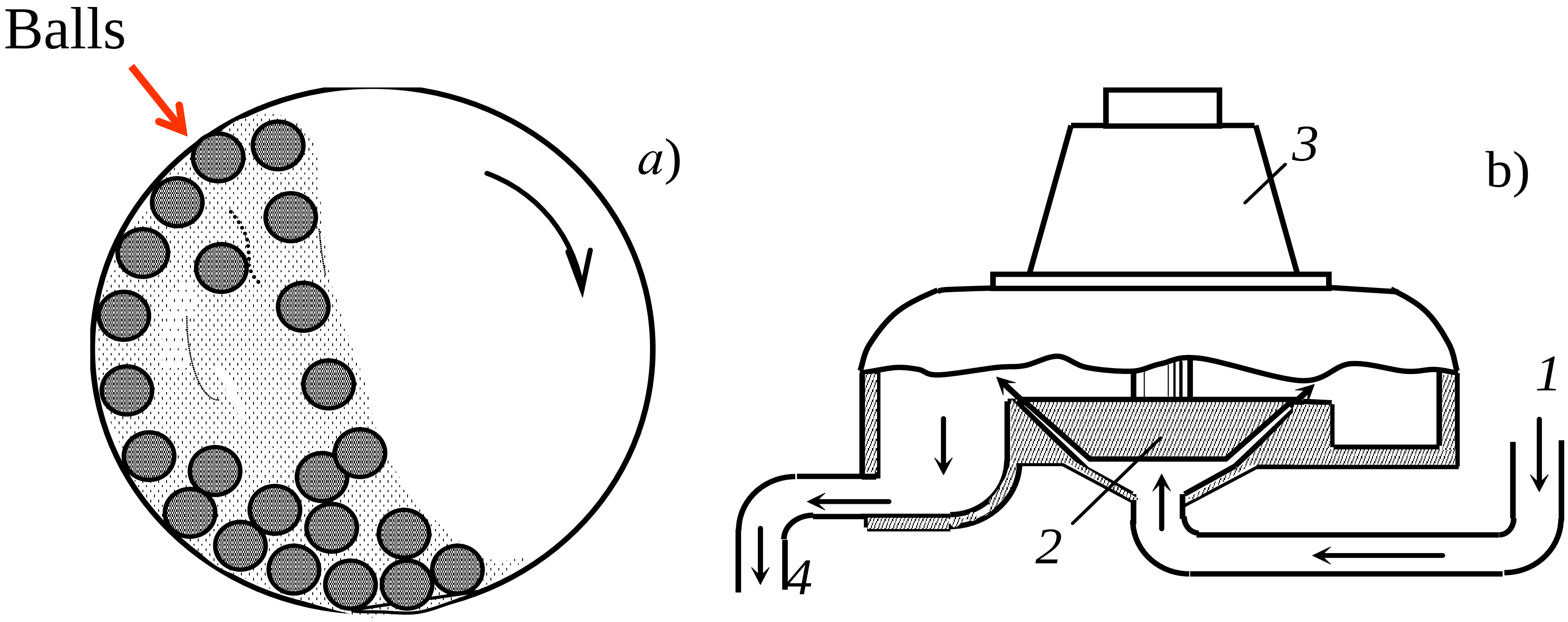

Ball mill (*a*) and colloidal mill (*b*): *1* – suspension pipe;
2 – rotor; *3* – electrical motor; 4 – outlet pipe.

As a rule, the top-down methods **do not allow obtaining nanosized** particles.

However, some **exceptions** are known, e.g., for fullerenes.

Hand-grinding in an agate (or glass) mortar

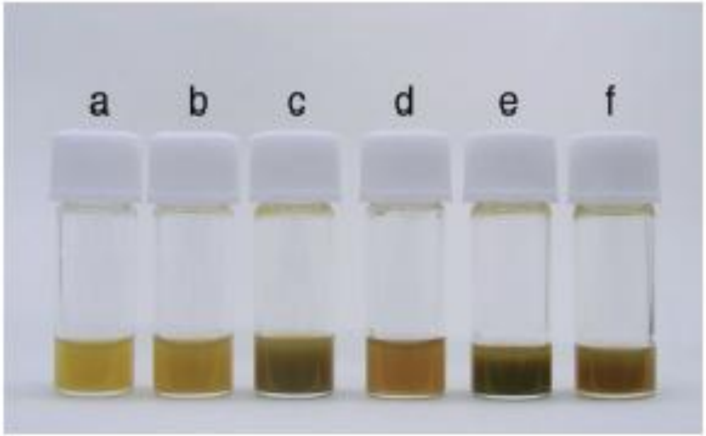

Figure 1. Photograph of dispersions of the C_{60} nanoparticles in various solvents. a) Methanol, b) ethanol, c) 2-propanol, d) 1-octanol, e) acetone, and f) silicone oil.

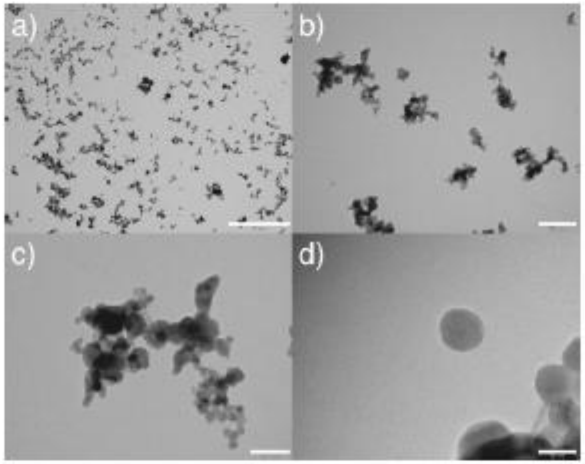

Figure 2. TEM images of the C_{60} nanoparticles dispersed in methanol at different magnifications. a) Scale bar, 5 µm. b) Scale bar, 500 nm. c) Scale bar, 200 nm. d) Scale bar, 50 nm.

Chemistry Letters Vol.35, No.4 (2006)

Top-down Preparation of Dispersions of C_{60} Nanoparticles in Organic Solvents

Shigeru Deguchi* and Sada-atsu Mukai

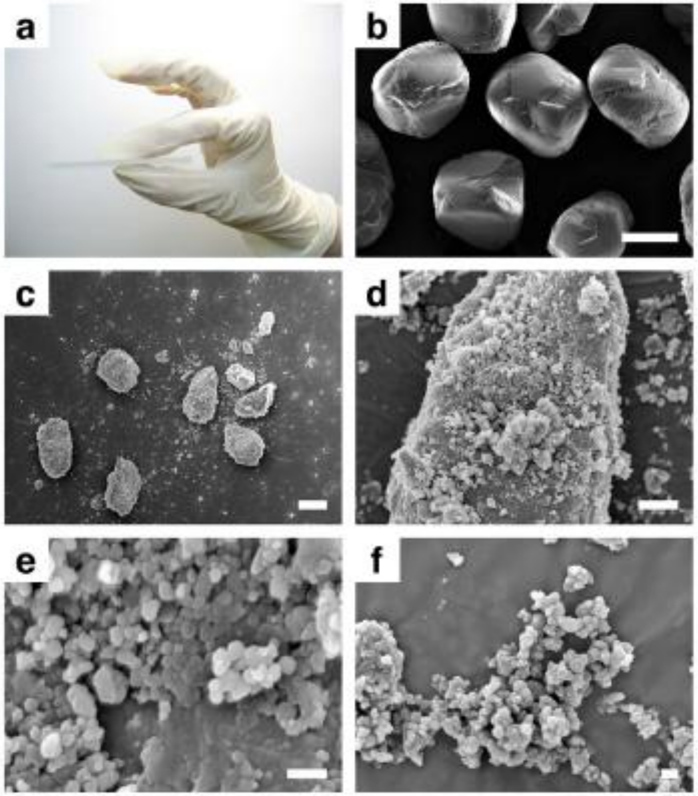

Figure 1 | Formation of nanoparticles by rubbing solid C_{60} between glass slides. (a) Experimental procedure. (b) SEM image of particles of as-received solid C_{60}. Scale bar represents 100 µm. (c, d, e and f) SEM images of nanoparticles of C_{60} formed by rubbing bulks solids between glass slides. Scale bars represent 10 µm (c), 2 µm (d), and 200 nm (e and f).

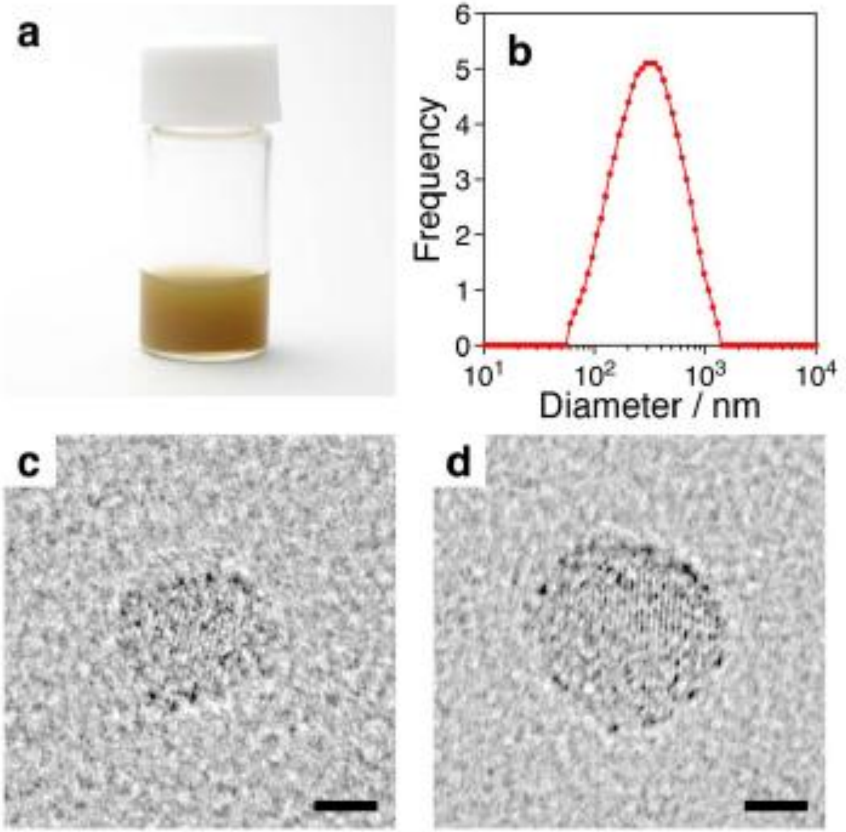

Figure 3 | Size distribution of nanoparticles produced by rubbing solid C_{60} between glass slides. (a) An optical photograph of a dispersion of nanoparticles of C_{60} in water containing 1 wt% SDS. (b) Size distribution of the nanoparticles of C_{60} in the dispersion. (c and d) HRTEM images of nanoparticles of C_{60} found in the dispersion. Scale bars represent 5 nm.

Non-Engineered Nanoparticles of C_{60}

Shigeru Deguchi[1], Sada-atsu Mukai[1,2,3], Hide Sakaguchi[4] & Yoshimune Nonomura[5]

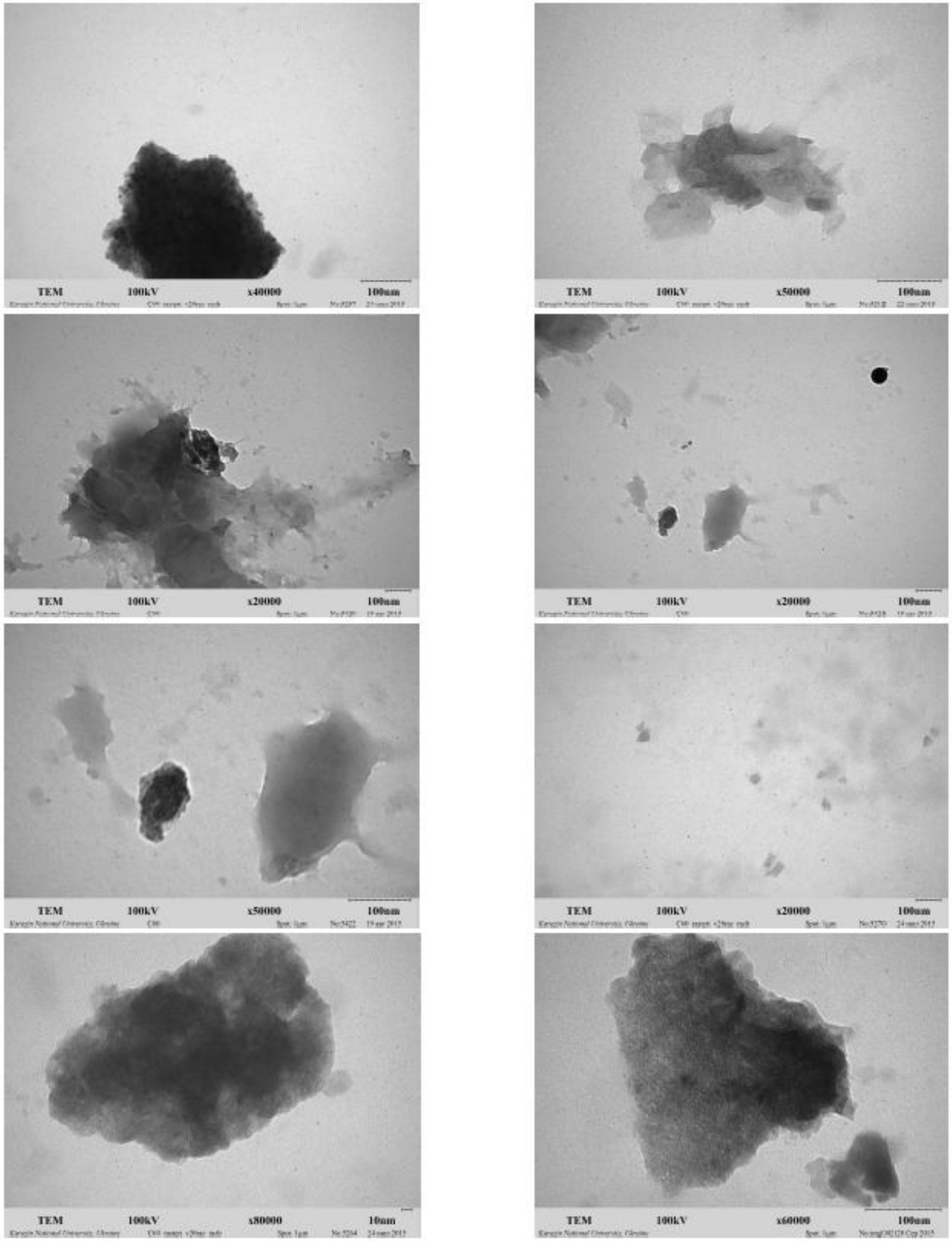

Figure 1. The TEM images of two independently prepared samples of C_{60} colloid, after evaporation of the 3-fold diluted solutions.

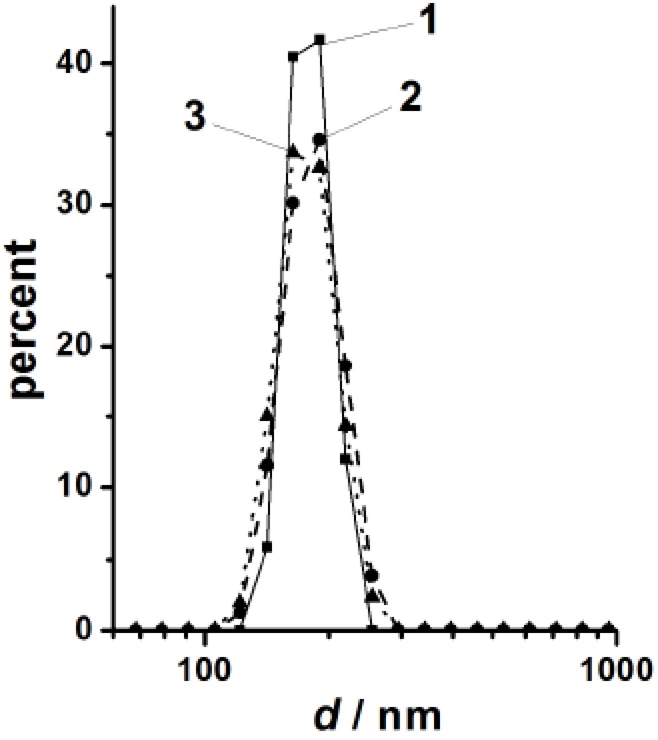

C_{60} sol in acetonitrile, prepared by hand-grinding in our laboratory

Detonation nanodiamond

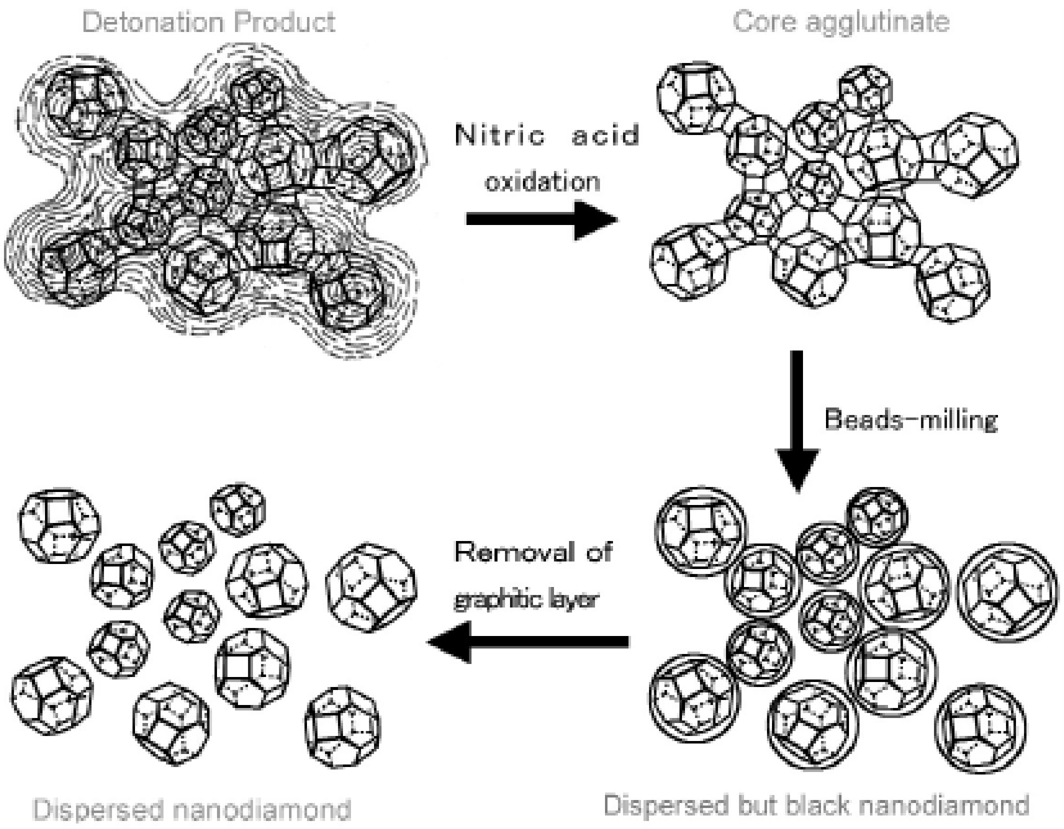

Presently, **splitting up macrospecies** is often made using laser beam, ultrasound (“sonication”), microwave radiation, etc.

Such procedures may be conducted either in liquids or in the gas phase.

Preparation of a metal colloid by using an electric arc, according to Bredig:

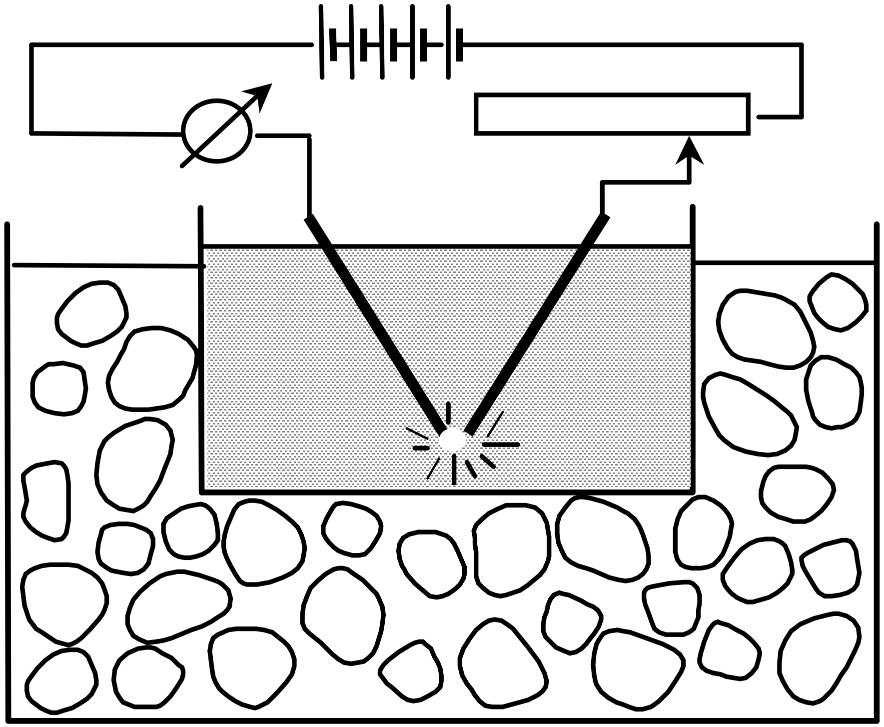

On the first glance, this method belongs to the “top-down” type. However, in fact it consists in aggregation of metal atoms evaporated from the electrodes.

Bottom-up methods

1. **Physical condensation** of atoms or molecules into small colloidal species as a result of phase transitions.

2. **Chemical condensation** as a result of chemical reactions of different types.

Despite different ways of obtaining nanoparticles of a new phase, there are some fundamental regularities governing the process.

Kinetics of formation of a new phase

According to Weimarn's theory, the rate of formation of crystallization centers is proportional to the relative oversaturation:

$$\omega = K\frac{c-L}{L}$$

Петр Петрович фон ВЕЙМАРН
Piotr Petrovych von WEIMARN
1879—1935

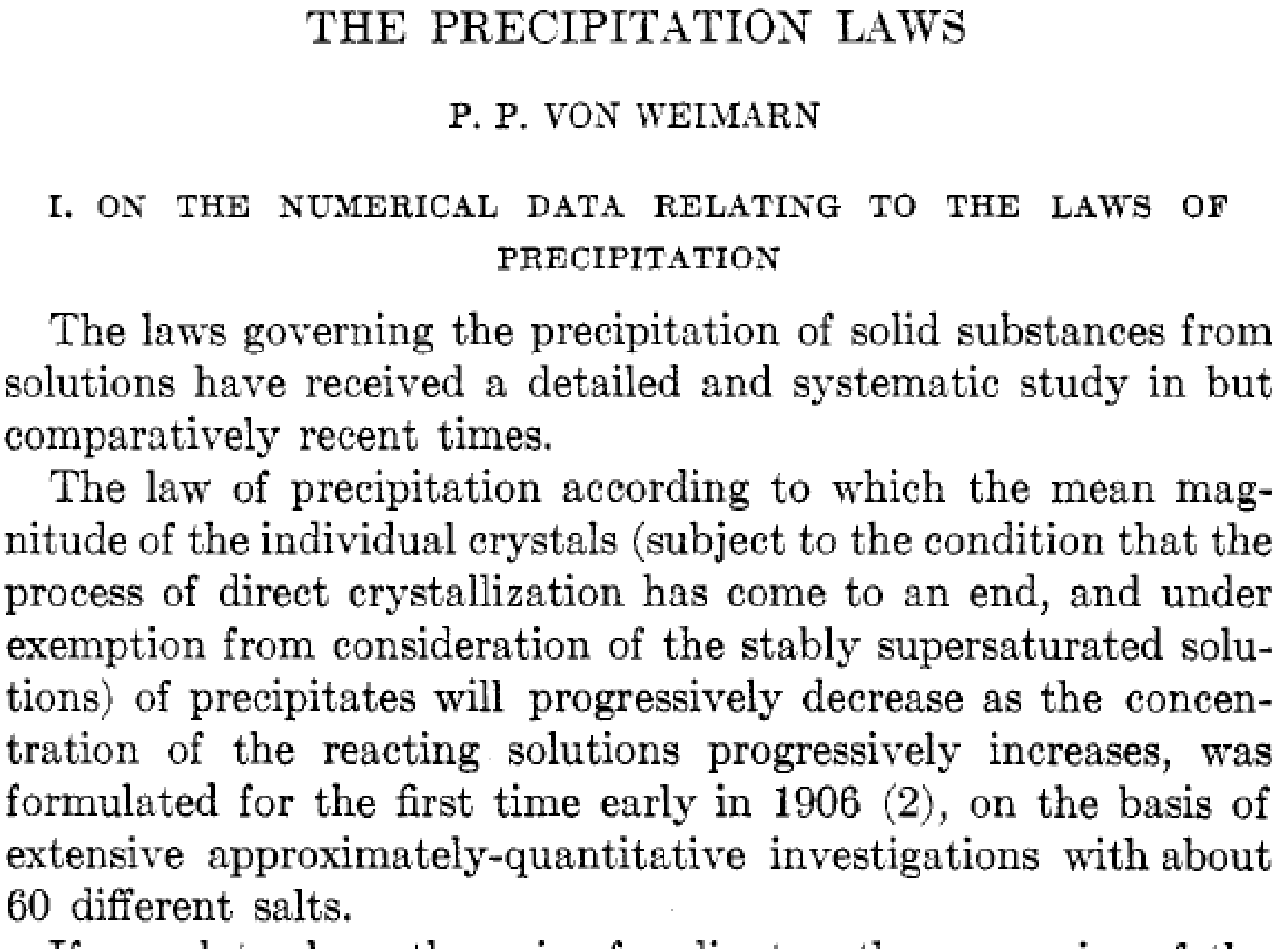

THE PRECIPITATION LAWS

P. P. VON WEIMARN

I. ON THE NUMERICAL DATA RELATING TO THE LAWS OF PRECIPITATION

The laws governing the precipitation of solid substances from solutions have received a detailed and systematic study in but comparatively recent times.

The law of precipitation according to which the mean magnitude of the individual crystals (subject to the condition that the process of direct crystallization has come to an end, and under exemption from consideration of the stably supersaturated solutions) of precipitates will progressively decrease as the concentration of the reacting solutions progressively increases, was formulated for the first time early in 1906 (2), on the basis of extensive approximately-quantitative investigations with about 60 different salts.

Chem. Rev. 1925, 217–242

https://doi.org/10.1021/cr60006a002

$$\Delta G = \Delta G_i + \Delta G_s = -\frac{(4/3)\pi a^3}{V_m} RT \ln \frac{C_s}{C_0} + 4\pi a^2 \gamma$$

Energy

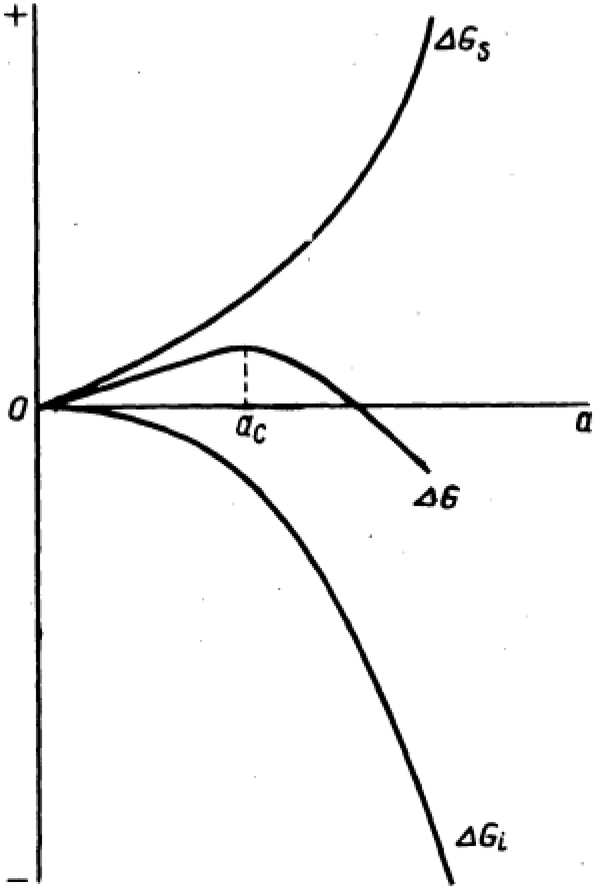

Energy of nucleation

particle size

General recommendations:

Optimal conditions for obtaining a colloidal system: low solubility and high supersaturation

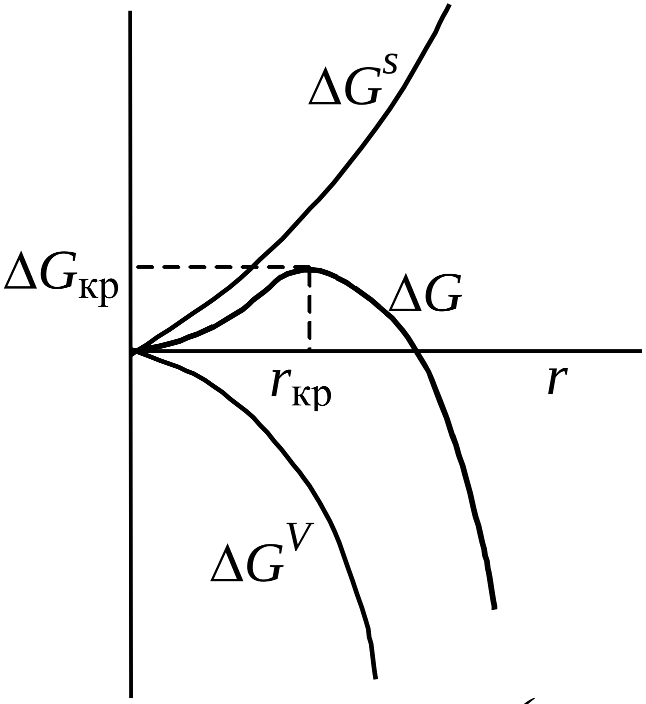

$$\Delta G = \frac{4\pi r^3(\mu_i^{liq} - \mu_i^{vap})}{3V_M} + 4\pi r^2\sigma$$

Let us find the extremum:

$$\left(\frac{\partial \Delta G}{\partial r}\right)_{extr} = 4\pi r_{crit}^2 \frac{\mu^{liq} - \mu^{vap}}{V_M} + 8\pi r_{crit}\sigma = 0$$

↓

$$\mu_i^{liq} - \mu_i^{vap} = -\frac{2\sigma V_M}{r_{crit}}$$

←

$$\ln\gamma_{crit} = \ln(p / p_0) = \frac{2\sigma V_M}{r_{crit}RT}$$

$$\Delta G_{crit} = -\frac{4}{3}\pi r_{crit}^2 \frac{2\sigma V_M}{r_{crit} V_M} + 4\pi r_{crit}^2 \sigma = 4\pi r_{crit}^2 (\sigma - \frac{2}{3}\sigma)$$

$$\boxed{\Delta G_{crit} = \frac{1}{3}\sigma s_{crit}}$$

$$\Delta G_{crit} = (4/3)\pi r_{crit}^2 \sigma$$

$$r_{crit} = \frac{2\sigma V_M}{RT \ln \gamma_{crit}}$$

$$\boxed{\Delta G_{crit} = \frac{16\pi \sigma^3 V_M^2}{3R^2 T^2 (\ln \gamma_{crit})^2}}$$

Condensation methods of synthesis of dispersed systems

Physical condensation

A molecular solution of a compound in an organic solvent

A small volume is poured into
a larger volume of water

Colloidal solution in water

In such way, hydrosols of P, S, Se, rosin (mixture of resinous substances, mainly acids $C_{19}H_{29}COOH$), mastic, gamboges, palmitic acid, parafin, antracene, cholesterol.

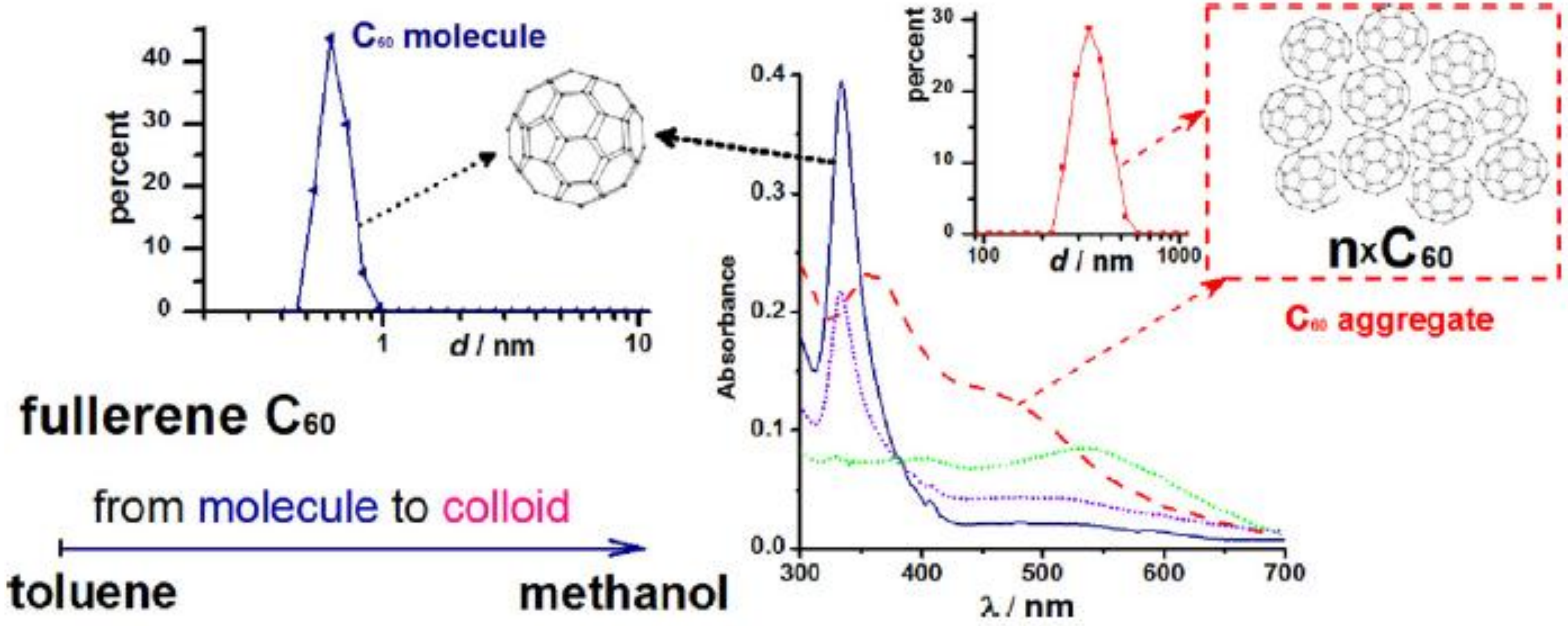

Colloids and Surfaces A: Physicochem. Eng. Aspects 509 (2016) 631–637

Contents lists available at ScienceDirect

Colloids and Surfaces A: Physicochemical and Engineering Aspects

journal homepage: www.elsevier.com/locate/colsurfa

The peculiar behavior of fullerene C_{60} in mixtures of ‘good’ and polar solvents: Colloidal particles in the toluene–methanol mixtures and some other systems

N.O. Mchedlov-Petrossyan[a,*], N.N. Kamneva[a], Y.T.M. Al-Shuuchi[a], A.I. Marynin[b], S.V. Shekhovtsov[a]

The data obey the Volmer’s principle:

The lower the solubility is,
the smaller the colloidal species appear

In 99 vol. % methanol, the size of C_{60} colloidal particles is 200 nm; increase of toluene content up to 30 % (70 % methanol) the size rises up to 500 nm.

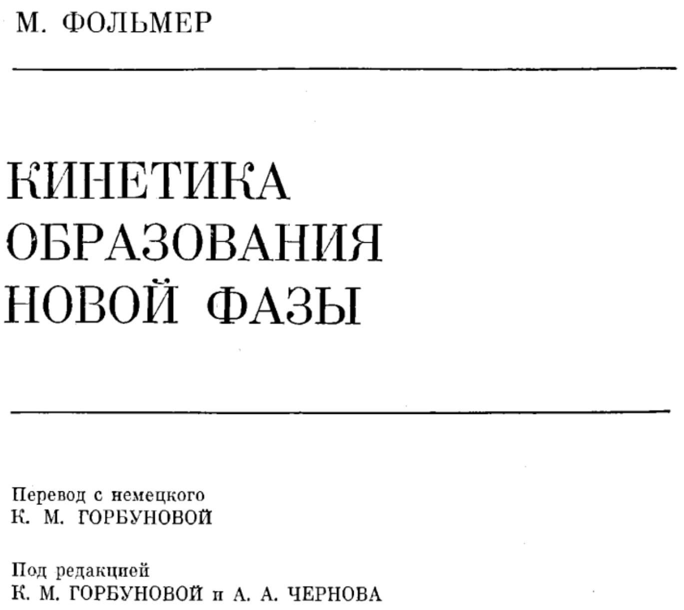

М. ФОЛЬМЕР

КИНЕТИКА
ОБРАЗОВАНИЯ
НОВОЙ ФАЗЫ

Перевод с немецкого
К. М. ГОРБУНОВОЙ

Под редакцией
К. М. ГОРБУНОВОЙ и А. А. ЧЕРНОВА

Chemical methods of synthesis of hydrosols

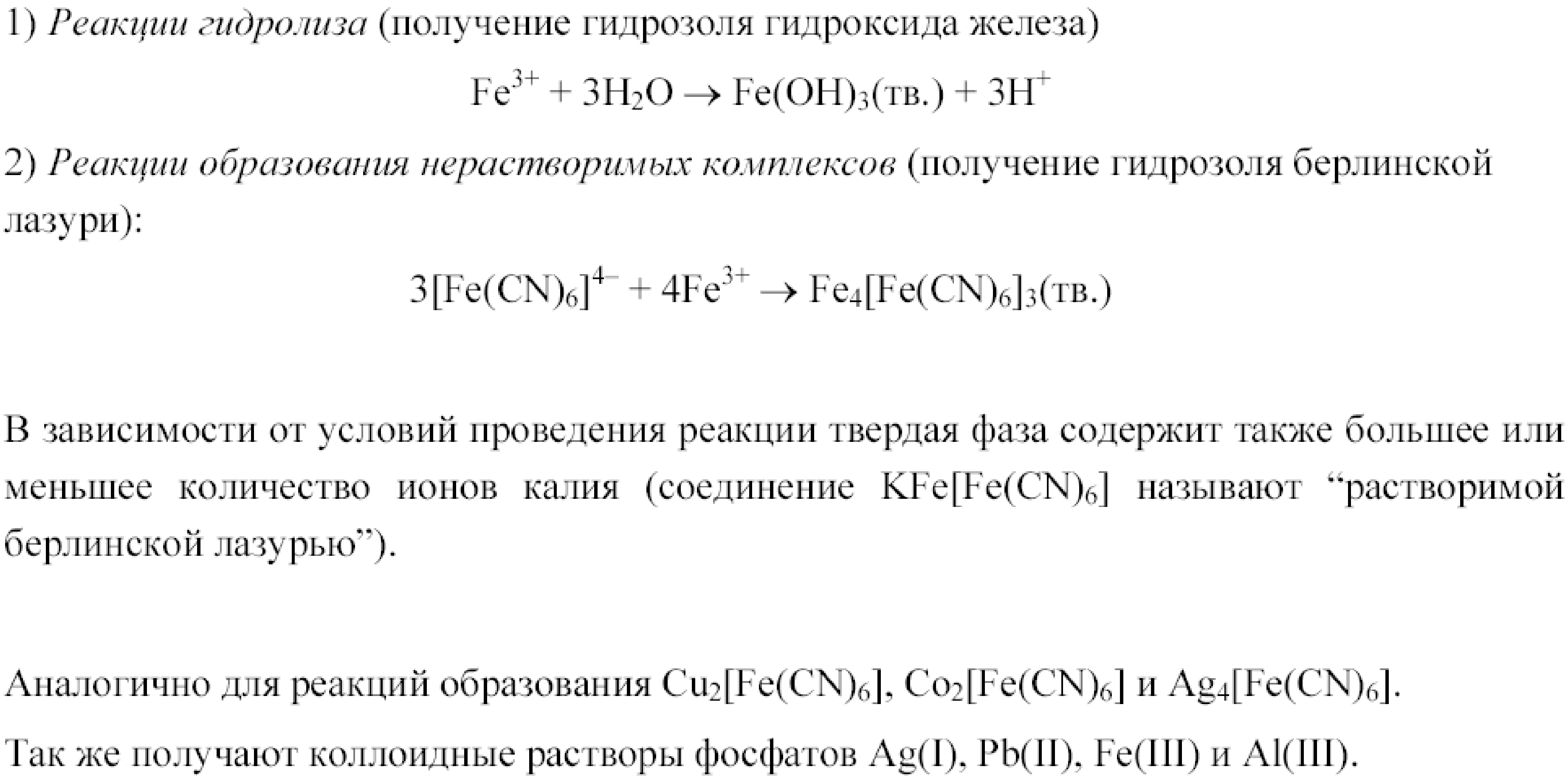

1) *Реакции гидролиза* (получение гидрозоля гидроксида железа)

$$Fe^{3+} + 3H_2O \rightarrow Fe(OH)_3(\text{тв.}) + 3H^+$$

2) *Реакции образования нерастворимых комплексов* (получение гидрозоля берлинской лазури):

$$3[Fe(CN)_6]^{4-} + 4Fe^{3+} \rightarrow Fe_4[Fe(CN)_6]_3(\text{тв.})$$

В зависимости от условий проведения реакции твердая фаза содержит также большее или меньшее количество ионов калия (соединение $KFe[Fe(CN)_6]$ называют “растворимой берлинской лазурью”).

Аналогично для реакций образования $Cu_2[Fe(CN)_6]$, $Co_2[Fe(CN)_6]$ и $Ag_4[Fe(CN)_6]$.

Так же получают коллоидные растворы фосфатов Ag(I), Pb(II), Fe(III) и Al(III).

3) *Реакции обмена* (получение гидрозоля сульфида мышьяка):

$$As_2O_3 + 3H_2S \rightarrow As_2S_3(\text{тв.}) + 3H_2O$$

4) *Реакции образования малорастворимых солей* (получение гидрозоля йодида серебра):

$$Ag^+ + I^- \rightarrow AgI\ (\text{тв.})$$

(Аналогичные уравнения можно записать для реакций образования AgBr и AgCl).

5) *Реакции образования малорастворимых кислот* (получение гидрозоля поликремниевой кислоты):

$$nSiO_3^{2-} + 2nH^+ \rightarrow (H_2SiO_3)_n(\text{тв.})$$

Эту реакцию можно, например, провести путем приливания серной кислоты к раствору силиката натрия.

6) *Редокс-реакции.* К ним относятся разные способы получения гидрозоля серы:

$$2H_2S + O_2 \rightarrow 2S(\text{тв.}) + 2H_2O$$

$$2H_2S + SO_2 \rightarrow 3S(\text{тв.}) + 2H_2O$$

$$3SO_3^{2-} + 4H^+ \rightarrow 4S(\text{тв.}) + 2HSO_4^- + H_2O$$

$$5H_2S + H_2S_5O_6 \rightarrow 10S + 6H_2O$$

Восстановлением селенистой кислоты гидразином или диоксидом серы можно получить гидрозоль селена:

$$H_2SeO_3 + N_2H_4 \rightarrow Se(\text{тв.}) + 3H_2O + N_2$$

$$H_2SeO_3 + 2SO_2 \rightarrow Se(\text{тв.}) + 2SO_3 + H_2O$$

Существует несколько способов получения гидрозоля золота из соединений золота (III). Обычно последние сначала переводят в аурат:

$$[AuCl_4]^- + 2CO_3^{2-} \rightarrow AuO_2^- + 2CO_2 + 4Cl^-$$

и затем добавляют формальдегид:

$$2AuO_2^- + 3HCHO + CO_3^{2-} \rightarrow 2Au(\text{тв.}) + 3HCO_2^- + HCO_3^- + H_2O$$

Возможно также восстановление аурата с помощью танина; восстановитель при этом окисляется до флобафена:

$$2AuO_2^- + 2H^+ + C_{76}H_{52}O_{46} \rightarrow 2Au(\text{тв.}) + H_2O + C_{76}H_{52}O_{49}$$

(Восстановлением иона Ag^+ танином можно получить и золь серебра). Другой вариант восстановление пероксидом водорода:

$$2[AuCl_4]^- + 3H_2O_2 \rightarrow 2Au(\text{тв.}) + 6H^+ + 8Cl^- + 3O_2$$

Ультрафиолетовое облучение оказывает сильное влияние на ход этой и других реакций получения гидрозоля Au.

Как восстановитель может применяться фосфор:

$$[AuCl_4]^- + 3H_2O + P \rightarrow Au(тв.) + H_3PO_4 + 4Cl^- + 3H^+$$

Фосфор можно вводить в систему в виде эфирного раствора; так в середине XIX века получал гидрозоли золота Фарадей.

Гидрозоли металлов можно также получить восстановлением осадков оксидов:

$$Ag_2O(тв.) + H_2 \rightarrow 2Ag\ (тв.) + H_2O$$

Редокс-реакции применяются и для получения гидрозолей оксидов металлов:

$$8H^+ + 6S_2O_3^{2-} + 2MnO_4^- \rightarrow 2MnO_2(тв.) + 3S_4O_6^{2-} + 4H_2O$$

Micelles as nano-reactors

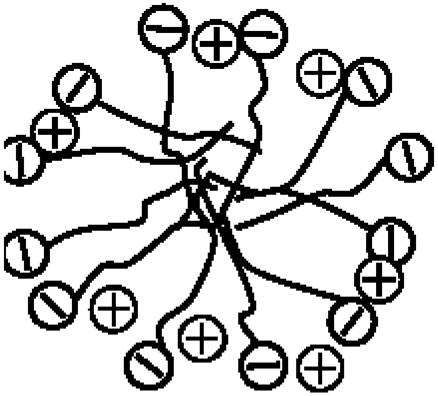

All the aforesaid chemical reactions may be conducted in the surfactant micelles.

The limited volume ensures formation of nanosized particles of metals, poorly soluble salts, etc.

Photochemical reduction of metal salts to metal sols is of special interest.

A method of synthesis of mesoporous molecular sieves (widely used as catalysts)

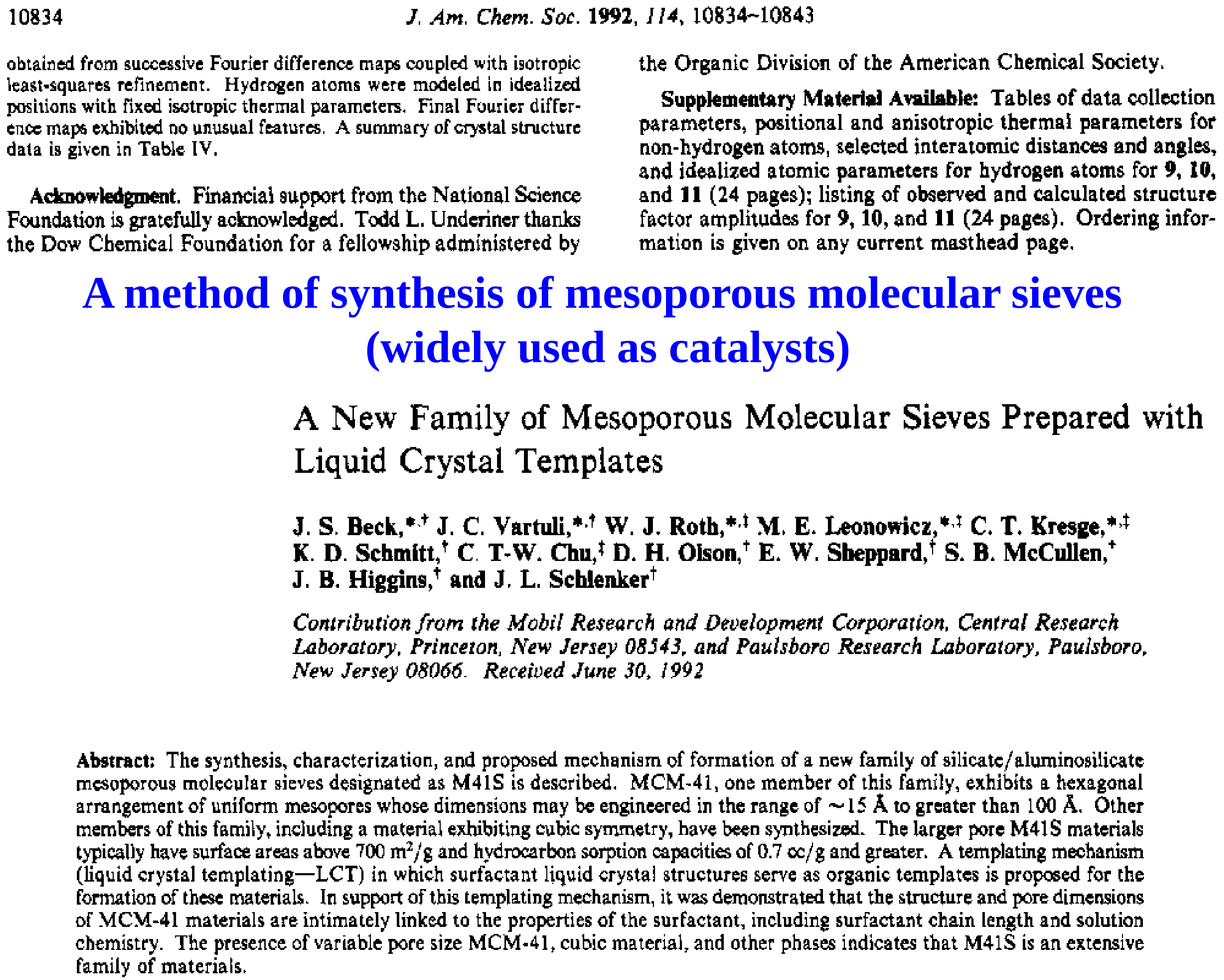

10834 J. Am. Chem. Soc. 1992, 114, 10834–10843

obtained from successive Fourier difference maps coupled with isotropic least-squares refinement. Hydrogen atoms were modeled in idealized positions with fixed isotropic thermal parameters. Final Fourier difference maps exhibited no unusual features. A summary of crystal structure data is given in Table IV.

Acknowledgment. Financial support from the National Science Foundation is gratefully acknowledged. Todd L. Underiner thanks the Dow Chemical Foundation for a fellowship administered by the Organic Division of the American Chemical Society.

Supplementary Material Available: Tables of data collection parameters, positional and anisotropic thermal parameters for non-hydrogen atoms, selected interatomic distances and angles, and idealized atomic parameters for hydrogen atoms for **9**, **10**, and **11** (24 pages); listing of observed and calculated structure factor amplitudes for **9**, **10**, and **11** (24 pages). Ordering information is given on any current masthead page.

A New Family of Mesoporous Molecular Sieves Prepared with Liquid Crystal Templates

J. S. Beck,[*,†] J. C. Vartuli,[*,†] W. J. Roth,[*,†] M. E. Leonowicz,[*,‡] C. T. Kresge,[*,‡] K. D. Schmitt,[†] C. T-W. Chu,[‡] D. H. Olson,[†] E. W. Sheppard,[†] S. B. McCullen,[†] J. B. Higgins,[†] and J. L. Schlenker[†]

Contribution from the Mobil Research and Development Corporation, Central Research Laboratory, Princeton, New Jersey 08543, and Paulsboro Research Laboratory, Paulsboro, New Jersey 08066. *Received June 30, 1992*

Abstract: The synthesis, characterization, and proposed mechanism of formation of a new family of silicate/aluminosilicate mesoporous molecular sieves designated as M41S is described. MCM-41, one member of this family, exhibits a hexagonal arrangement of uniform mesopores whose dimensions may be engineered in the range of ~15 Å to greater than 100 Å. Other members of this family, including a material exhibiting cubic symmetry, have been synthesized. The larger pore M41S materials typically have surface areas above 700 m^2/g and hydrocarbon sorption capacities of 0.7 cc/g and greater. A templating mechanism (liquid crystal templating—LCT) in which surfactant liquid crystal structures serve as organic templates is proposed for the formation of these materials. In support of this templating mechanism, it was demonstrated that the structure and pore dimensions of MCM-41 materials are intimately linked to the properties of the surfactant, including surfactant chain length and solution chemistry. The presence of variable pore size MCM-41, cubic material, and other phases indicates that M41S is an extensive family of materials.

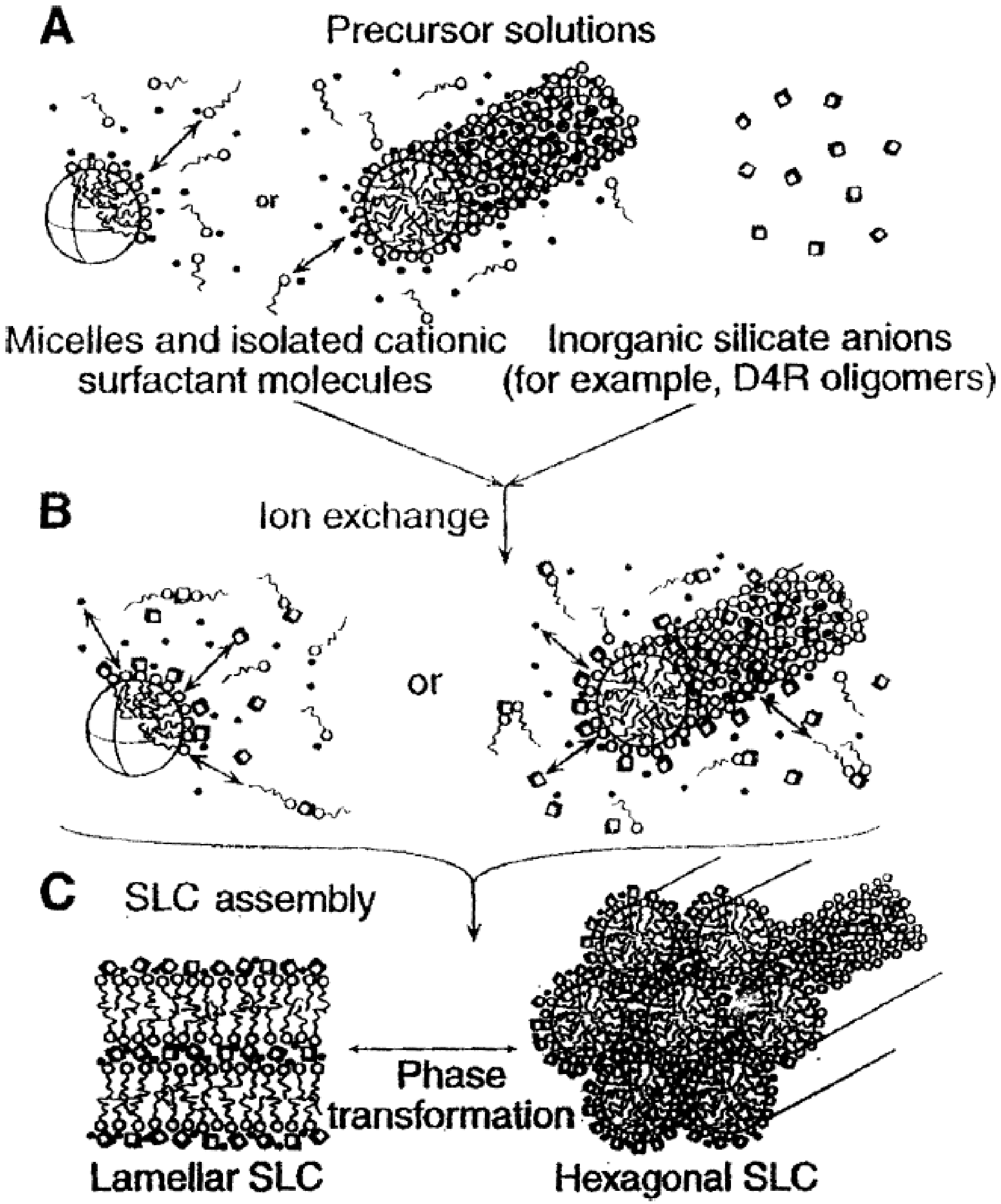
A
Precursor solutions
or
Micelles and isolated cationic surfactant molecules
Inorganic silicate anions (for example, D4R oligomers)
B
Ion exchange
or
C
SLC assembly
Phase transformation
Lamellar SLC
Hexagonal SLC

Common chemical reactions used for preparation of colloids may be performed within “**water pools**” in reversed micelles (or microemulsions).

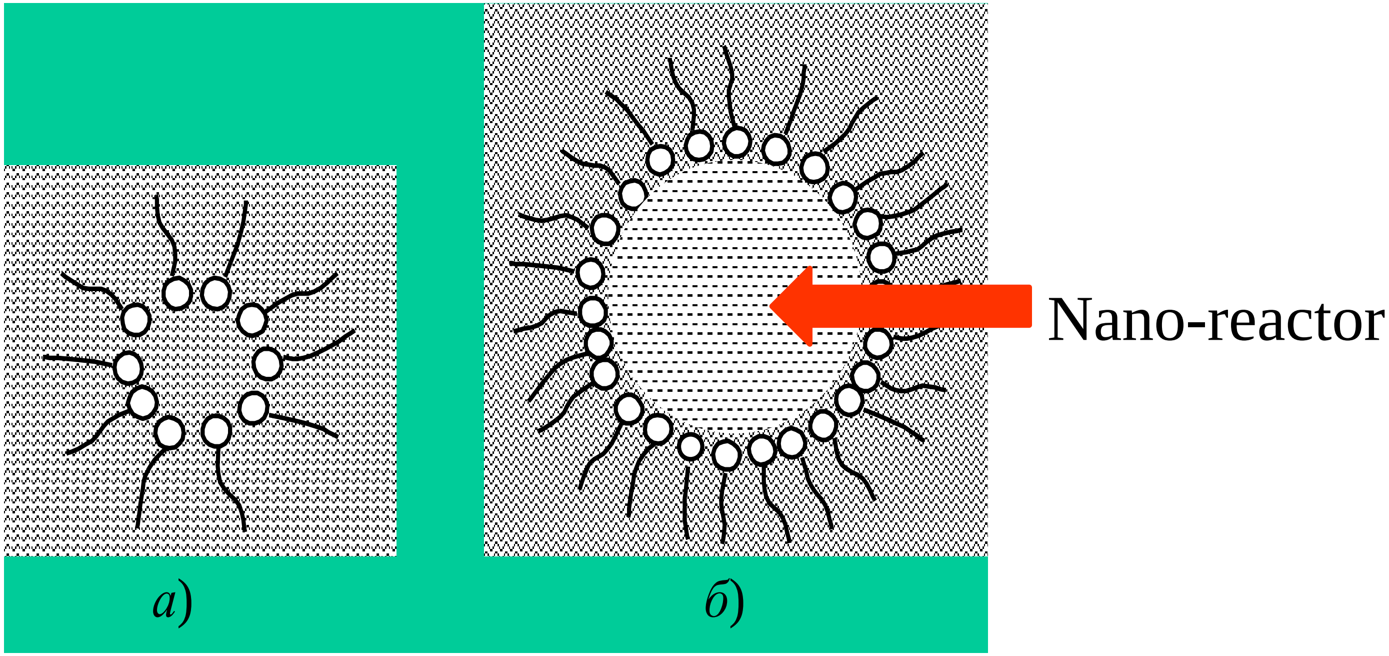

This ensures nanometric size of solid phase thus formed. For example:

$$Si(OC_2H_5)_4 + 2H_2O \rightarrow SiO_2(solid) + 4C_2H_5OH$$

Gamma-radiolysis and the synthesis of sub-colloidal species

Гамма-радиолиз проводится с помощью “кобальтовой пушки” (^{60}Co):

“Cobalt cannon”

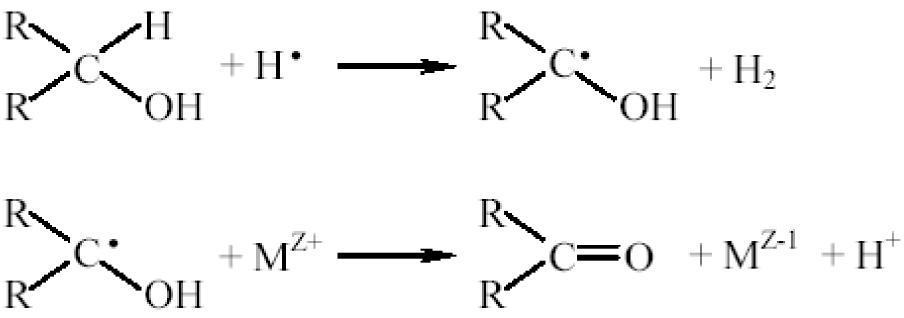

и далее, вплоть до образования электронейтральных атомов металлов.

Импульсный радиолиз позволяет получить частицы серебра размером от 1 до 10 нм, палладия – от 1 до 4 нм, и так далее.

На разных стадиях образуются так называемые *субколлоидные* частицы, например, Ag_2^+, Ag_2, Ag_4^{2+}, Ag_4^+, и так далее – образования, промежуточные между ионами (или малыми группами атомов) и коллоидными частицами.

Main requirements for the synthesis of systems for nanotechnology:

The method should allow synthesizing practically **monodisperse** nanoparticles of **a given size**

STRUCTURE AND PROPERTIES OF COLLOIDAL PARTICLES OF DIFFERENT NATURE

Thomson-Kelvin effect
Solubility of solid nanoparticles:
Gibbs – Freundlich – Ostwald equation

$$\ln \frac{L}{L_s} = \pm \frac{\sigma V_M}{RT}\left(\frac{1}{r_1} + \frac{1}{r_2}\right)$$

“Ostwald’s ripening”
Dispersion and chemical reactivity

Why does this effect not lead to the dissolution of colloidal particles and the formation of a macrophase?

Metal nanoparticles

The origin of the majority of specific “nano” properties is the so-called **quantum effect:** the electrical, magnetic, optical, and other properties of the macroscopic body disappear. Instead, some new features are observed.

Colloidal nano-sized state of metals is sometimes called as the **fifth aggregate state**, in addition to solid, liquid, gas, and plasma.

Their properties are well-documented. One of the most interesting phenomenon is the so-called **plasmon resonance** (sols of Cu, Ag, Au).

Structure of a colloidal particle of a hydrophobic sole: Metal iodides

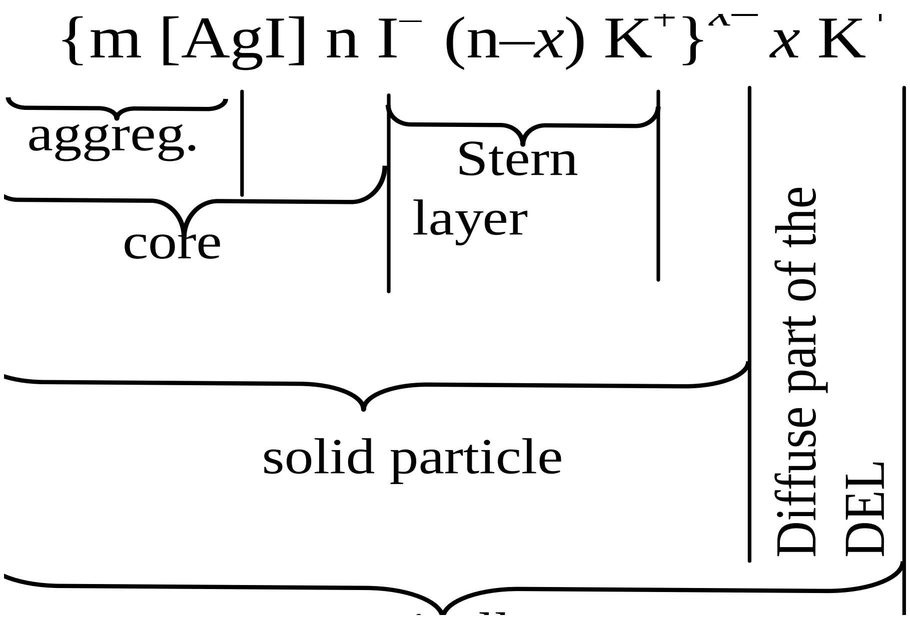

$\{m\,[AgI]\,n\,I^-\,(n-x)\,K^+\}^{x-}\,x\,K^+$

aggreg.

core

Stern layer

solid particle

Diffuse part of the DEL

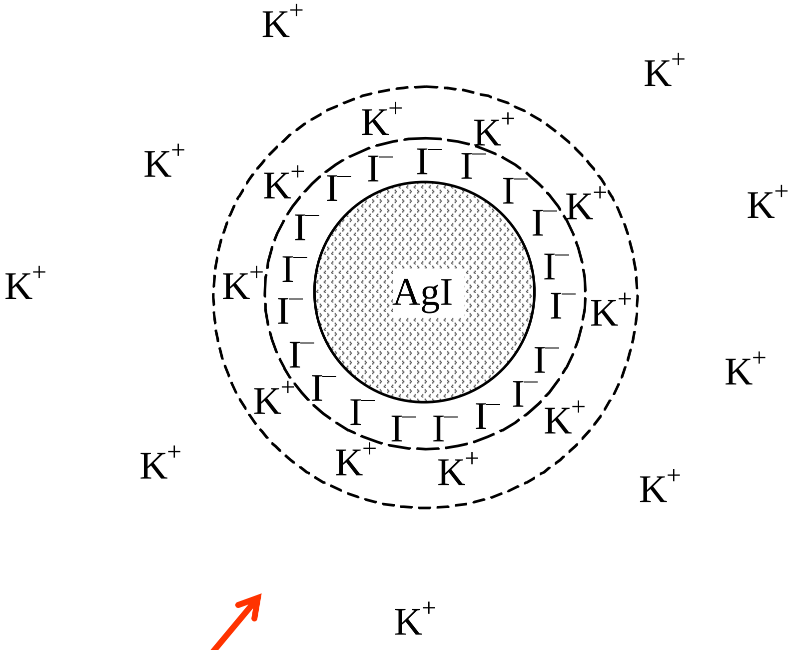

Micelle of a lyophobic sole

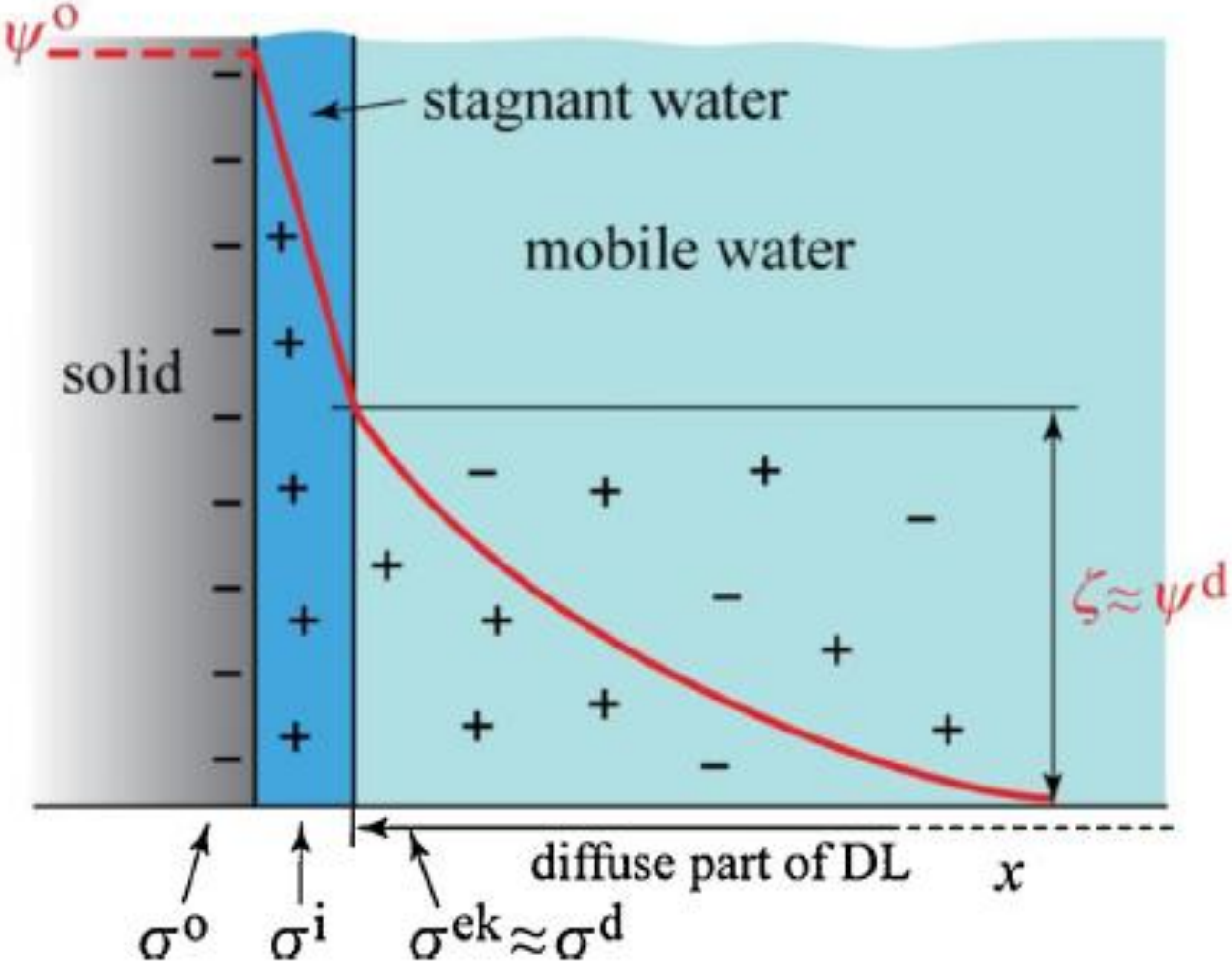

Fig. 1. Gouy–Stern picture of the electrical double layer.

J. Lyklema, 2014

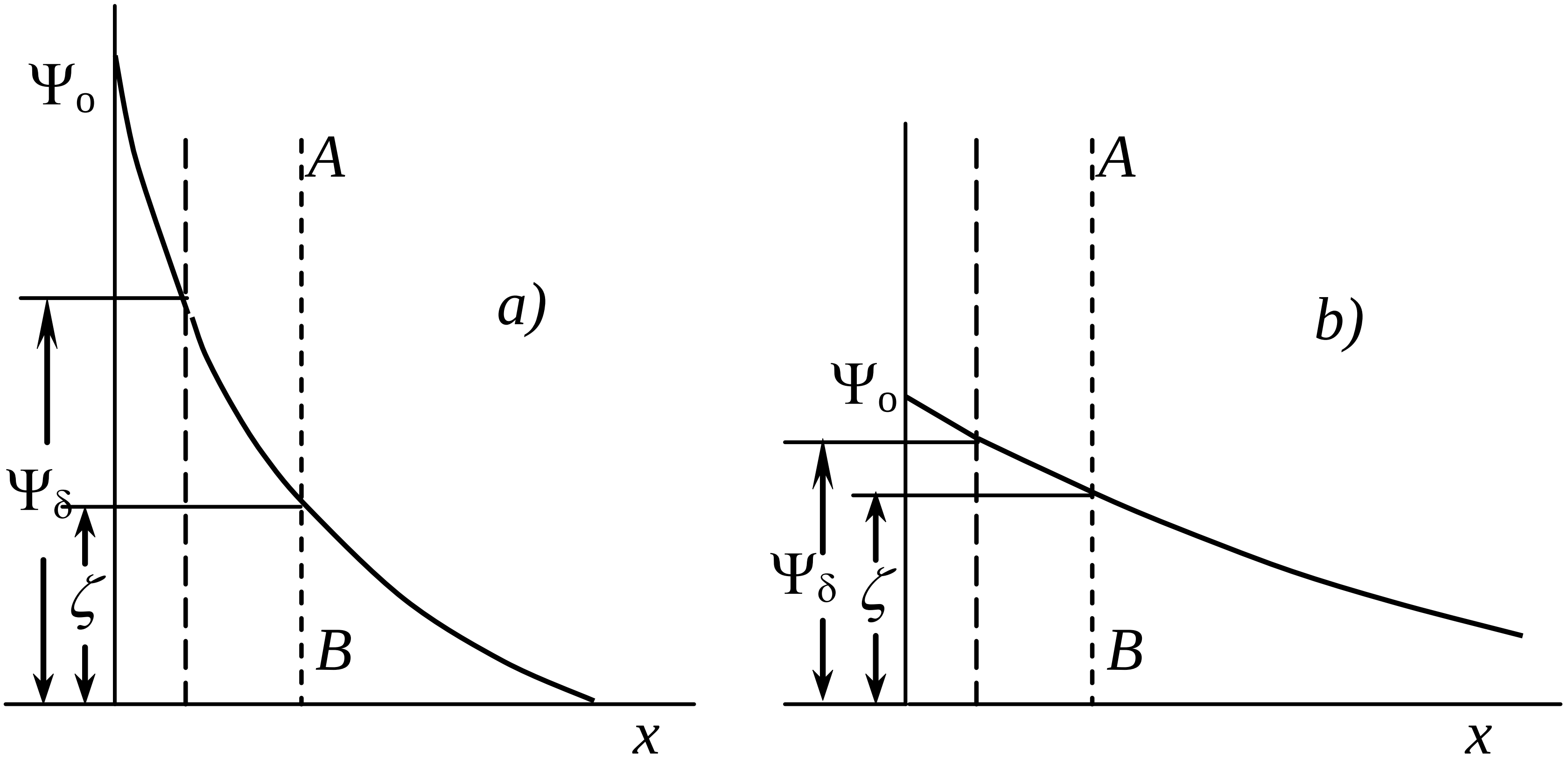

Correlation between Ψ_{δ} and ζ potentials:

For highly charged particles in concentrated enough electrolytic solution (*a*) and for low charged colloid particles in diluted solution of an electrolyte (b).

The influence of the ionic strength on the electrostatic and electrokinetic potentials

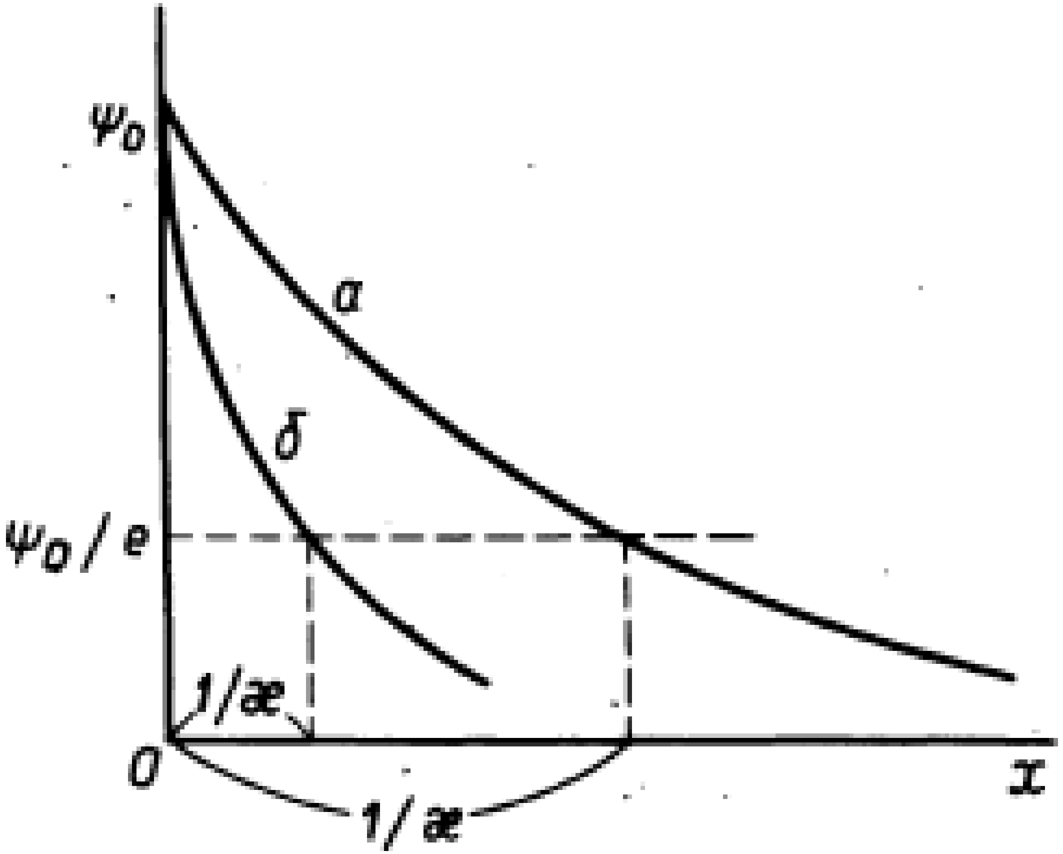

A universal method for stabilization of nanoparticles: adsorption of polymeric molecules

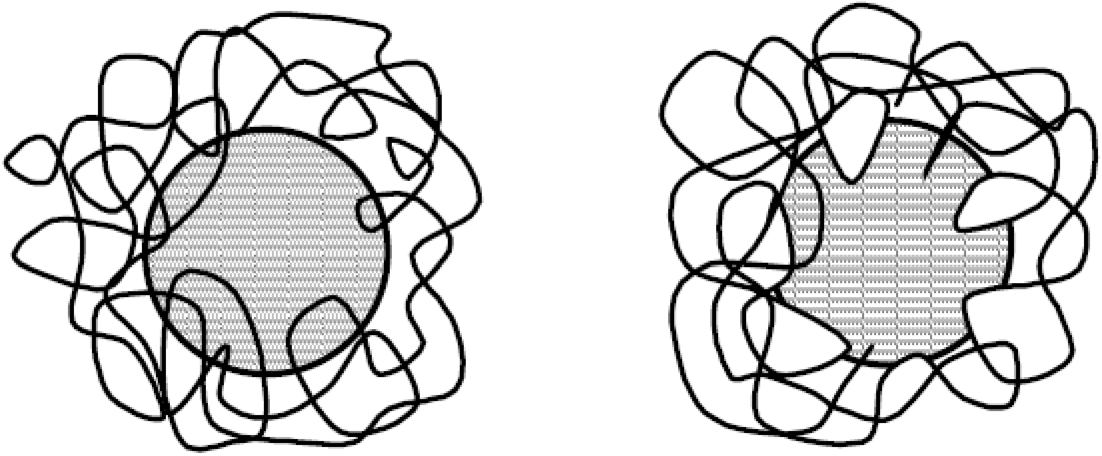

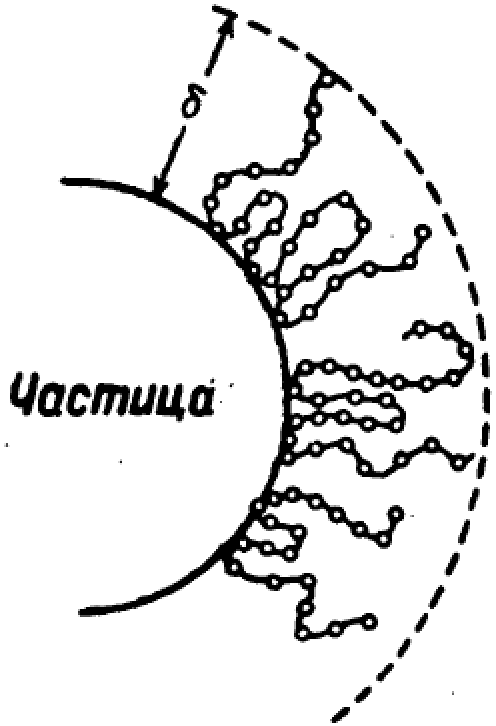
δ
Частица

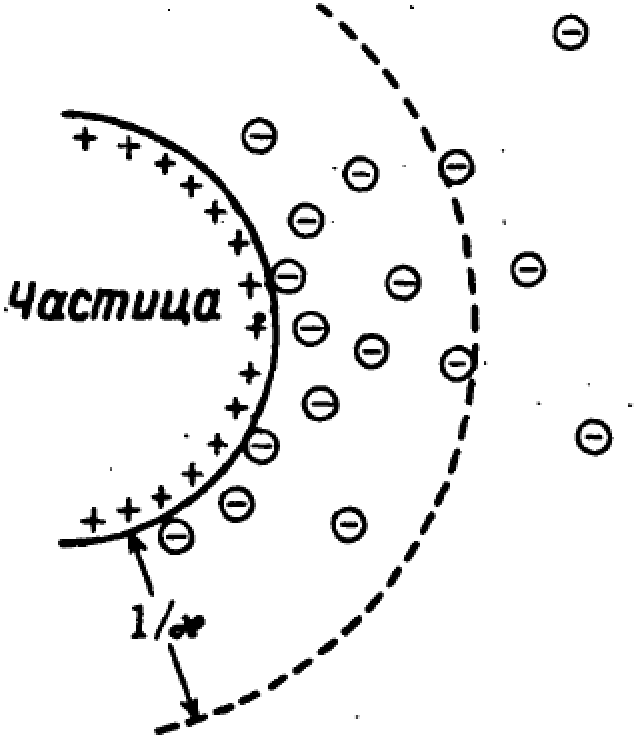
Частица
$1/\varkappa$

SiO_2 nanoparticles

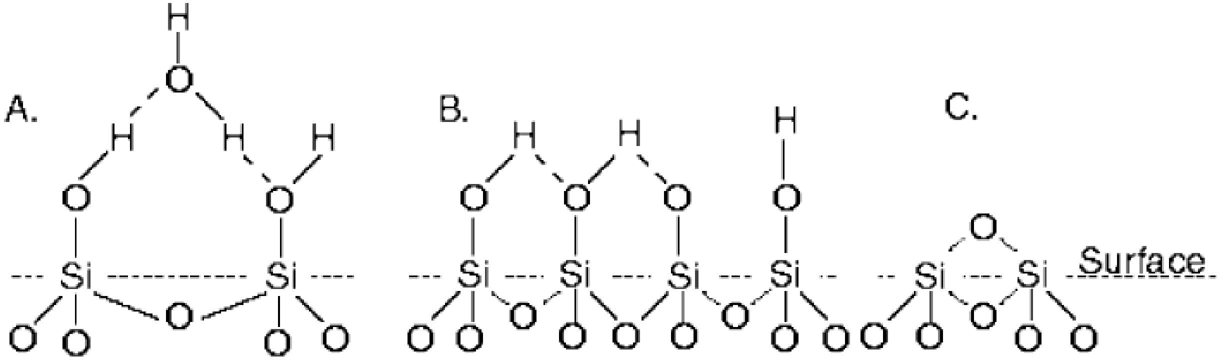

Fig. 1. Schematic representation of the types of functional groups that occur on the silica surface. (a) Hydrated and (b) anhydrous silanol groups are associated with the hydroxylated surface whereas (c) siloxane-dehydrated groups occur mainly on the pyrogenic surface. Redrawn after Ref. [5](a).

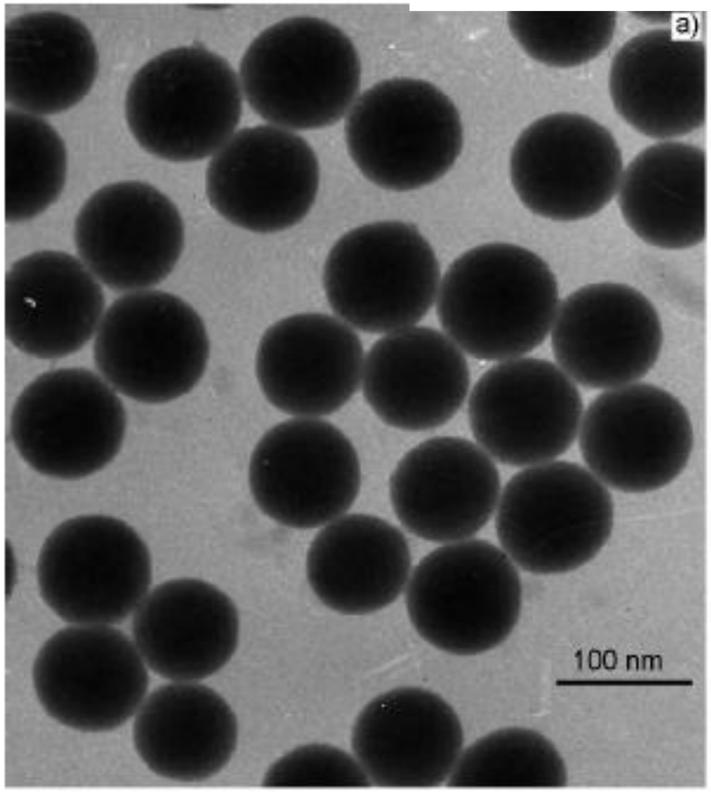

Низкий pH (кислотная область):

$$-\mathrm{Si}-OH + H^+ + OH^- \rightarrow -\mathrm{Si}-OH_2^+ + OH^-$$

(избыток) (положительный заряд)

Высокий pH (щелочная область):

$$-\mathrm{Si}-OH + H^+ + OH^- \rightarrow -\mathrm{Si}-O^- + H_2O + H^+$$

(избыток) (отрицательный заряд)

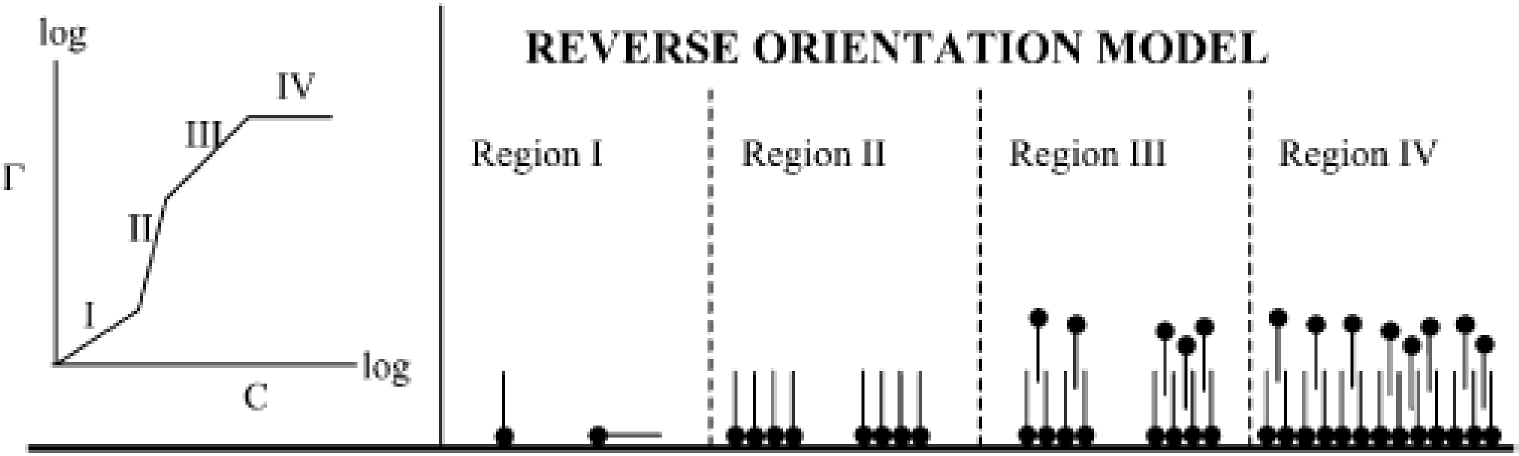

ELSEVIER

Advances in Colloid and Interface Science
103 (2003) 219–304

ADVANCES IN
COLLOID AND
INTERFACE
SCIENCE

www.elsevier.com/locate/cis

Mechanism of cationic surfactant adsorption at the solid–aqueous interface

R. Atkin[a], V.S.J. Craig[b], E.J. Wanless[c,*], S. Biggs[d]

SiO_2 + cationic surfactant: coagulation and overcharging

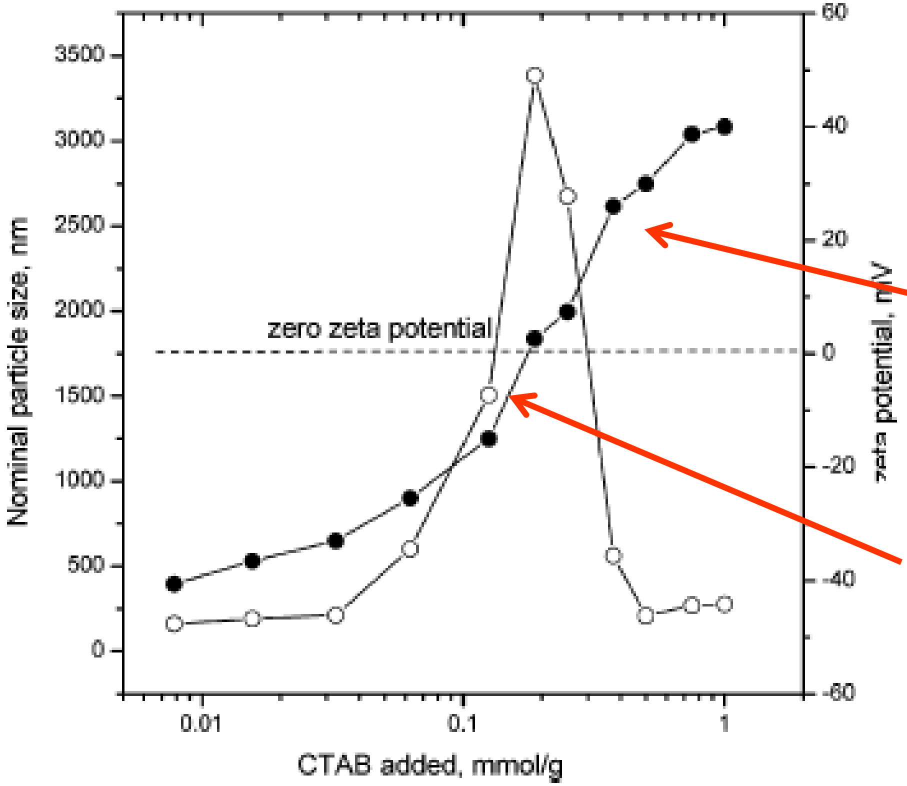

Figure 3. Effects of CTAB sorption on nominal colloidal particle sizes (open circle) and corresponding ζ potentials (solid circle) as determined by dynamic light scattering measurements. Silica colloid concentration is 0.5 wt %.

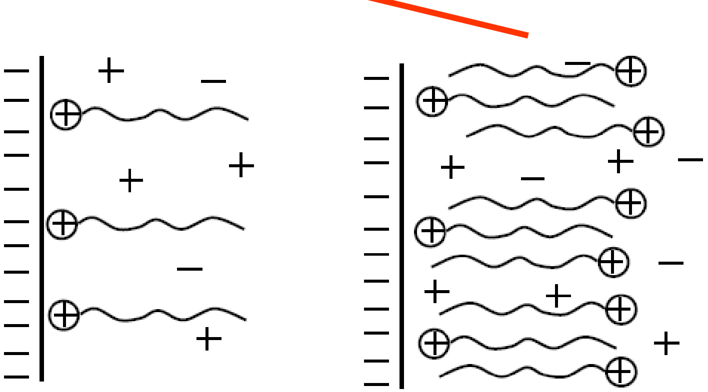

J. Phys. Chem. B **2004,** *108,* 17477−17483 174

Adsorption and Structural Arrangement of Cetyltrimethylammonium Cations at the Silica Nanoparticle−Water Interface

Wei Wang,*,† Baohua Gu,† Liyuan Liang,†,§ and William A. Hamilton‡

SiO_2 + cationic surfactant

Adsorption of CTAB on silica nanoparticles (d = 106 nm)

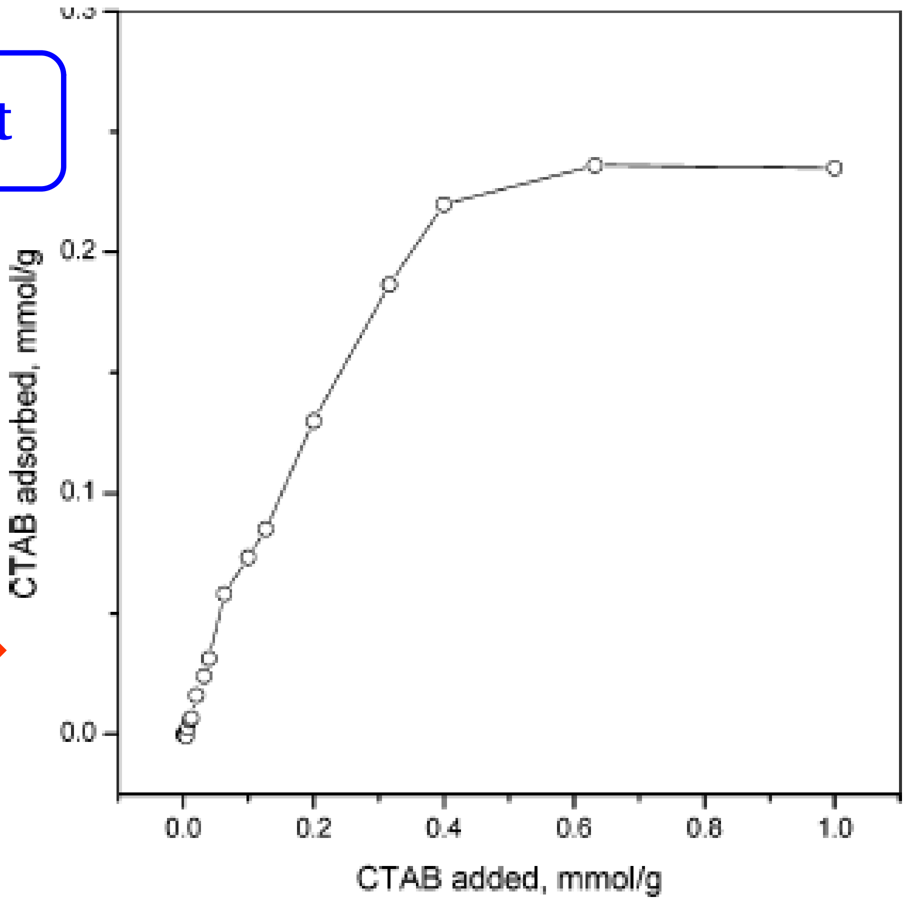

Figure 1. Adsorption of CTA^+ cations on SiO_2 nanoparticles (*d* = 106 nm) in deionized water at 23 °C.

J. Phys. Chem. B **2004,** *108,* 17477−17483 **174**

Adsorption and Structural Arrangement of Cetyltrimethylammonium Cations at the Silica Nanoparticle−Water Interface

Wei Wang,*,† Baohua Gu,† Liyuan Liang,†,§ and William A. Hamilton‡

SiO_2 + cationic surfactant
(our experiments)

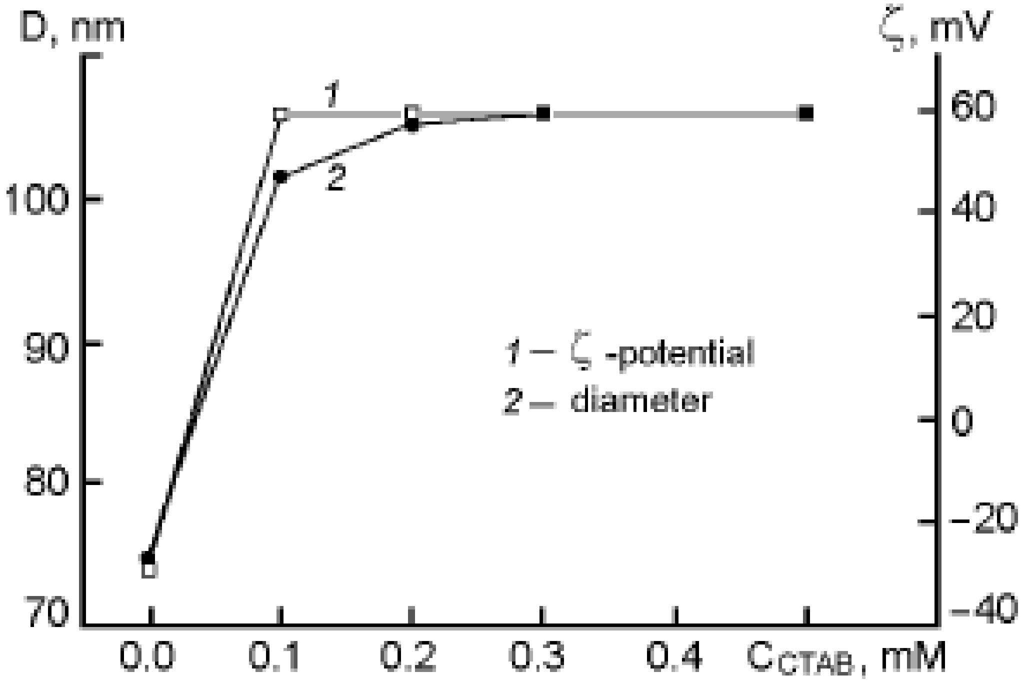

Fig. 2. The ζ-potential (*1*) and particle diameter (*2*) of silica vs CTAB concentration.

overcharging

Heteronanoparticles

SiO_2/Au (diameter 40 nm)

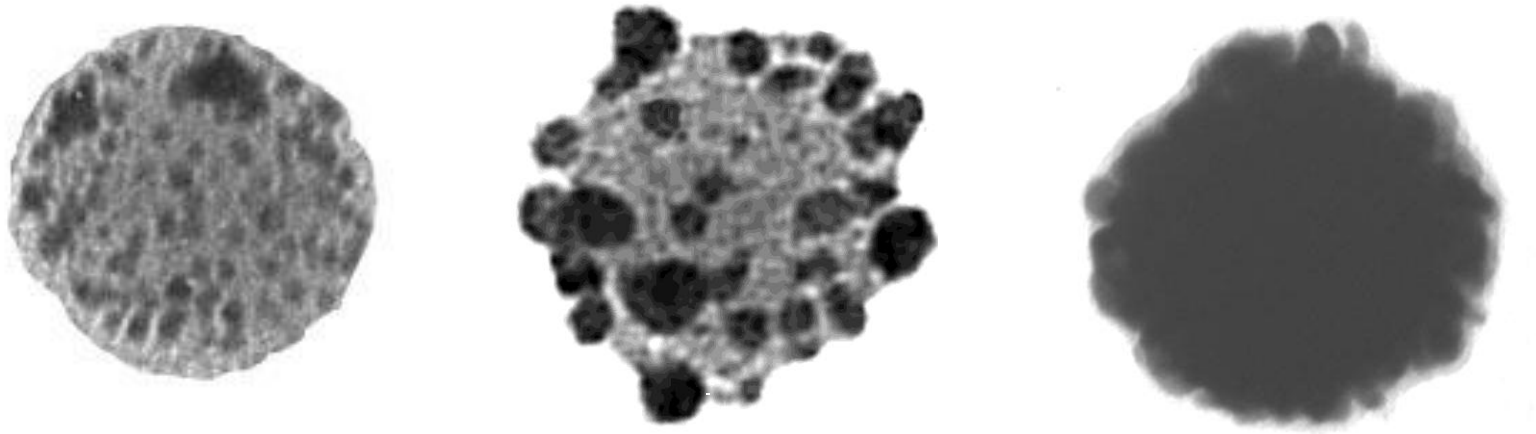

Separate Au clusters on the surface

Rise of Au clusters

A thick Au shell of 7 nm

TEM image of heteronanoparticles

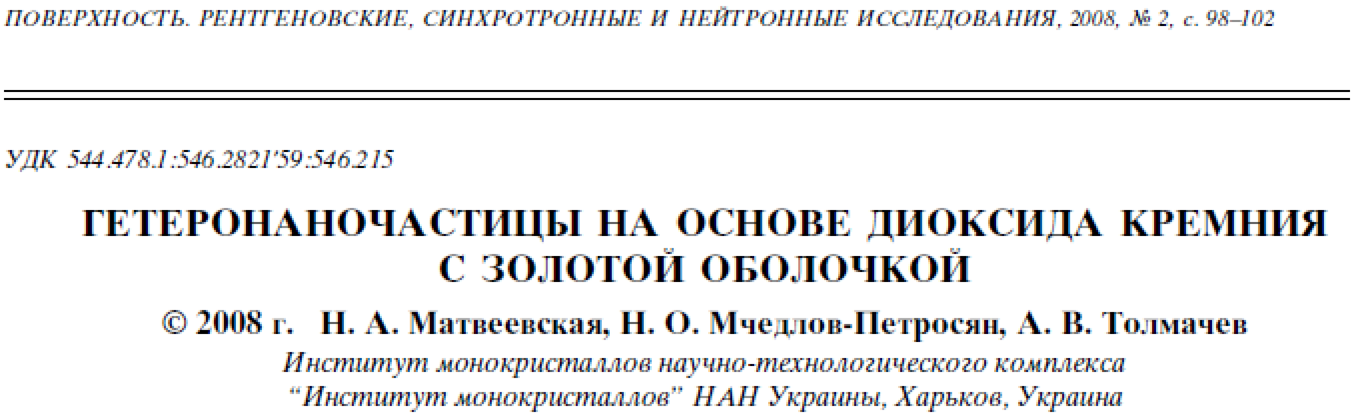

ПОВЕРХНОСТЬ. РЕНТГЕНОВСКИЕ, СИНХРОТРОННЫЕ И НЕЙТРОННЫЕ ИССЛЕДОВАНИЯ, 2008, № 2, с. 98–102

УДК 544.478.1:546.2821'59:546.215

ГЕТЕРОНАНОЧАСТИЦЫ НА ОСНОВЕ ДИОКСИДА КРЕМНИЯ С ЗОЛОТОЙ ОБОЛОЧКОЙ

© 2008 г. Н. А. Матвеевская, Н. О. Мчедлов-Петросян, А. В. Толмачев

Институт монокристаллов научно-технологического комплекса
"Институт монокристаллов" НАН Украины, Харьков, Украина

coagulation and overcharging

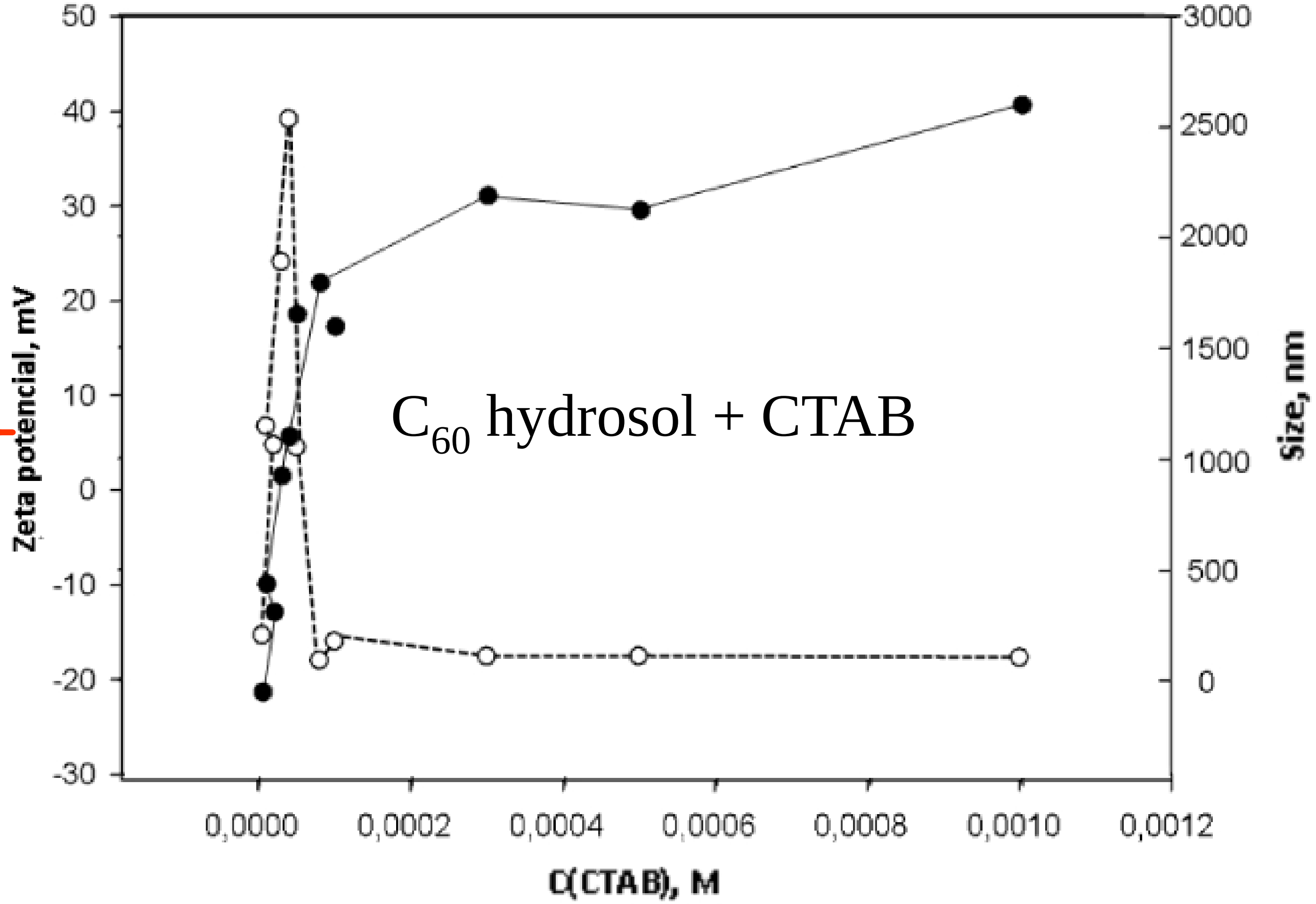

Dependence of the zeta potential and size values (full and empty circles, respectively) of the 1.94x10^{-5} M C$_{60}$ colloid on CTAB concentration. Measurements made within 4 min after preparation of each working solution.

coagulation
and
overcharging

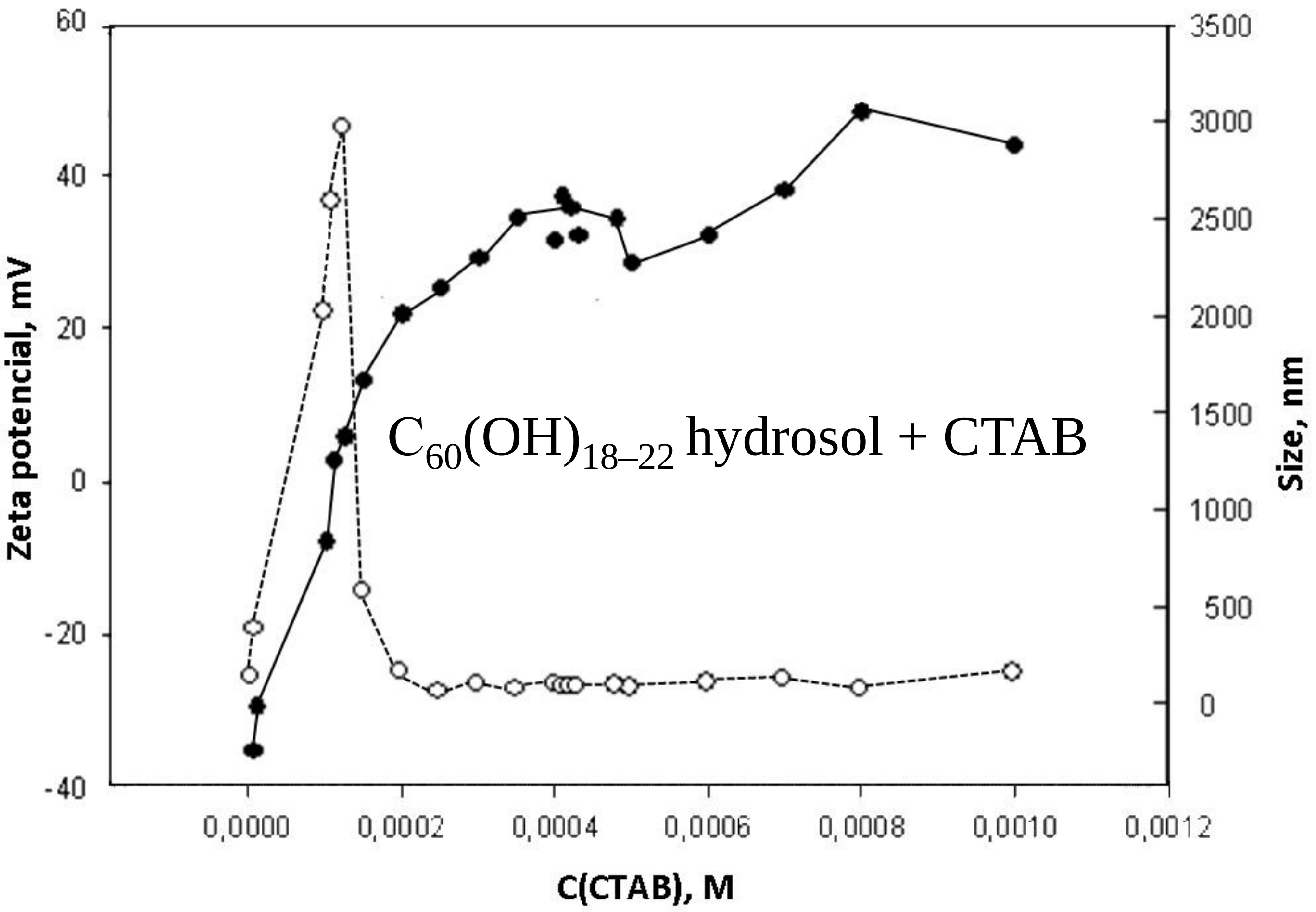

$C_{60}(OH)_{18–22}$ hydrosol + CTAB

$C_{60}(OH)_{18–22}$ (0.0114 g $dm^{–3}$) + cetyltrimethylammonium bromide

Colloidal particles with positive charge (e.g., metal oxides):

Interaction with anionic and cationic surfactants

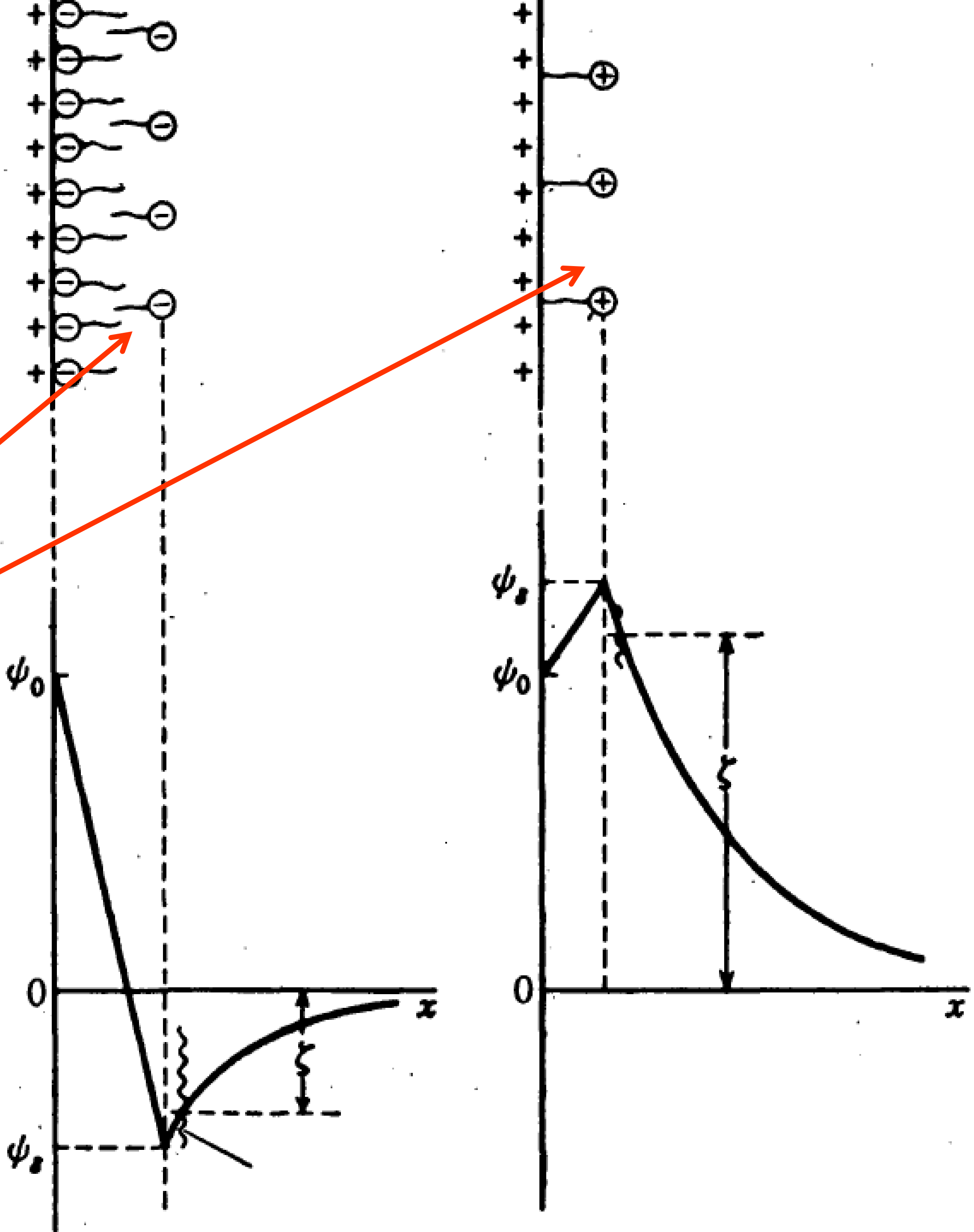

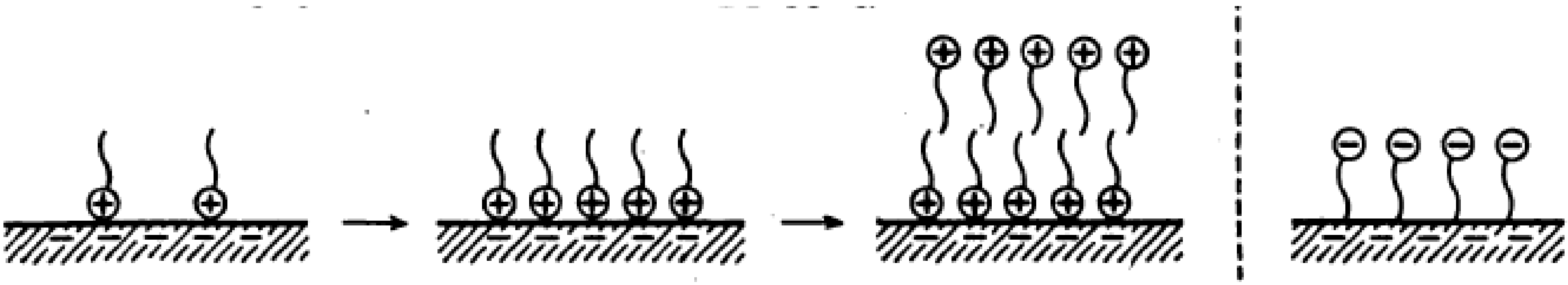

Overcharging of positively charged colloidal particles in water by anionic surfactants

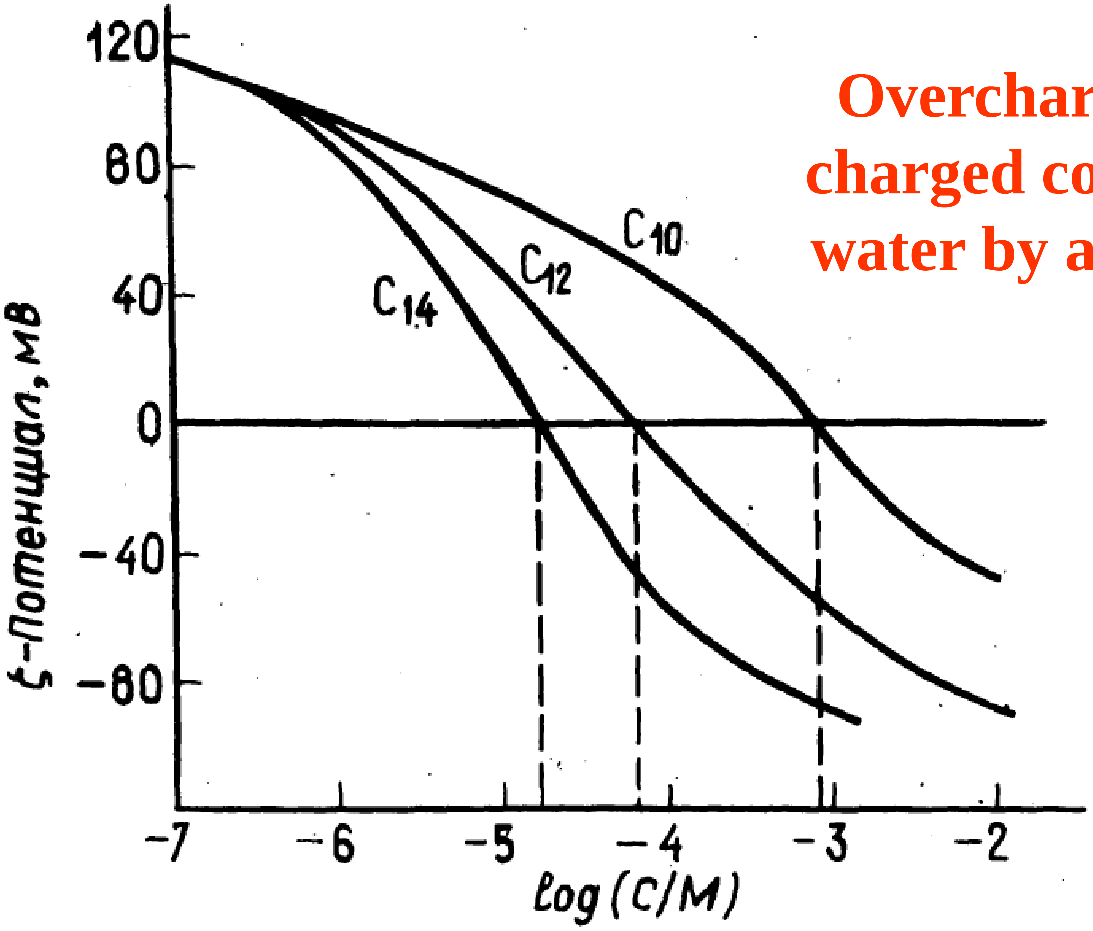

Рис. 6.28. Влияние анионогенных поверхностно-активных веществ на ζ-потенциал коллоидного раствора AgI
[*Ottewill R. H.*, *Watanabe A.*, Kolloid-Z., **170**, 132 (1960)].

C_{10}— натриевая соль децилсульфокислоты, C_{12} — натриевая соль додецилсульфокислоты; C_{14}— натриевая соль тетрадецилсульфокислоты.

TiO_2 colloidal particles in water

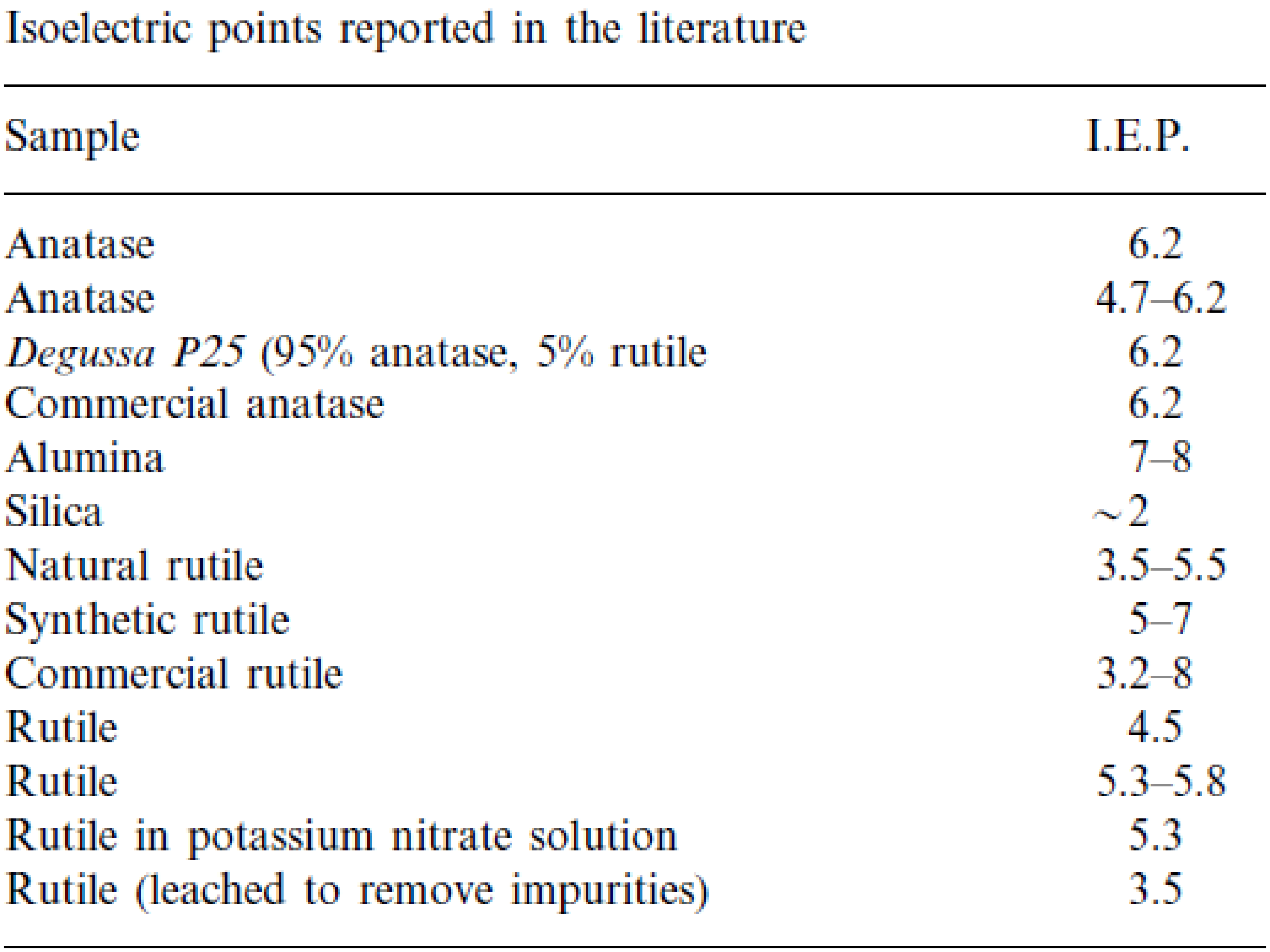

Isoelectric points reported in the literature

Sample	I.E.P.
Anatase	6.2
Anatase	4.7–6.2
Degussa P25 (95% anatase, 5% rutile	6.2
Commercial anatase	6.2
Alumina	7–8
Silica	~2
Natural rutile	3.5–5.5
Synthetic rutile	5–7
Commercial rutile	3.2–8
Rutile	4.5
Rutile	5.3–5.8
Rutile in potassium nitrate solution	5.3
Rutile (leached to remove impurities)	3.5

(Chadwick et al. 2002)

TiO_2 colloidal particles in water

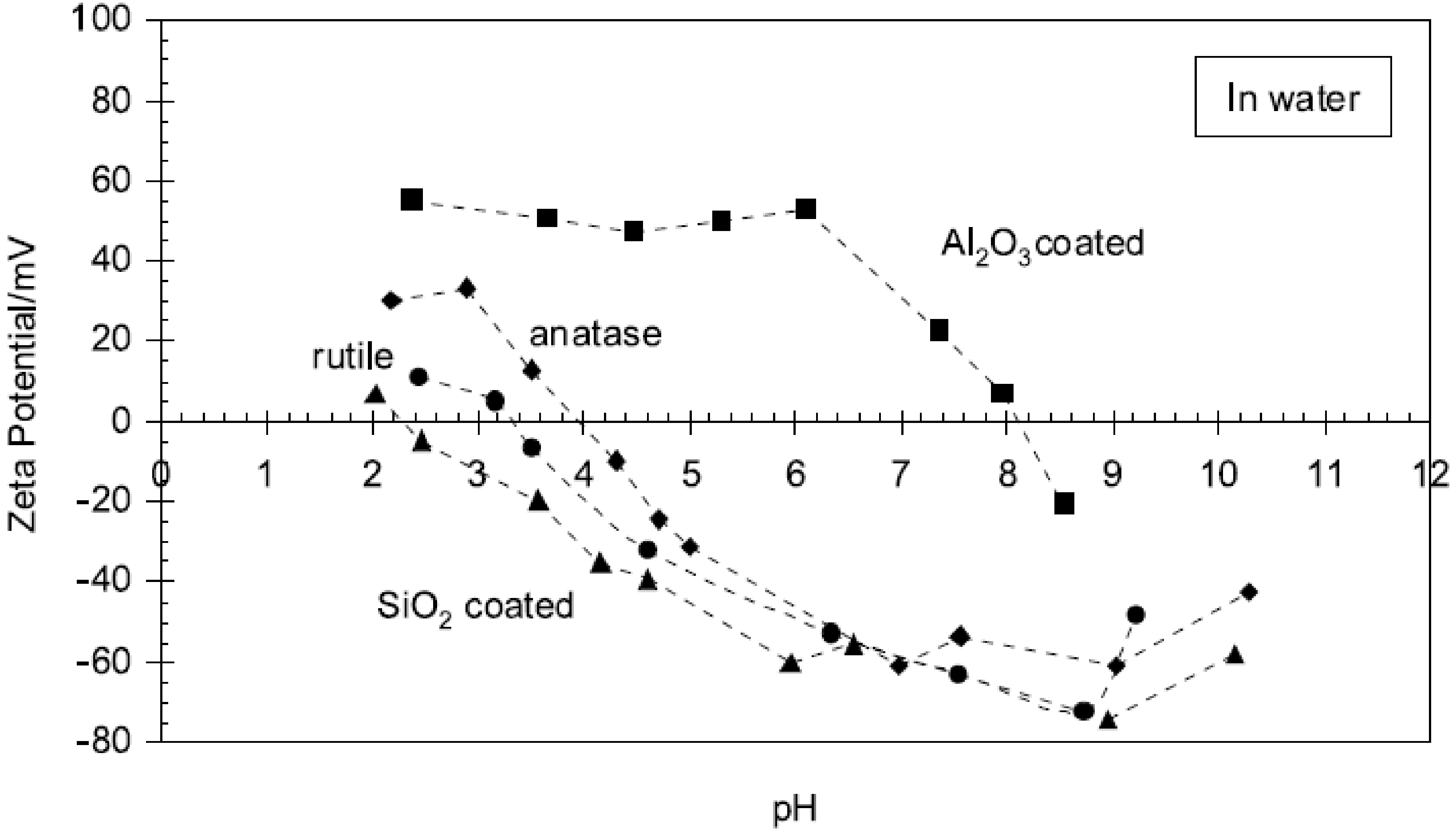

(Chadwick et al. 2002)

Nano-TiO_2 is the most popular nanoproduct !!

Oil micro- (or nano-) drops in water: negatively charged particles

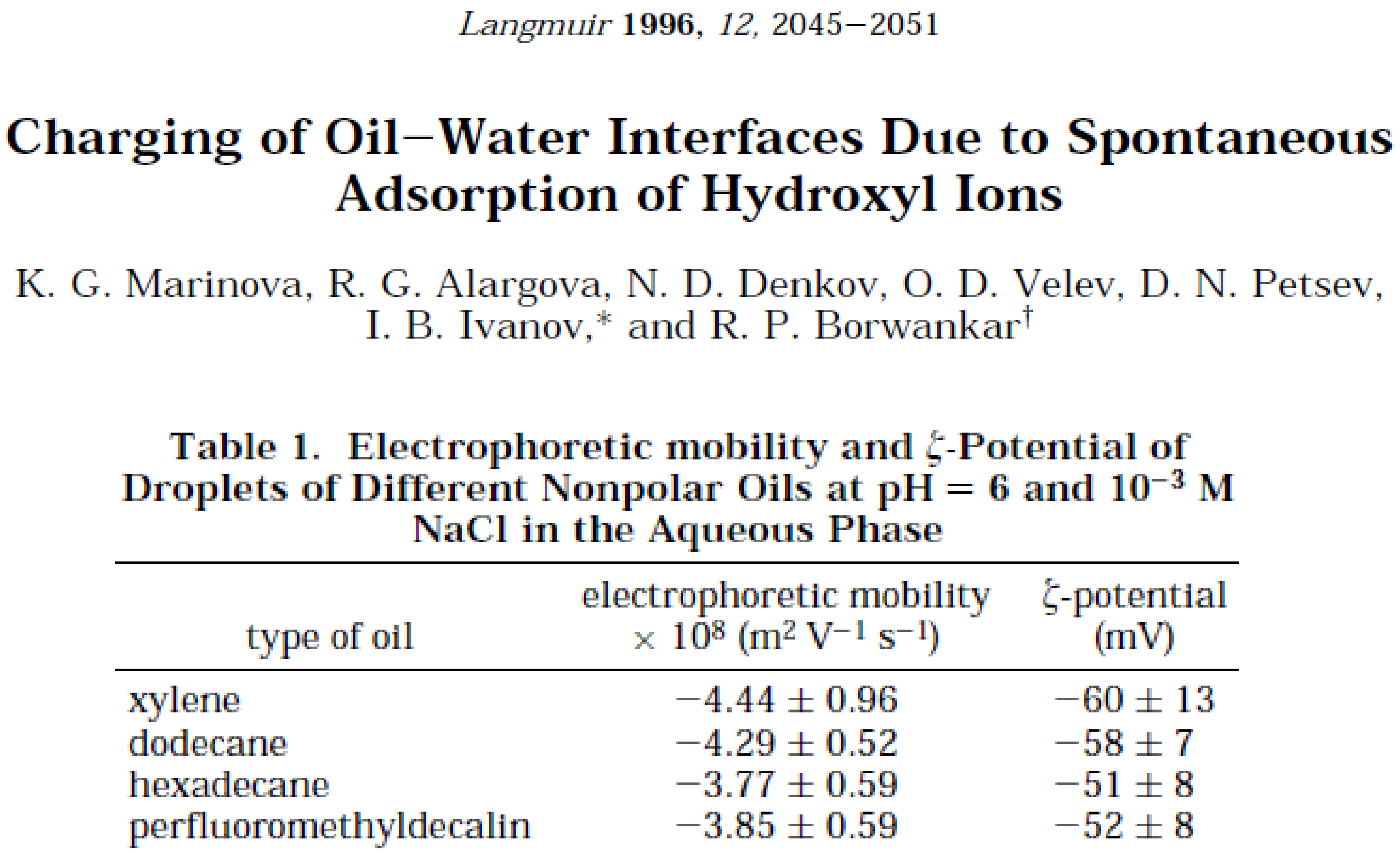

Langmuir **1996**, *12*, 2045–2051

Charging of Oil–Water Interfaces Due to Spontaneous Adsorption of Hydroxyl Ions

K. G. Marinova, R. G. Alargova, N. D. Denkov, O. D. Velev, D. N. Petsev,
I. B. Ivanov,* and R. P. Borwankar†

Table 1. Electrophoretic mobility and ζ-Potential of Droplets of Different Nonpolar Oils at pH = 6 and 10^{-3} M NaCl in the Aqueous Phase

type of oil	electrophoretic mobility $\times 10^8$ ($m^2\ V^{-1}\ s^{-1}$)	ζ-potential (mV)
xylene	-4.44 ± 0.96	-60 ± 13
dodecane	-4.29 ± 0.52	-58 ± 7
hexadecane	-3.77 ± 0.59	-51 ± 8
perfluoromethyldecalin	-3.85 ± 0.59	-52 ± 8

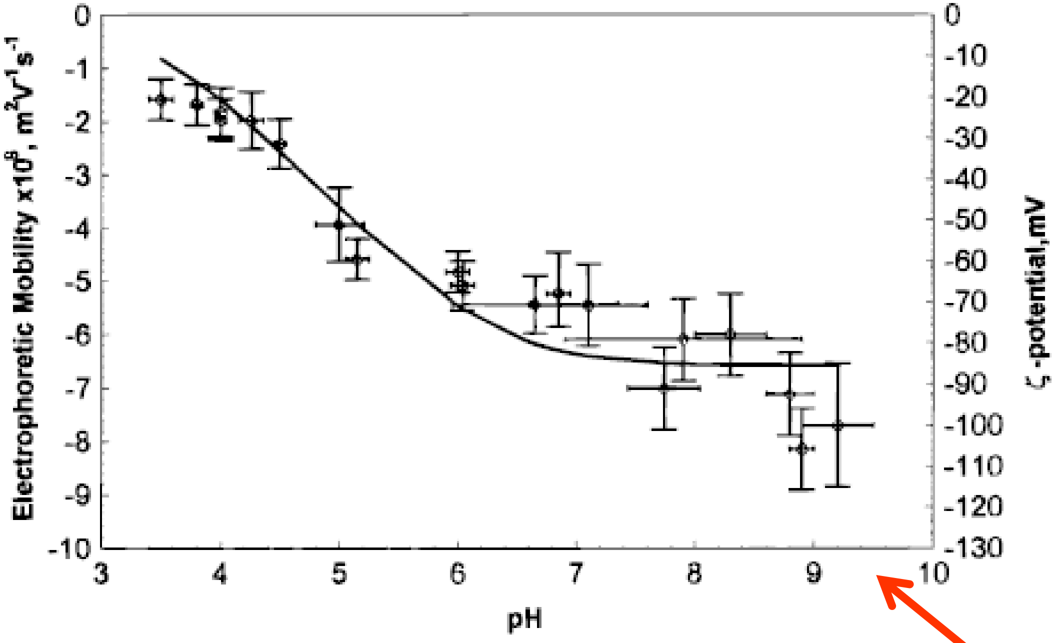

Oil in water: electrophoretic mobility and zeta-potential versus pH and ionic strength

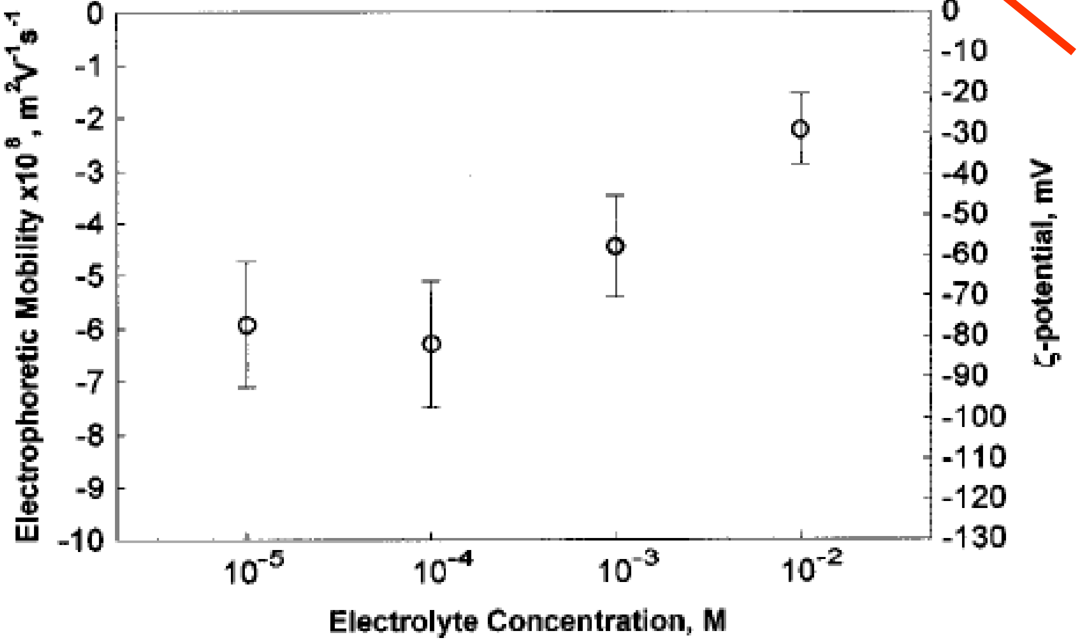

Dipolar water molecules around the oil surface

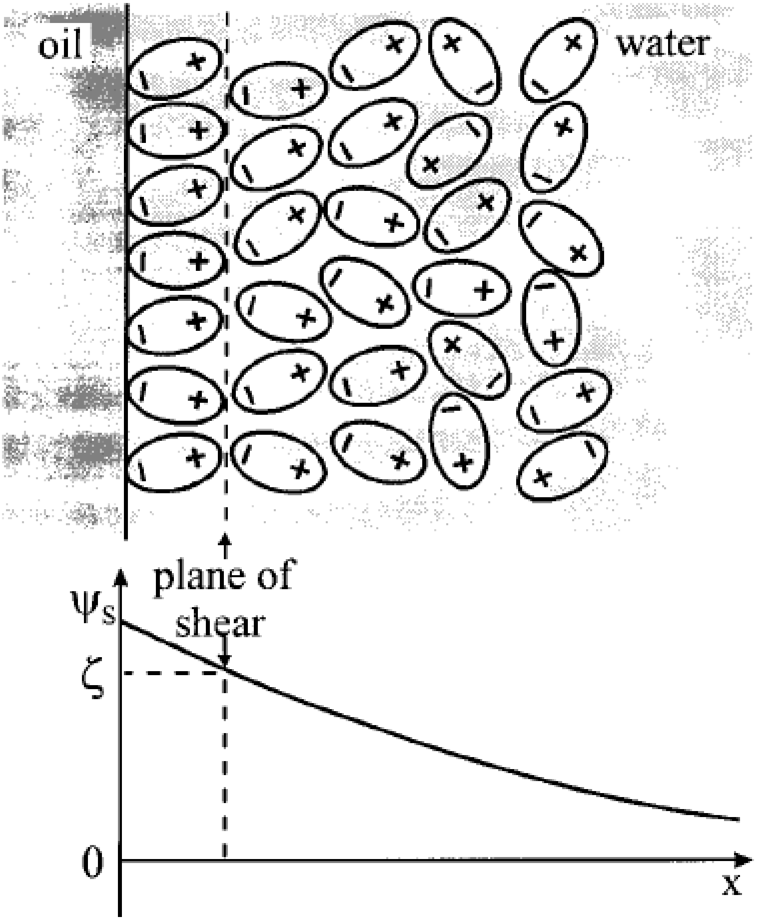

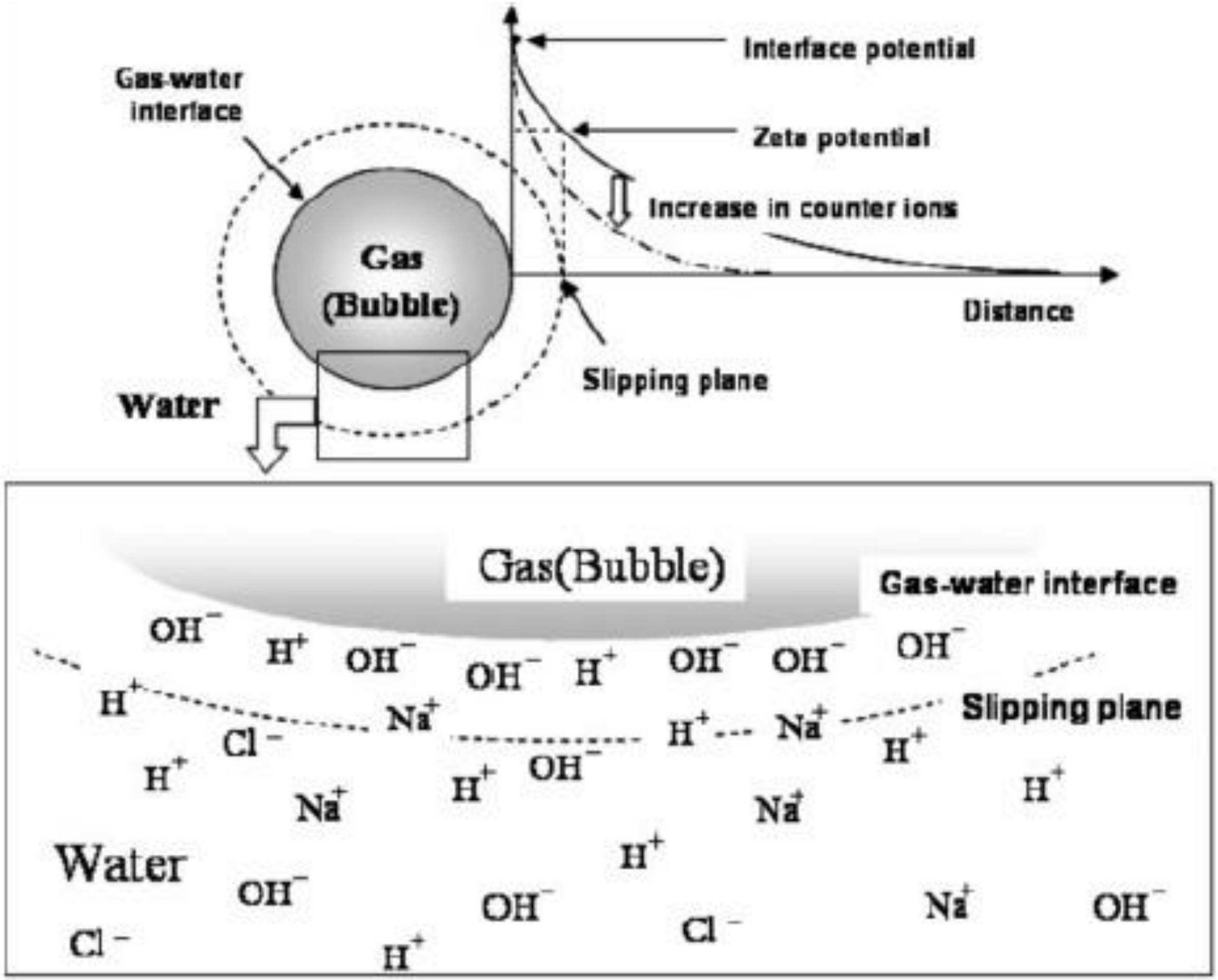

Takahashi, 2005

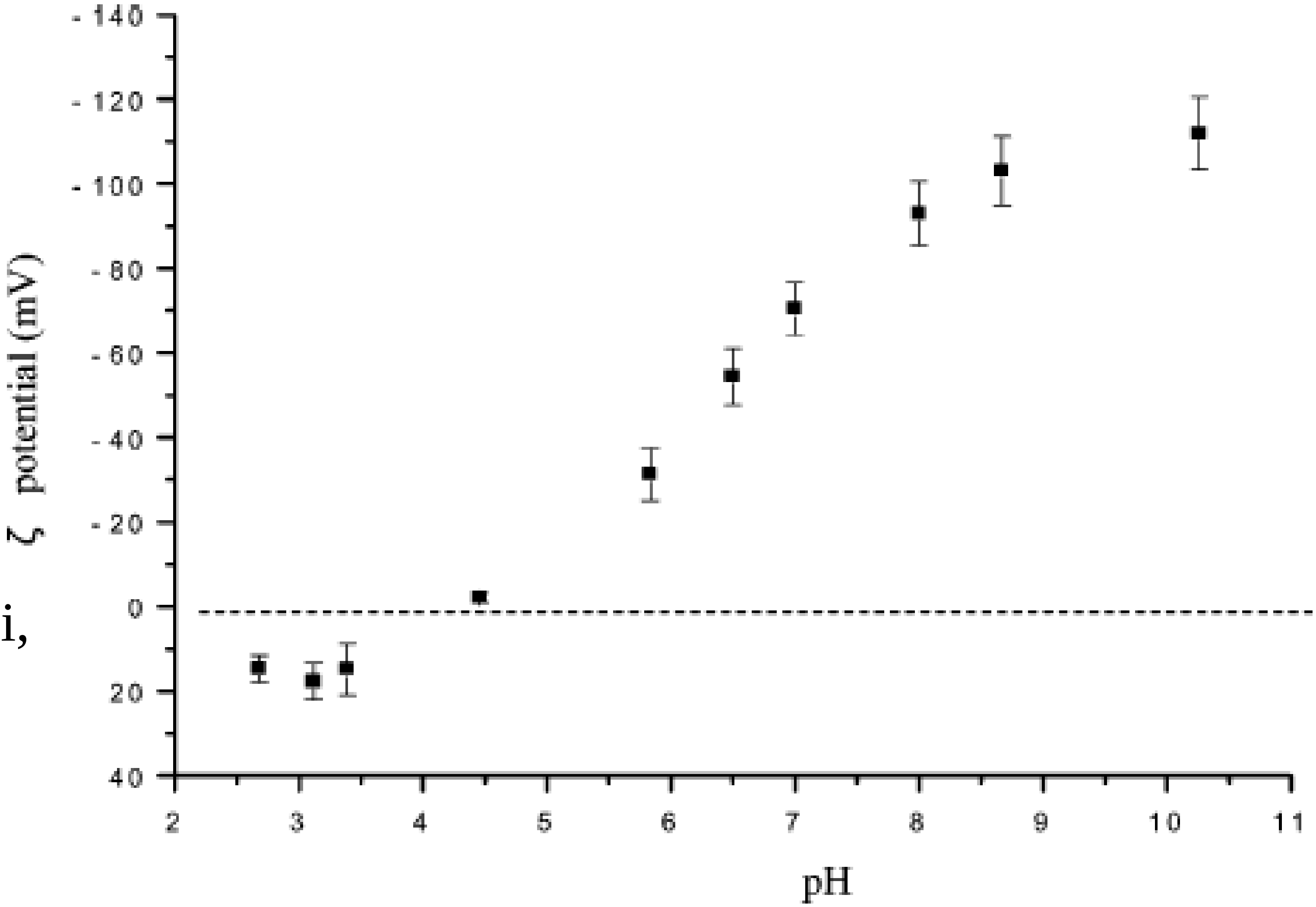

Takahashi, 2005

Figure 11. Relationship between the ζ potential of the microbubbles and the pH of the water, determined by HCl and NaOH. The surface charge of the gas−water interface was strongly affected by the pH of the water. The result indicated the important role of H^+ and OH^- in the surface charge.

Water/air surface: zeta-potential versus pH

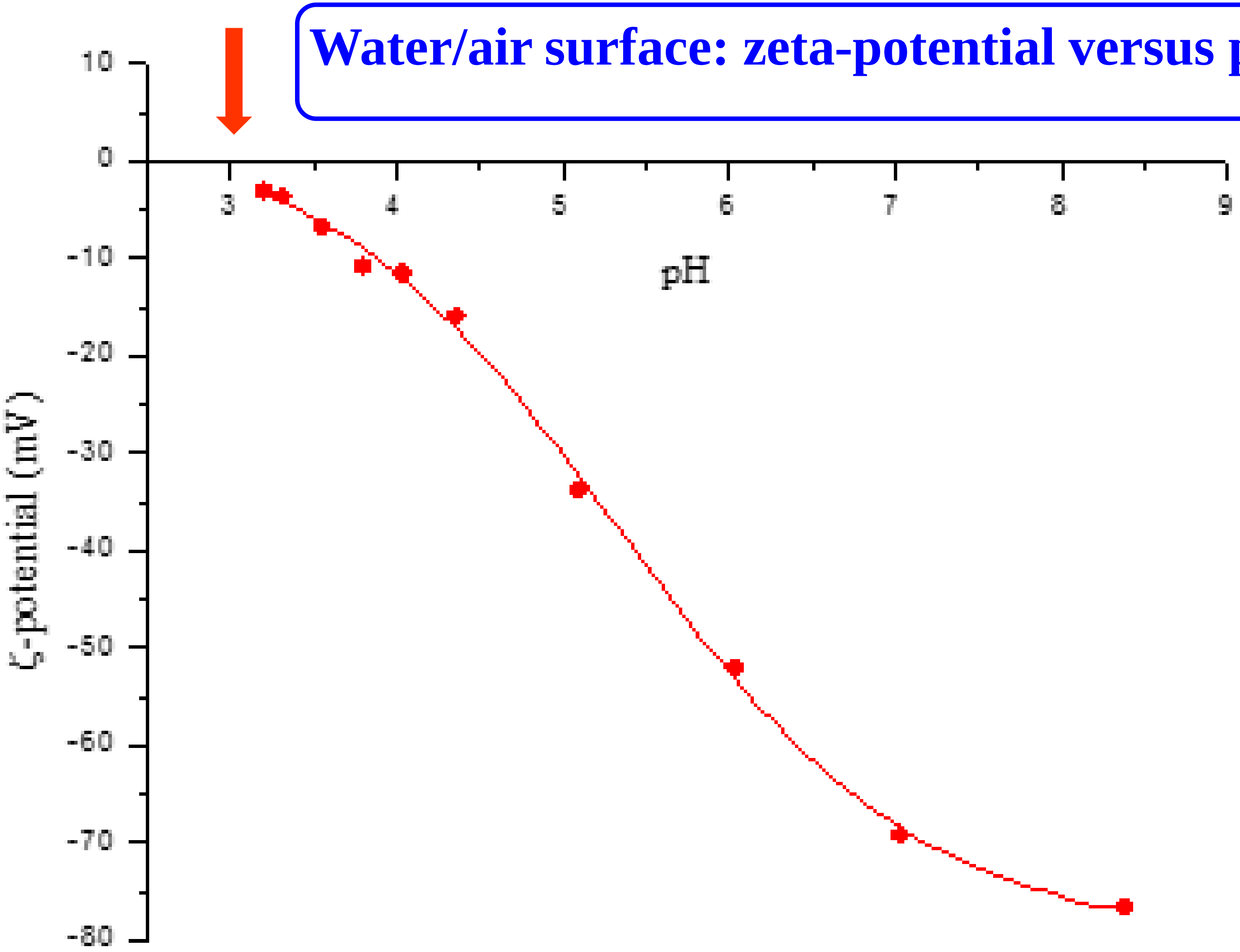

(Prof. James Beattie; Sydney, Australia)

The possible structure of fullerene C60 particles hydrosol

(Analogous to the oil-in-water and air-in-water particles)

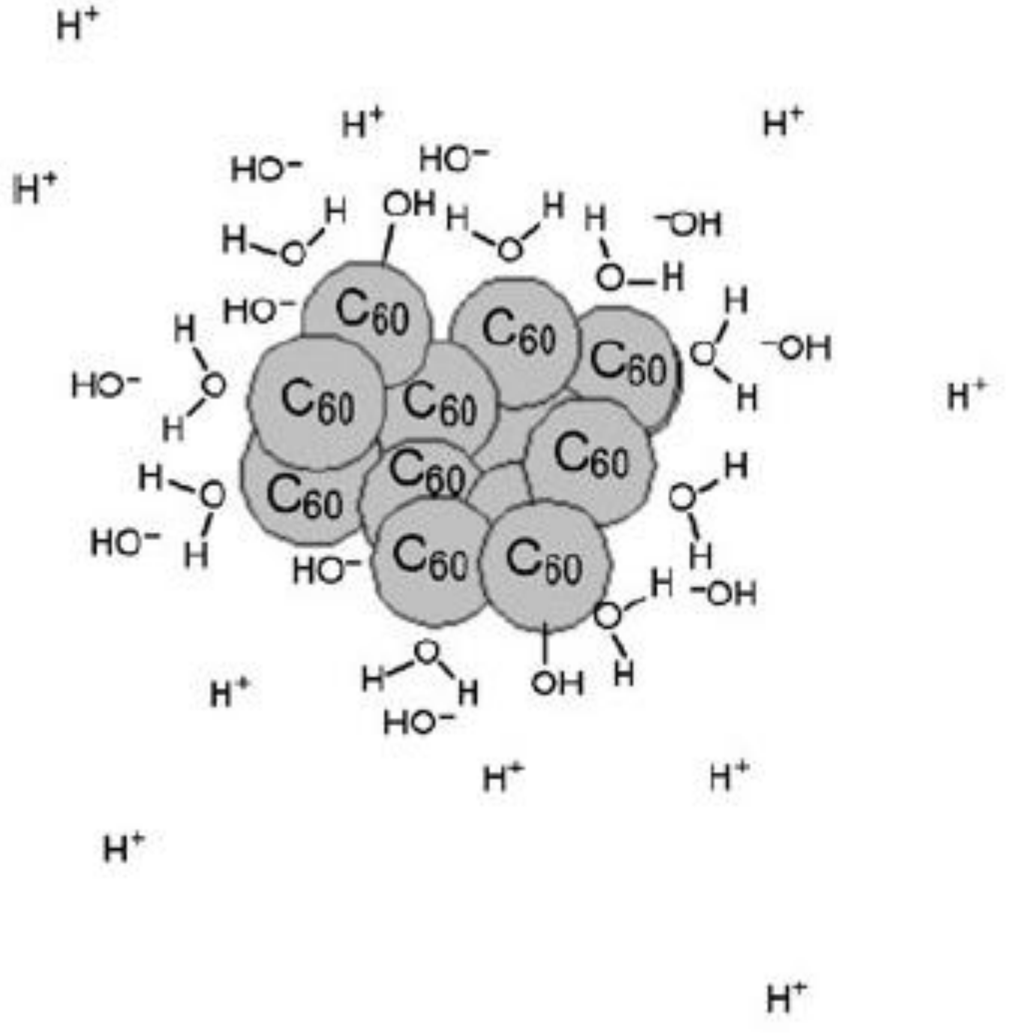

Particle size distribution in a 5.3

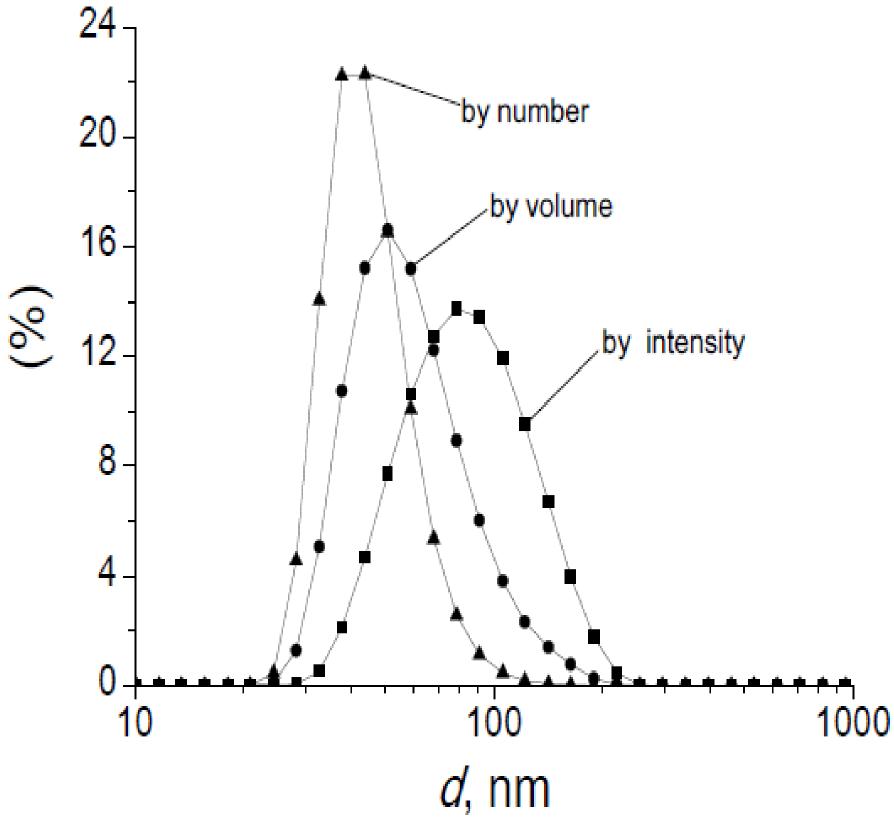

Particle size distribution in a 5.3 10^{-5} M C_{60} hydrosol

Nanocarbon structures in water: TEM of dried samples

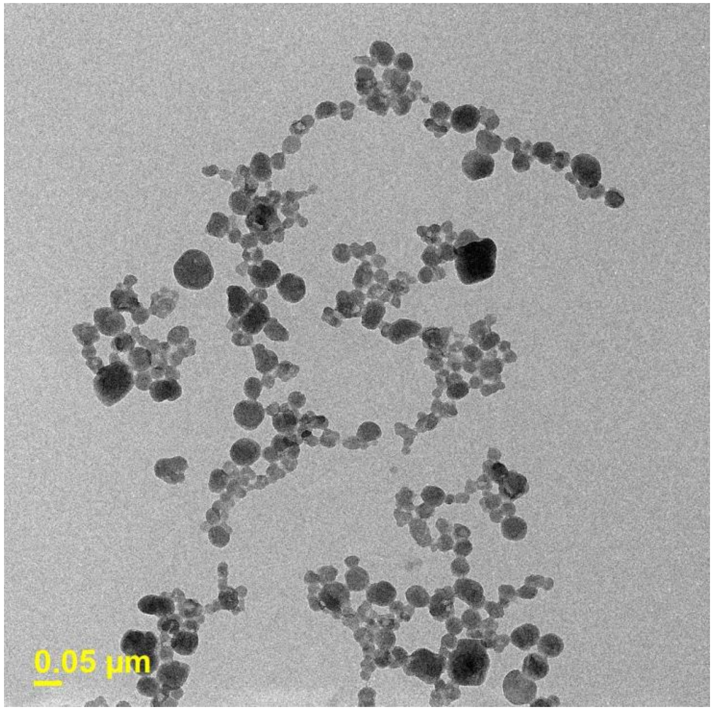

C_{60} hydrosol

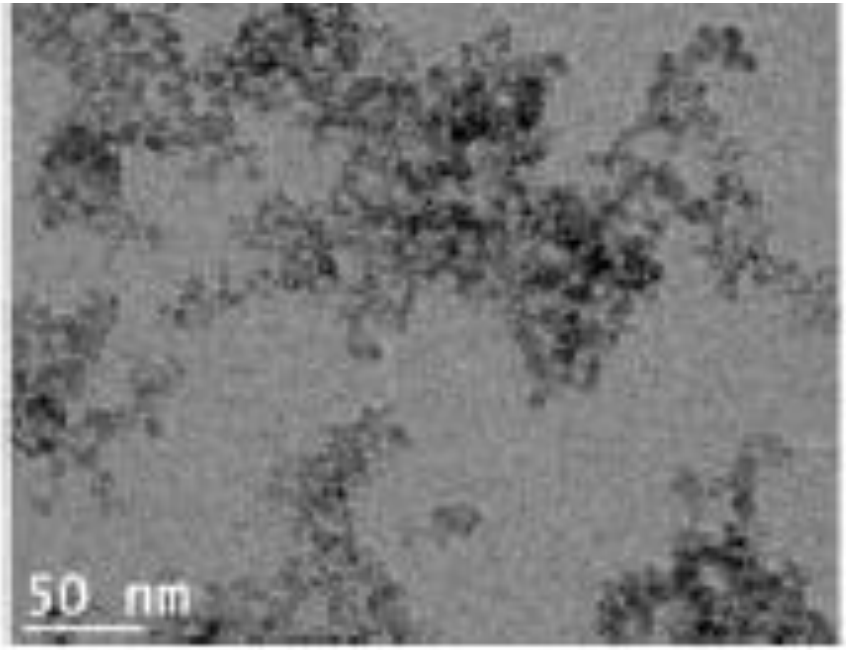

Detonation nanodiamond hydrosol

Nanocarbon structures in water: TEM of dried samples

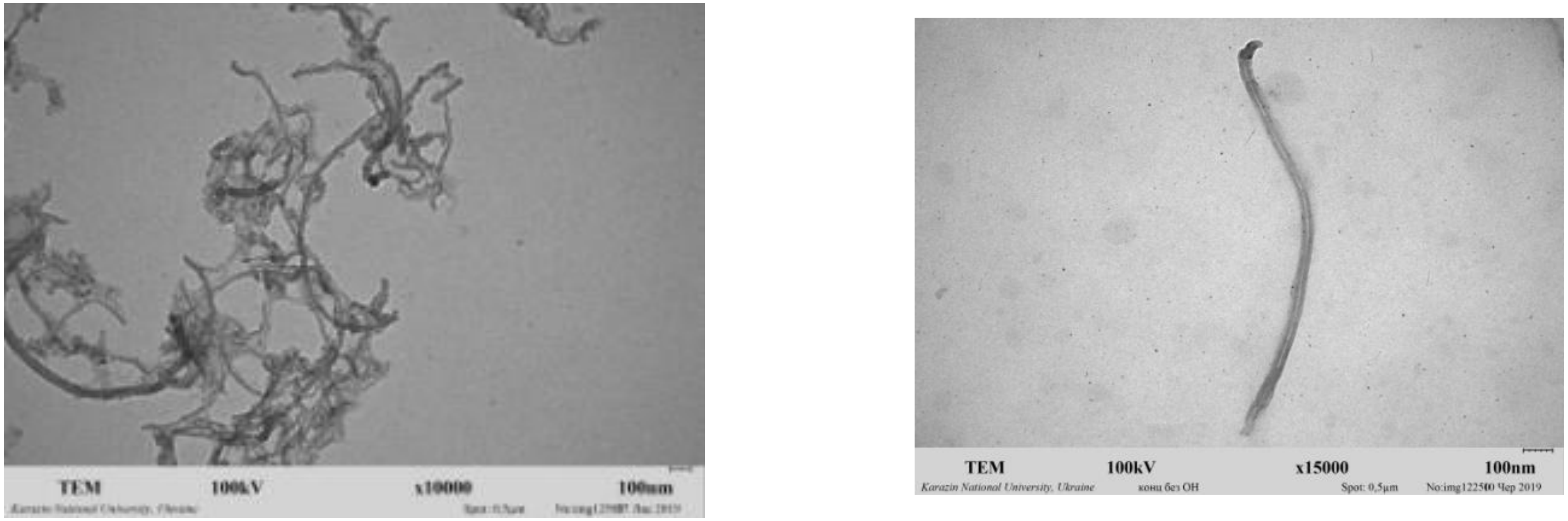

Aqueous suspension of single-walled carbon nanotubes (SWCNT)

COAGULATION OF THE LYOPHOBIC DISPERSED SYSTEMS

Main feature of the lyophobic (in water – hydrophobic) nanodispersed system is their **coagulation in the presence of electrolytes.**

Aggregation or agglutination of initial colloidal species finally results in phase separation and sedimentation of the colloids. **This allows escaping the excessive surface energy.**

The reason is the **relatively weak protective action** of the double electrical layer.

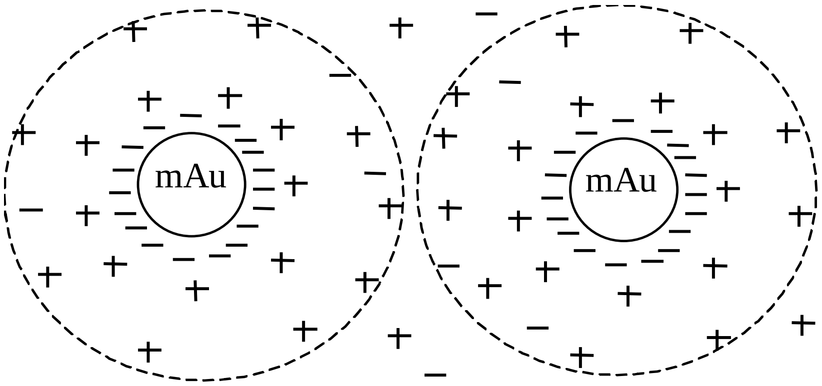

Nowadays, the generally recognized approach to the problem is based on the Derjaguin approach and the **DLVO** (Derjaguin – Landau – Verwey – Overbeek) theory. In this theory, the Hamaker diagram “Interaction energy vs. distance” is constructed using the electrostatic and molecular contributions.

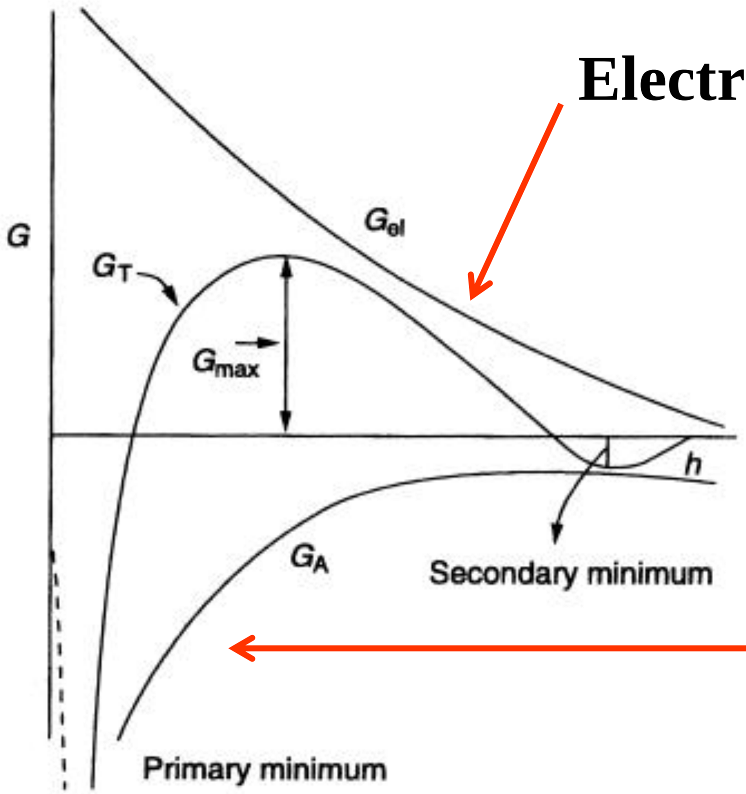

Electrostatic repulsion

Hamaker diagram

Molecular attraction

Fig. 1.1 Energy–distance curve for electrostatically stabilized systems.

T. Tadros, 2007

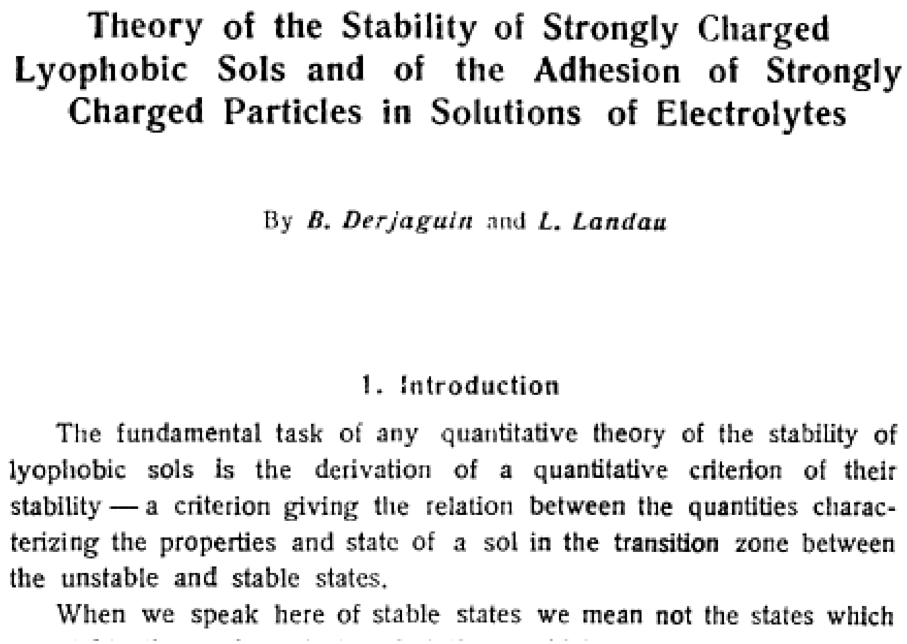

Theory of the Stability of Strongly Charged Lyophobic Sols and of the Adhesion of Strongly Charged Particles in Solutions of Electrolytes

By *B. Derjaguin* and *L. Landau*

1. Introduction

The fundamental task of any quantitative theory of the stability of lyophobic sols is the derivation of a quantitative criterion of their stability — a criterion giving the relation between the quantities characterizing the properties and state of a sol in the transition zone between the unstable and stable states.

When we speak here of stable states we mean not the states which

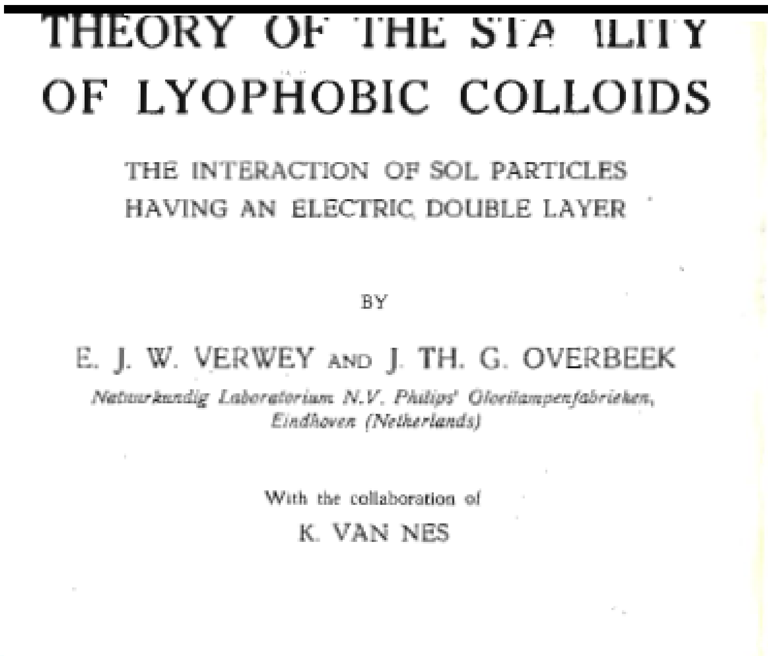

THEORY OF THE STA ILITY OF LYOPHOBIC COLLOIDS

THE INTERACTION OF SOL PARTICLES
HAVING AN ELECTRIC DOUBLE LAYER

BY

E. J. W. VERWEY AND J. TH. G. OVERBEEK
Natuurkundig Laboratorium N.V. Philips' Gloeilampenfabrieken,
Eindhoven (Netherlands)

With the collaboration of
K. VAN NES

Hugo Hamaker

Overbeek, Derjaguin and Verwey
(at Portmeirion, Wales, 1968)

Lev Landau

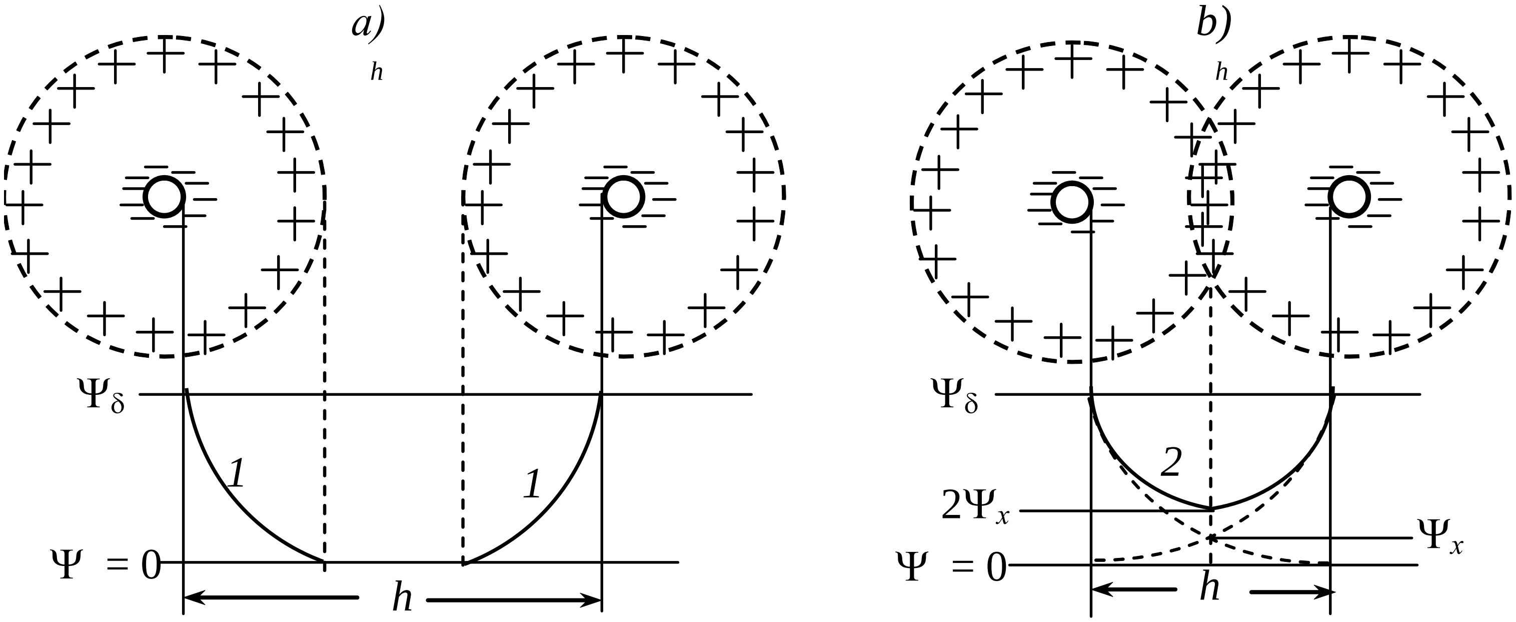

The interaction between two colloidal particles in an electrolyte solution is replaced by the interaction between two plates (see the next slide).

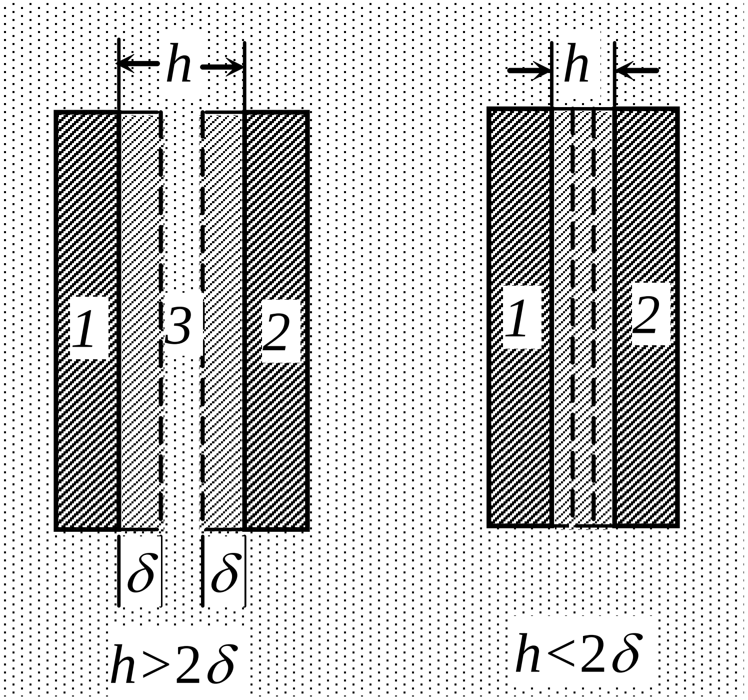

a) b)

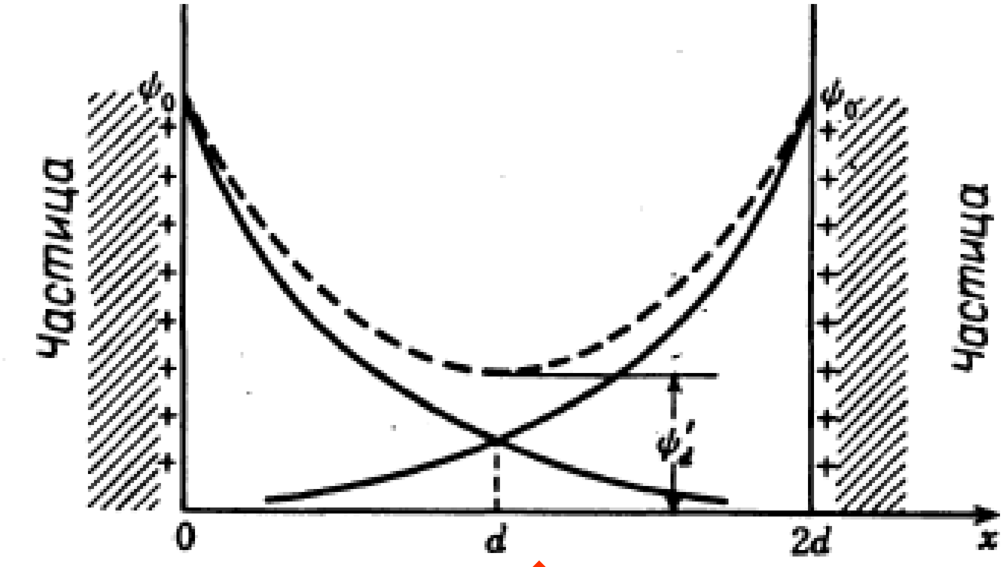

Overlapping of the diffuse parts of the double electrical layers

As result, the following equations were obtained:

For highly charged surfaces

$$U_{el} = \frac{64 c_{\circ} RT}{\kappa} \gamma^2 e^{-\kappa h}$$

For low charged surfaces:

$$U_{el} = 2\varepsilon_{\circ}\varepsilon_{\mathrm{r}}\kappa\Psi_{\delta}^{2} e^{-\kappa h}$$

where $\gamma = \dfrac{\exp[zF\Psi_{\delta}/(2RT)]-1}{\exp[zF\Psi_{\delta}/(2RT)]+1}$

Here c is the electrolyte concentration, Ψ is the electrostatic potential, κ is the reciprocal Debye length, h is the distance between the plates.

Molecular contribution (attraction) → $\boxed{U_{\mathrm{mol}} = -\dfrac{A_{12}}{12\pi h^{2}}}$

Here A_{12} is the so-called Hamaker constant, with the order of magnitude of 10^{-19} J.

$$A_{12} = (\sqrt{A_{11}} - \sqrt{A_{22}})^{2}$$

Increasing in the ionic strength (electrolyte concentration) decreases the height of the potential barrier

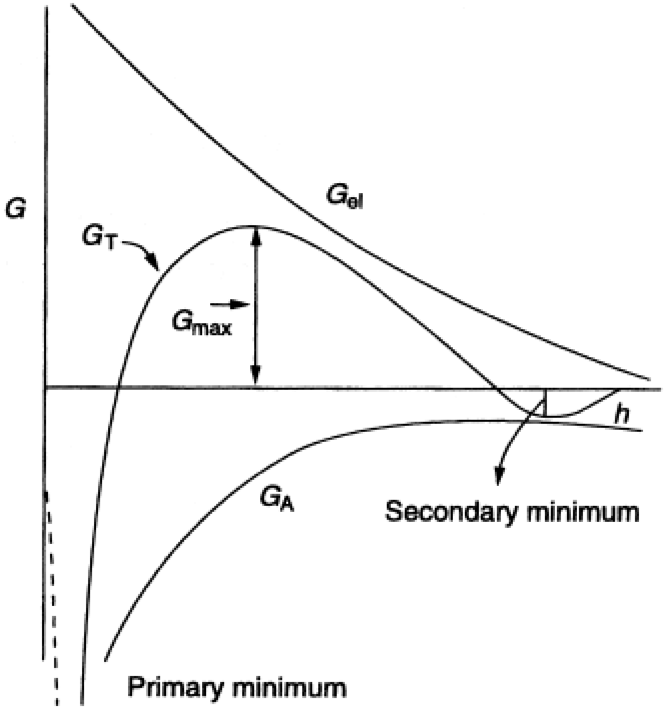

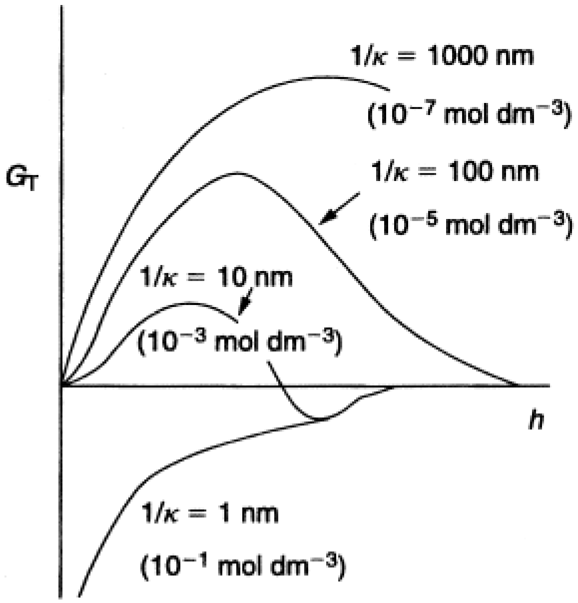

$$U_{el} = \frac{64 c_o RT}{\kappa}\gamma^2 e^{-\kappa h} - \frac{A_{12}}{12\pi h^2}$$

Modification of the equations for the interaction of two spherical particles

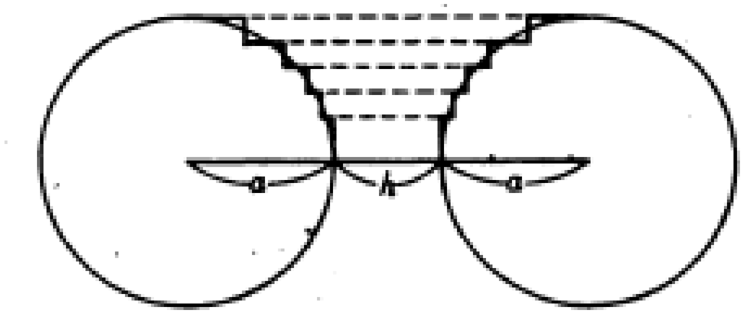

Derjaguin's integration results in the following equation:

$$\boxed{U(h) = 2\pi\varepsilon_0\varepsilon_r r\Psi_\delta^2 \ln(1+e^{-\kappa h}) - \frac{A^* r}{12h}}$$

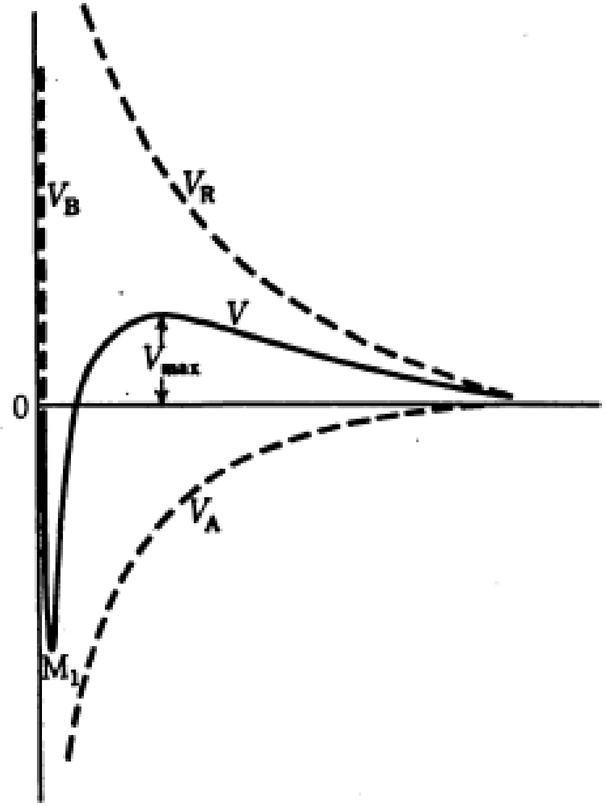

Slow coagulation

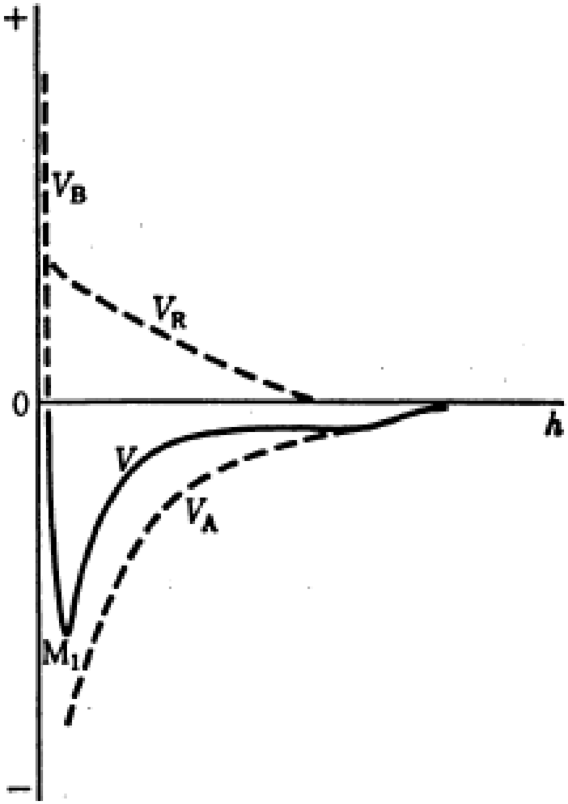

Fast coagulation

Threshold of coagulation = Coagulation point = Critical concentration of coagulation, or CCC

Nikolai Fuchs

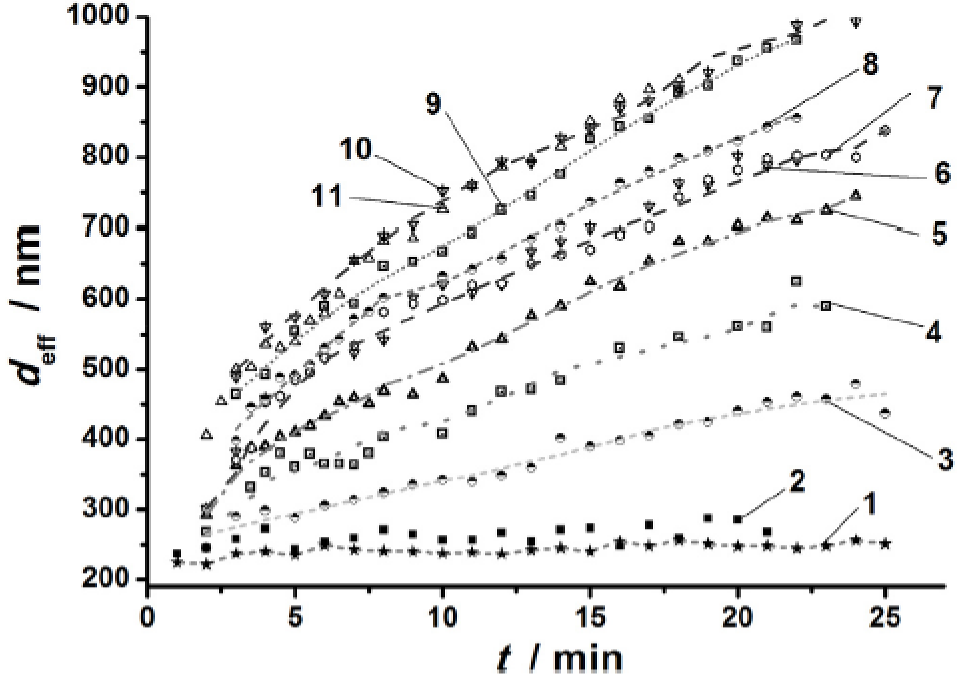

Fig. 7. C_{60} in acetonitrile (1), with $Ba(ClO_4)_2$: 0.0003 mM (2); 0.0006 mM (3); 0.0008 mM (4); 0.001 mM (5); 0.002 mM (6); 0.01 mM (7); 0.05 mM (8); 0.1 mM (9); 0.2 mM (10); 0.5 mM (11). Size uncertainty: 10–15%.

The Fuchs function

$$W = \frac{k_{\text{rapid}}}{k} = \frac{[(\partial r/\partial t)_{t\to 0}]_{\text{rapid}}}{(\partial r/\partial t)_{t\to 0}}$$

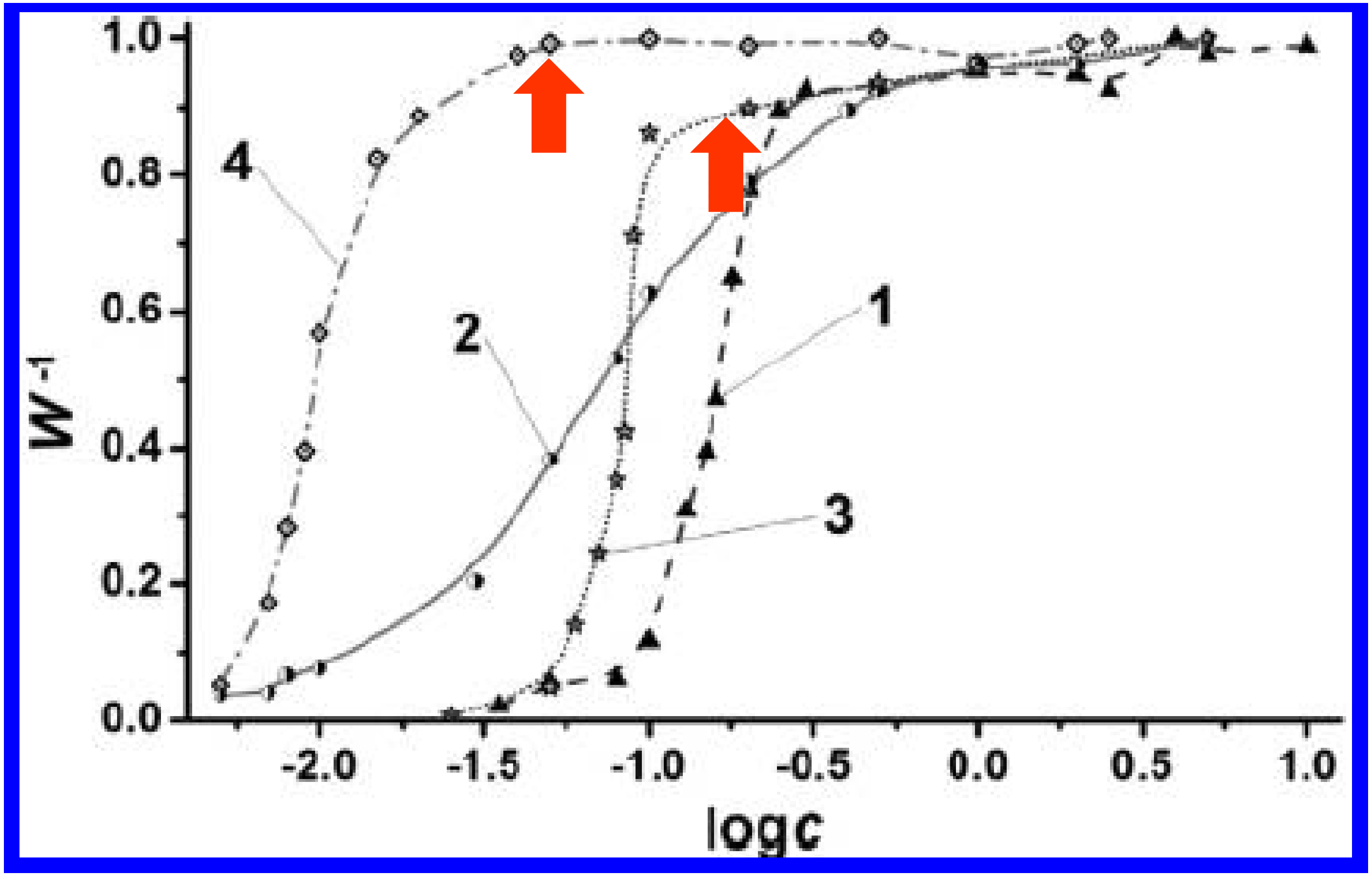

Figure 3. Reciprocal Fuchs function (i.e., the coagulation efficiency coefficient) vs the logarithm of the electrolyte concentration (mM) in methanol: $NaClO_4$ (1), $HClO_4$ (2), $TBAClO_4$ (3), and $Ca(ClO_4)_2$ (4)

Interactions of Nanosized Aggregates of Fullerene C_{60} with Electrolytes in Methanol: Coagulation and Overcharging of Particles

Nikolay O. Mchedlov-Petrossyan,*[†] Younis T. M. Al-Shuuchi,[†] Nika N. Kamneva,[†] Andriy I. Marynin,[‡] and Vladimir K. Klochkov[§]

CCC

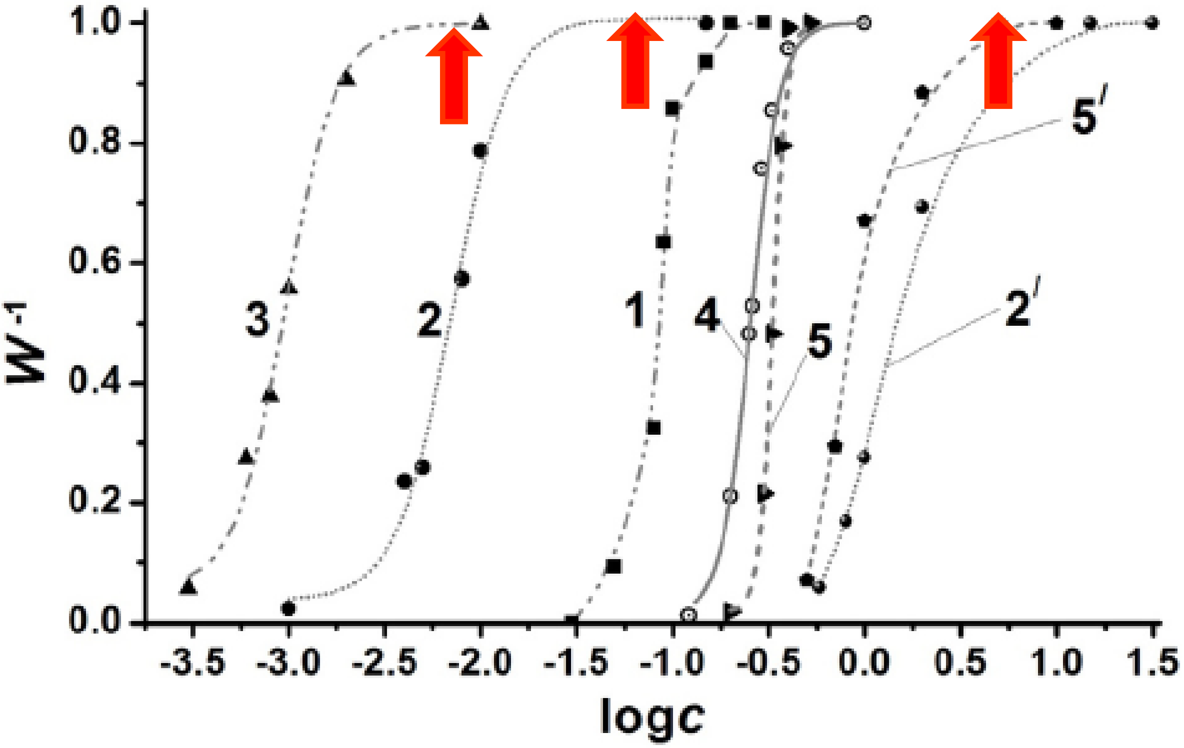

Fig. 8. The reciprocal Fuchs function (= coagulation efficiency coefficient) vs. logarithm of the electrolyte concentration (mM) in acetonitrile: NaClO$_4$ (1); Ca(ClO$_4$)$_2$ (2); Ba(ClO$_4$)$_2$ (3); TBAClO$_4$ (4); and CTAClO$_4$ (5). The second stage of coagulation: Ca(ClO$_4$)$_2$ (2$^/$) and CTAClO$_4$ (5$^/$).

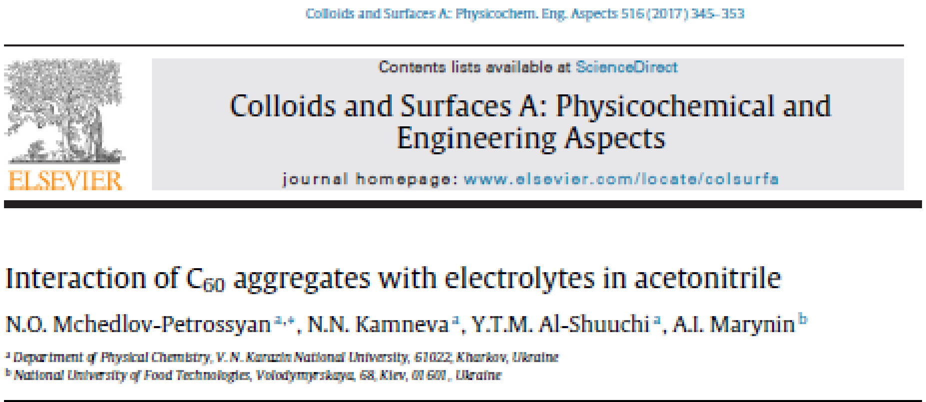
Colloids and Surfaces A: Physicochem. Eng. Aspects 516 (2017) 345–353

Contents lists available at ScienceDirect

Colloids and Surfaces A: Physicochemical and Engineering Aspects

journal homepage: www.elsevier.com/locate/colsurfa

Interaction of C$_{60}$ aggregates with electrolytes in acetonitrile

N.O. Mchedlov-Petrossyan [a,*], N.N. Kamneva [a], Y.T.M. Al-Shuuchi [a], A.I. Marynin [b]

[a] Department of Physical Chemistry, V. N. Karazin National University, 61022, Kharkov, Ukraine
[b] National University of Food Technologies, Volodymyrskaya, 68, Kiev, 01 601, Ukraine

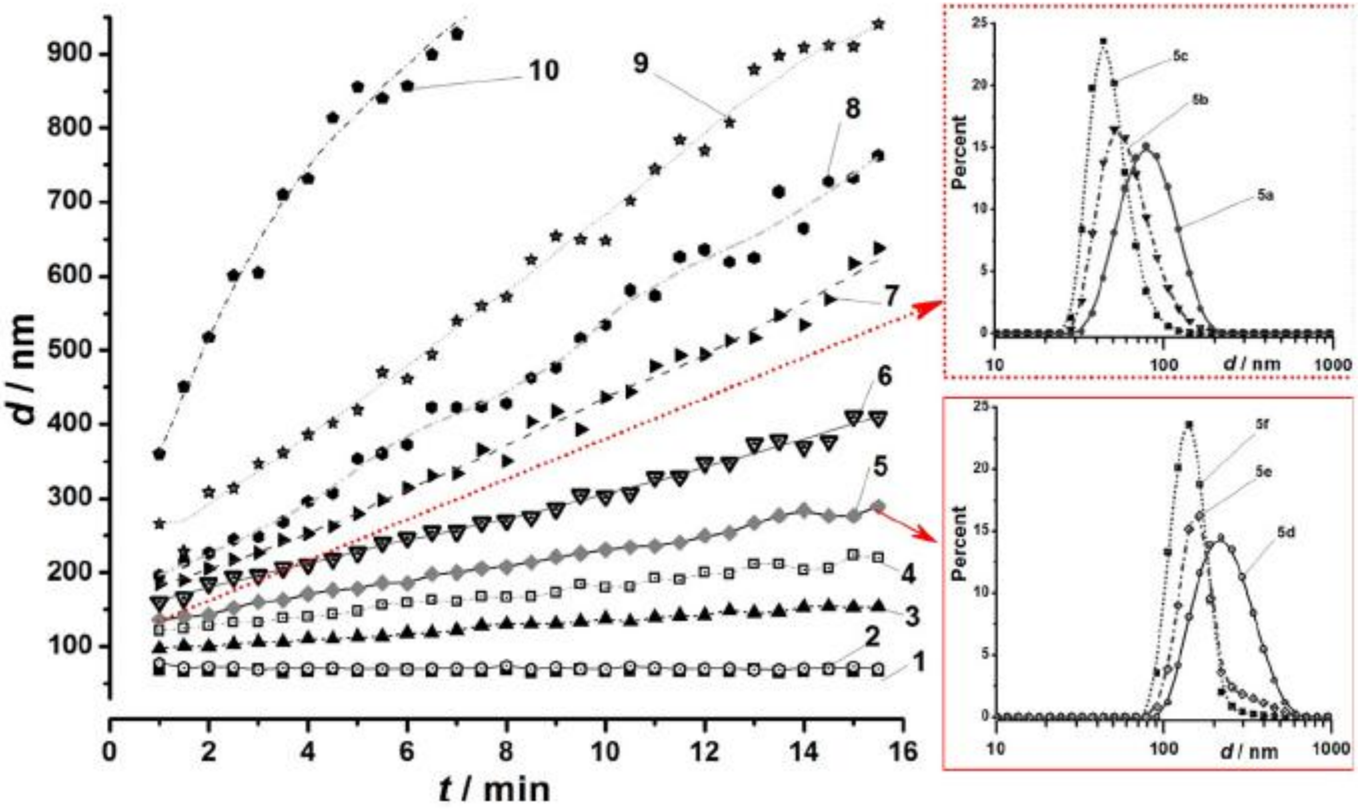

Hydrosol of detonation nanodiamonds: coagulation by NaCl and NaOH

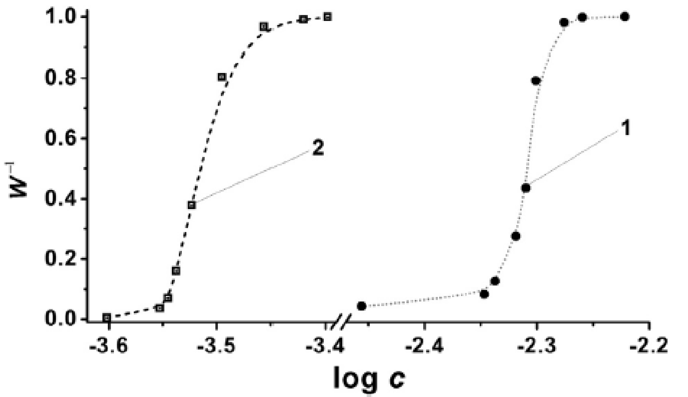

Fig. 13. The reciprocal Fuchs function, or coagulation efficiency coefficient of DND colloidal particles, W^{-1}, on logarithm of NaCl (1) and NaOH (2) molar concentrations; 0.0036 wt/vol% hydrosol; 25 °C.

Hans Schulze

Sir William Bate Hardy

Coagulation with multi-charged counter-ions: the Schulze – Hardy rule

$$CCC = \frac{const}{z^n}$$

$$\{m\mathrm{As_2S_3}\ n\mathrm{HS^-}\ (n-x)\ \mathrm{H^+}\}^{x-}\ x\ \mathrm{H^+}$$

Относительное коагулирующее действие Y^{-1} катионов
с зарядами z = 1, 2 и 3

	K^+	Ba^{2+}	Al^{3+}
по С. Линдеру и М. Пиктону	1	83	1590
по Ф. Повису	1	40	267
по Г. Фройндлиху	1	72	528

The coagulating effect of the counter-ion is proportional to some high degree of its charge

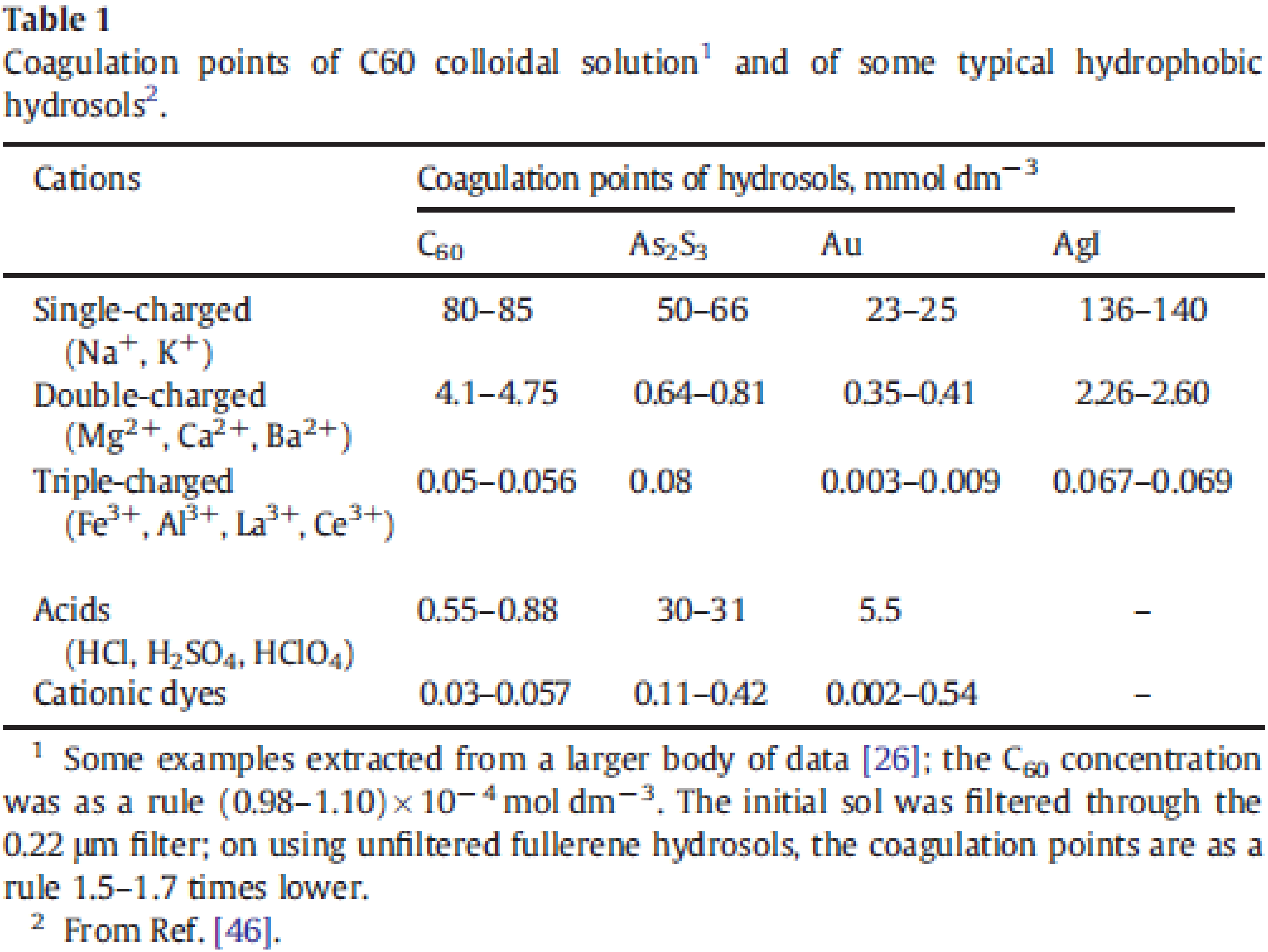

Table 1

Coagulation points of C60 colloidal solution[1] and of some typical hydrophobic hydrosols[2].

Cations	Coagulation points of hydrosols, mmol dm^{-3}			
	C_{60}	As_2S_3	Au	AgI
Single-charged (Na^+, K^+)	80–85	50–66	23–25	136–140
Double-charged (Mg^{2+}, Ca^{2+}, Ba^{2+})	4.1–4.75	0.64–0.81	0.35–0.41	2.26–2.60
Triple-charged (Fe^{3+}, Al^{3+}, La^{3+}, Ce^{3+})	0.05–0.056	0.08	0.003–0.009	0.067–0.069
Acids (HCl, H_2SO_4, $HClO_4$)	0.55–0.88	30–31	5.5	–
Cationic dyes	0.03–0.057	0.11–0.42	0.002–0.54	–

[1] Some examples extracted from a larger body of data [26]; the C_{60} concentration was as a rule (0.98–1.10) × 10^{-4} mol dm^{-3}. The initial sol was filtered through the 0.22 µm filter; on using unfiltered fullerene hydrosols, the coagulation points are as a rule 1.5–1.7 times lower.

[2] From Ref. [46].

Table 4. Values of Coagulation Points of C_{60} Hydrosol[a,b,c]

electrolyte	z[d]	$10^3 \times Y$, M[e]	Y(NaCl):Y(electrolyte)
NaCl	1	85[f]	1
$^1/_2Na_2SO_4$	1	85	1
NH_4Cl	1	80	1.06
KI	1	80	1.06
KOH	1	27.5	3.1
HNO_3	1	1.2	71
HCl	1	0.88	97
$HClO_4$	1	0.55	155
$CaCl_2$	2	4.1	21
$MgSO_4$	2	4.75	18
$^1/_2Fe_2(SO_4)_3$	3	0.05	1.7×10^3
$La(NO_3)_3$	3	0.056	1.5×10^3
$Th(NO_3)_4$	4	0.027	3.1×10^3
$C_5H_{11}N(C_2H_5)_3HSO_4$	1	1.8	47
$N(C_4H_9)_4HSO_4$	1	0.8	106
$C_{12}H_{25}N(CH_3)_3Br$	1	0.032	2.6×10^3
$C_{16}H_{33}N(CH_3)_3Br$	1	0.0052[g]	1.6×10^4
quinaldine red	1	0.047	1.8×10^3
methylene blue	1	0.032	2.6×10^3
neutral red	1	0.028	3.0×10^3
indotricarbocyanine	1	0.025	3.4×10^3
1,1′-dimethylquino-2-carbocyanine	1	0.025	3.4×10^3

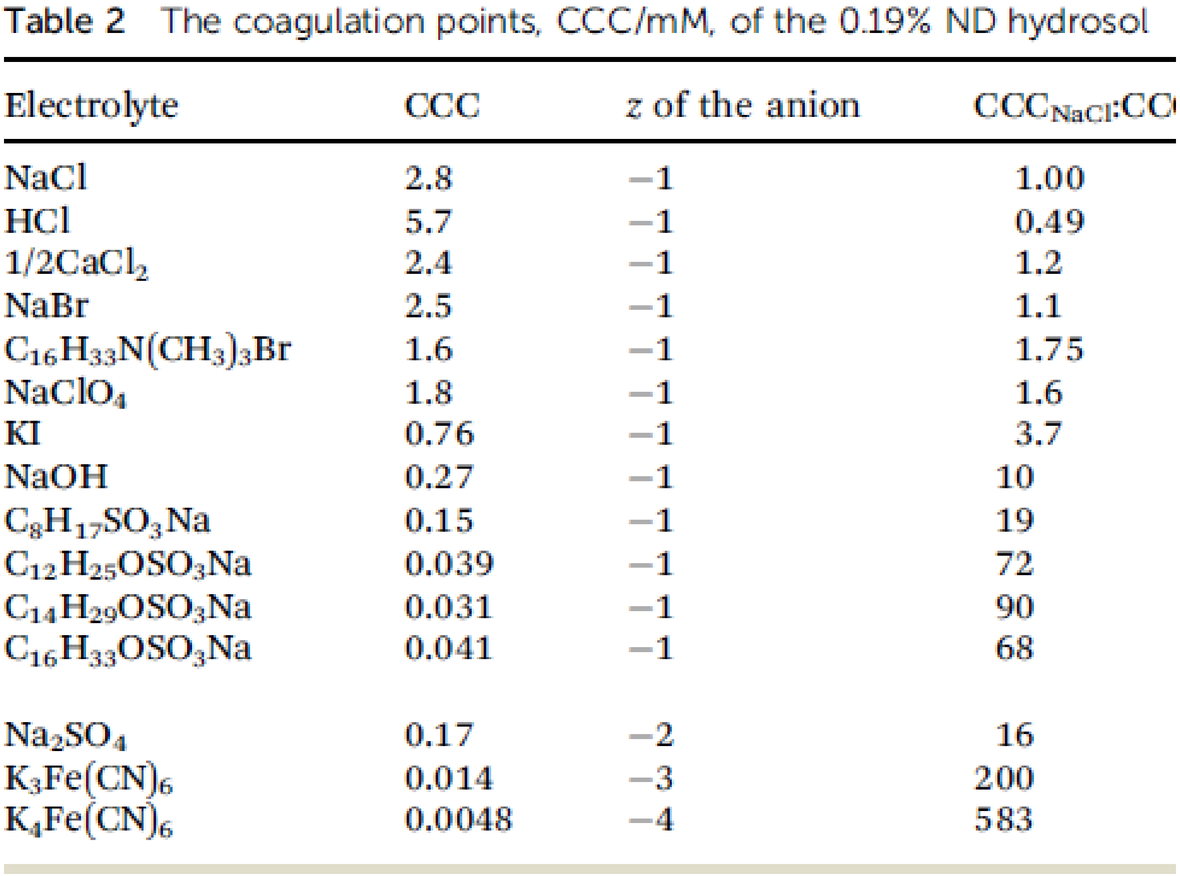

Table 2 The coagulation points, CCC/mM, of the 0.19% ND hydrosol

Electrolyte	CCC	*z* of the anion	CCC_{NaCl}:CC
NaCl	2.8	−1	1.00
HCl	5.7	−1	0.49
$1/2CaCl_2$	2.4	−1	1.2
NaBr	2.5	−1	1.1
$C_{16}H_{33}N(CH_3)_3Br$	1.6	−1	1.75
$NaClO_4$	1.8	−1	1.6
KI	0.76	−1	3.7
NaOH	0.27	−1	10
$C_8H_{17}SO_3Na$	0.15	−1	19
$C_{12}H_{25}OSO_3Na$	0.039	−1	72
$C_{14}H_{29}OSO_3Na$	0.031	−1	90
$C_{16}H_{33}OSO_3Na$	0.041	−1	68
Na_2SO_4	0.17	−2	16
$K_3Fe(CN)_6$	0.014	−3	200
$K_4Fe(CN)_6$	0.0048	−4	583

$$CCC = \frac{const}{z^n}$$

The DLVO theory predicts *n* = 6 for highly charged colloidal particles, in the absence of adsorption:

The ratio of 1/(*CCC)* for z = 1, 2, 3, and 4
Should be 1 : 64 : 729 : 4096

Besides numerous results published in the literature, let us consider our data for hydrosols:

Fullerene C_{60} ("negative" sol): 1: 20 : 1500 : 3100
Detonation nanodiamond ("positive" sol): 1 : 16 : 200 : 583
SWCNT suspension ("negative"): 1 : 111 : 6000

The reasons of deviations from the classical DLVO theory:

(1) Adsorption of counter ions on the colloidal particles

(2) Polydispersity

(3) Influence of solvation (hydration) of ions: “Lyotropic series”

Overcharging

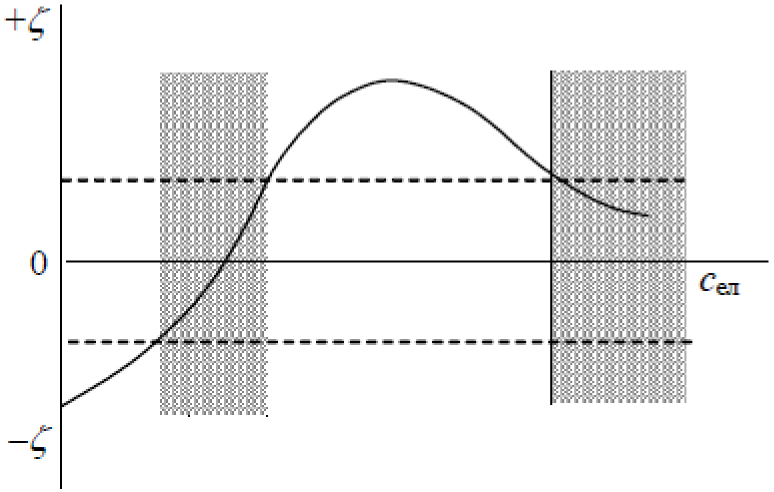

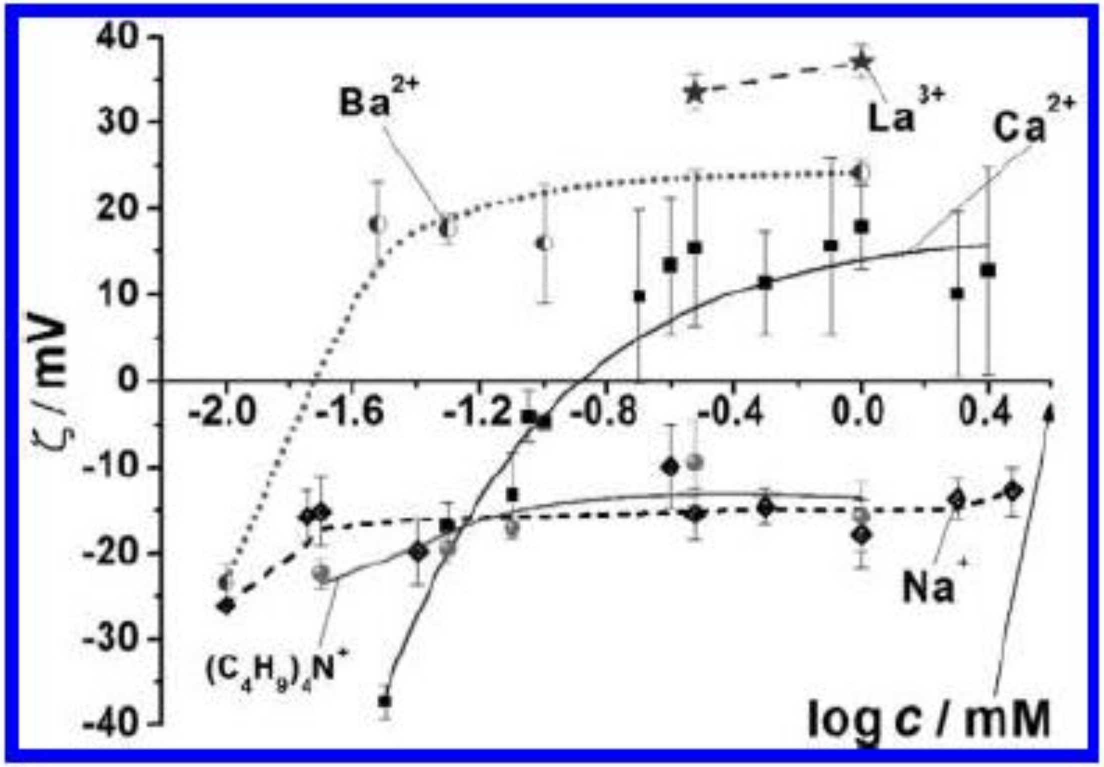

Figure 4. Dependence of the zeta potential of the C_{60} colloid in methanol on the concentrations of the electrolytes.

Table 2. Values of the Zeta Potential of C_{60} Colloidal Particles in Methyl Alcohol with Electrolytes

added electrolyte	κr	f	ζ/mV
$Ca(ClO_4)_2$, mM			
0.020	5.920	1.18	−15 ± 2
0.050	9.360	1.25	−12 ± 1
0.080	11.85	1.28	−4 ± 1
0.090	12.56	1.29	−2 ± 2
0.10	13.24	1.30	+4 ± 2
0.20	18.73	1.34	+21 ± 1
0.25	20.94	1.36	+25 ± 2
0.50	29.61	1.39	+26 ± 1
0.80	37.46	1.41	+23 ± 1
1.0	41.88	1.42	+9 ± 1
2.0	59.23	1.44	+11 ± 3
2.5	66.22	1.45	+26 ± 1
$Ba(ClO_4)_2$, mM			
0.010	4.190	1.13	−24 ± 2
0.030	7.250	1.21	+18.2 ± 0.5
0.050	9.360	1.25	+18 ± 2
0.10	13.24	1.30	+23 ± 2
1.00	41.88	1.42	+24 ± 2
$La(ClO_4)_3$, mM			
0.30	32.40[a]	1.40	+34 ± 2
1.00	59.23[a]	1.44	+37 ± 3

[a] Calculated for the complete dissociation of $La(ClO_4)_3$.

The overcharging and polydispersity leads to deviations from the classical DLVO theory

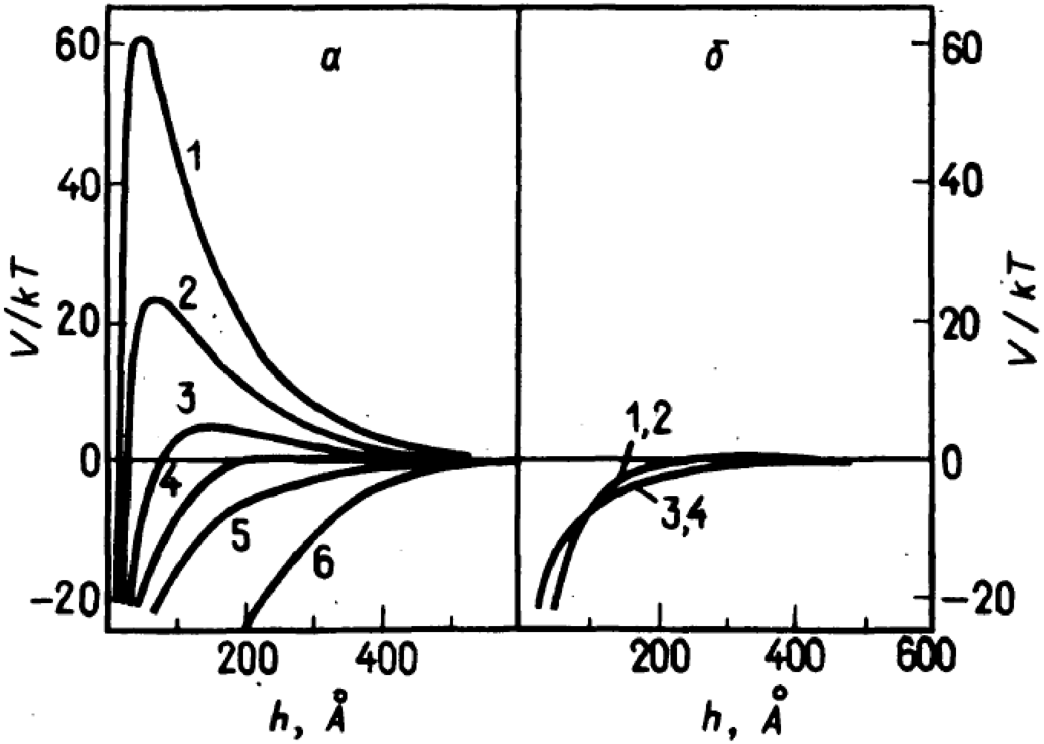

Рис. 6.31. Полная энергия взаимодействия двух частиц с различными поверхностными потенциалами.

Радиусы частиц $a_1 = a_2 = 1250$ Å; $A = 5 \cdot 10^{-20}$ Дж; $1/\kappa = 10^{-8}$ м [*Parfitt G.D.* Dispersion of Powders in Liquids (2 nd ed.), Applied Science, 1973, Chap. 1].

Рис. 6.31, а.	ψ_1, мВ	ψ_2, мВ	Рис. 6.31, б	ψ_1, мВ	ψ_2, мВ
Кривая *1*	+35,86	+ 35,86	Кривая *1*	+ 5,12	+ 35,86
2	+ 35,86	+ 20,48	2	+ 5,12	+ 20,48
3	+ 35,86	+ 10,24	*3*	+ 5,12	+ 10,24
4	+ 35,86	+ 5,12	*4*	+ 5,12	+ 5,12
5	+ 35,86	0			
6	+ 35,86	– 35,86			

Coagulation via surfactants

The logarithm of the CCC values of alkylammonium chlorides for the AgI hydrosol versus the number of carbon atoms

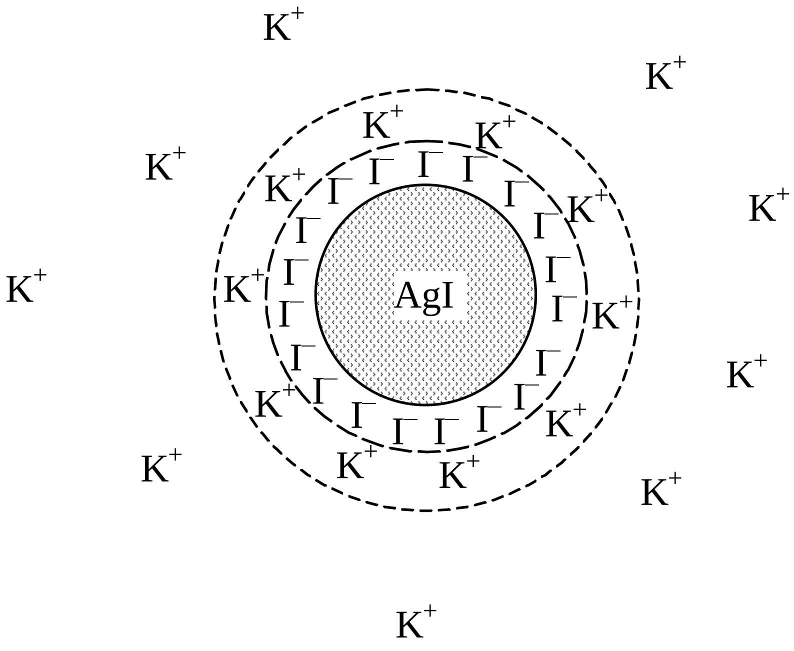

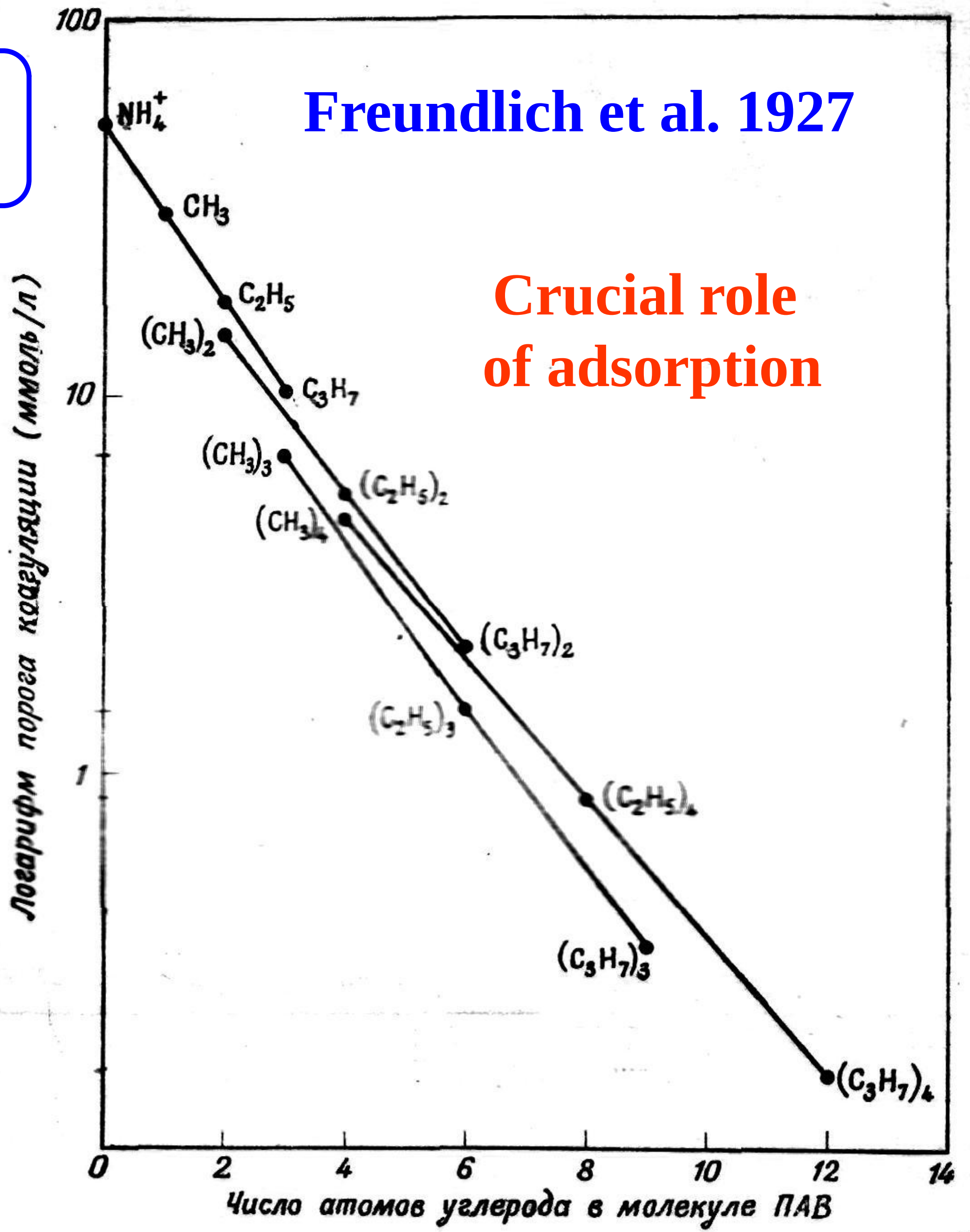

Freundlich et al. 1927

Crucial role of adsorption

Stabilization of lyophobic sols using polymers

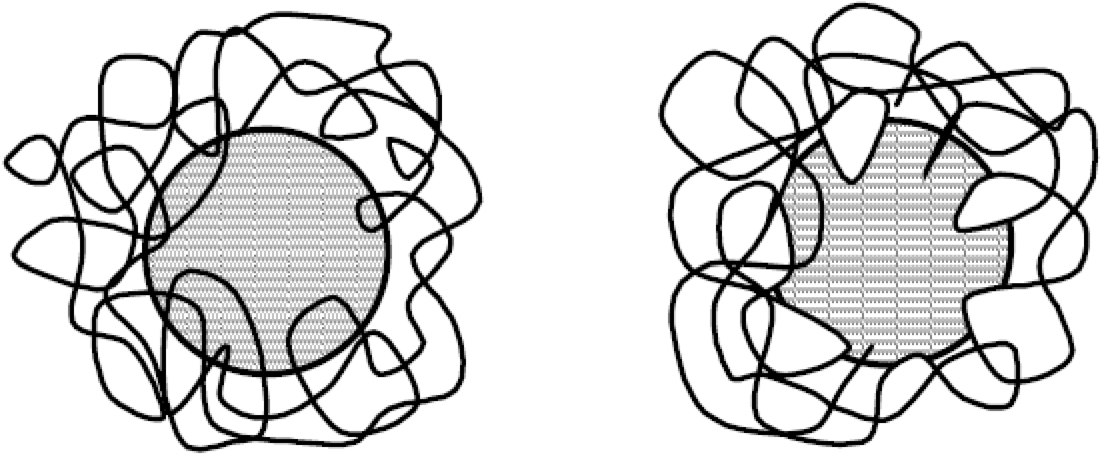

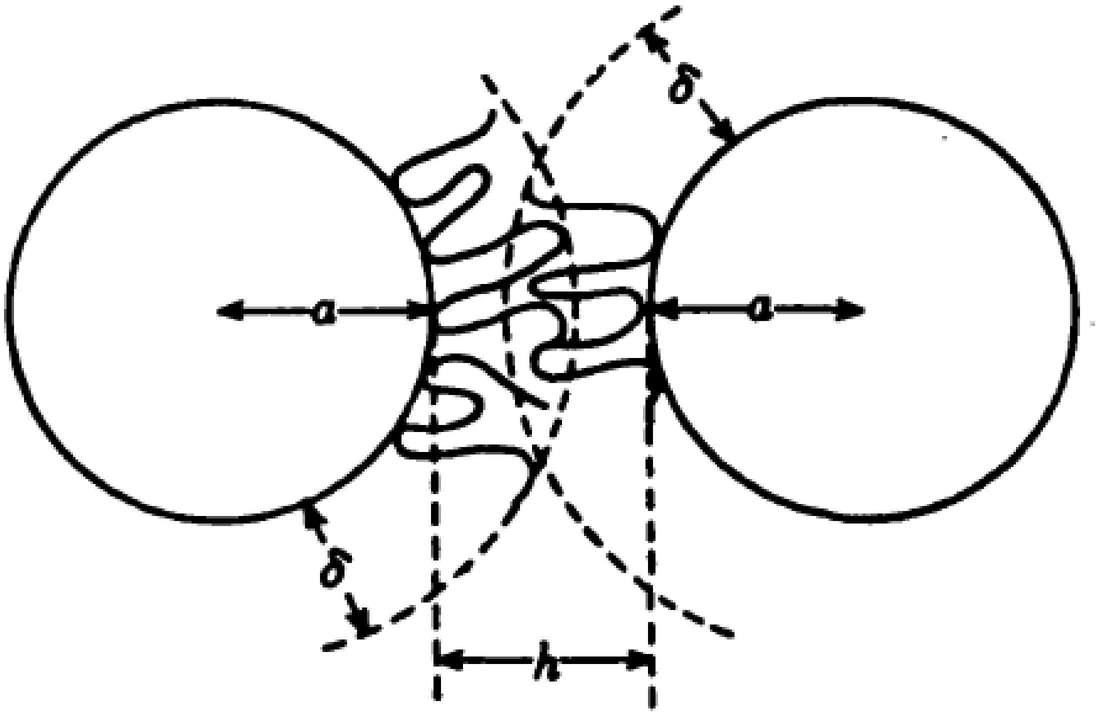

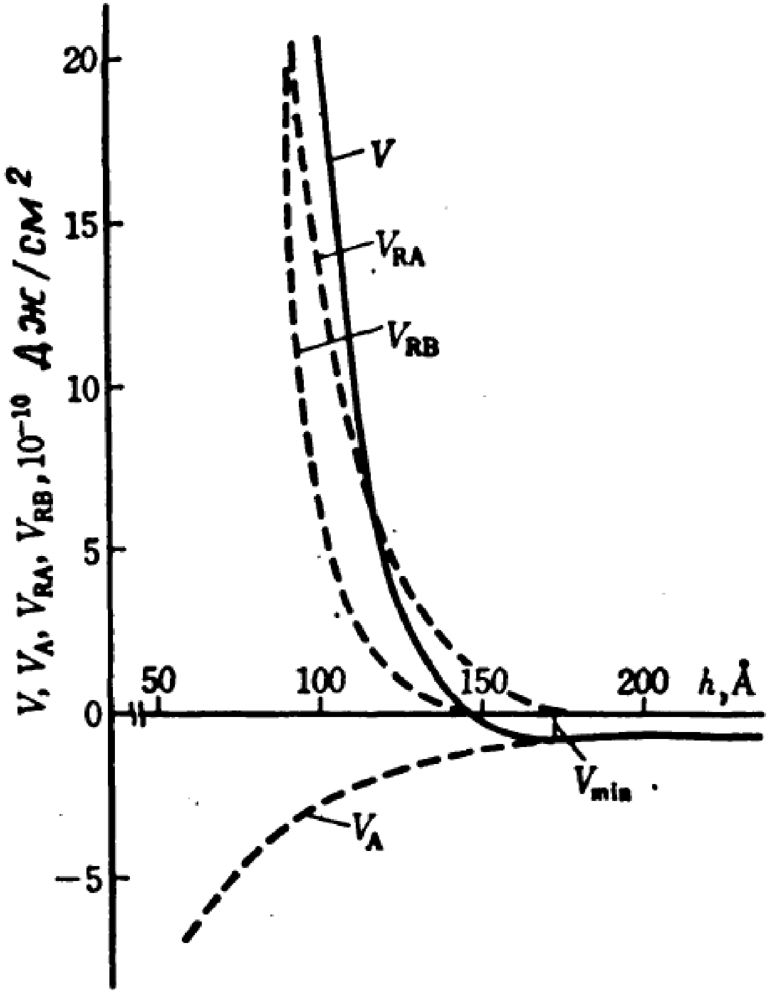

Рис. 6.34. Энергия взаимодействия двух частиц с адсорбированным на поверхности слоем полимера [*Hesselink J. Th., Vrij A., Overbeek J. Th. G.,* J. Phys. Chem., **75**, 2094 (1971)].

Молекулярный вес полимера 6000 (средняя длина макромолекулы 54 Å) поверхностная плотность адсорбента $2 \cdot 10^{-8}$ г/см^2; постоянная Гамакера $A = 10^{-20}$ Дж.

Stabilization **Flocculation**

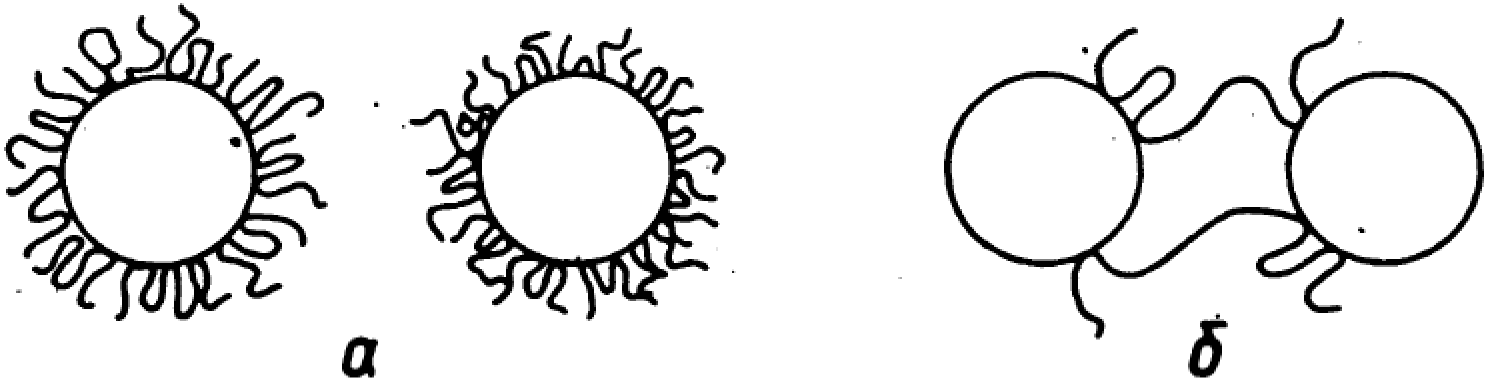

Рис. 6.35. Модели взаимодействия частиц с адсорбированными на поверхно
ти полимерными молекулами.

а — плотная адсорбция приводит к отталкиванию, *б* — рыхлая адсорбция — к
коагуляции путем сшивания.